

A Computational Approach for the Study of Color Modulation and Contrasts in
Visual Art

by

Anissa Agahchen
B.Sc., University of Victoria, 2014

A Dissertation Submitted in Partial Fulfillment of the
Requirements for the Degree of

MASTER OF SCIENCE

in the Department of Computer Science

© Anissa Agahchen, 2014
University of Victoria

All rights reserved. This dissertation may not be reproduced in whole or in part, by
photocopying or other means, without the permission of the author.

A Computational Approach for the Study of Color Modulation and Contrasts in
Visual Art

by

Anissa Agahchen
B.Sc., University of Victoria, 2014

Supervisory Committee

Dr. A. Branzan Albu, Supervisor
(Department of Computer Science)

Dr. G. Tzanetakis, Departmental Member
(Department of Computer Science)

Supervisory Committee

Dr. A. Branzan Albu, Supervisor
(Department of Computer Science)

Dr. G. Tzanetakis, Departmental Member
(Department of Computer Science)

ABSTRACT

This thesis describes a computational approach for analyzing the color aesthetics of images from the perspective of color theory. Our work has been informed by the works of Johannes Itten, one of the most influential theorists of color aesthetics. To the best of our knowledge, developing computational models that are based on Itten's theories is our unique contribution to Computer Vision. We focus on three aspects of color usage in visual art, namely *modulation*, *contrast of hue* and *cold-warm contrast*. For modulation, we introduce the color palette, a novel 3D visualization of the chromatic information of an image in the HSL space and propose a set of simple descriptors for evaluating color modulation. For *contrast of hue*, we assess the spatial color composition of the homogeneous regions. For *cold-warm contrast*, we assess the spatial color composition of the homogeneous regions and the hue adjacencies. Further, we assess the relative warmth of the homogeneous regions and adjacent hues. We also propose a visualization, namely a 3D histogram to visualize the patterns of the contrasts in an artist's paintings. We validate our methods by comparing our results with Itten's descriptions and comments. We hope that this computational approach improves the color-based features used in the aesthetic classification of images.

Contents

Supervisory Committee	ii
Abstract	iii
Table of Contents	iv
List of Tables	vi
List of Figures	vii
Acknowledgements	xii
Dedication	xiii
1 Introduction	1
1.1 Motivation	1
1.2 Overview of thesis	4
2 Related Work	5
2.1 Visual features in aesthetic classification	7
2.1.1 Low-level features	7
2.1.2 High level concepts	11
2.2 Databases	15
2.3 Discussion	16
3 Proposed Approach	18
3.1 A summary of Itten’s Color Theory	19
3.2 Modulation	22
3.3 Computational model for modulation	23
3.3.1 Descriptors for modulation	23

3.4	Contrasts	27
3.5	Computational models for color contrasts	29
3.5.1	Contrast of hue	31
3.5.2	Cold-warm contrast	33
3.5.3	Worked example	37
3.5.4	Analysis of paintings with the proposed computational models	41
3.5.5	Analysis of artists' chromatic style	43
4	Experiments	57
4.1	Database	57
4.2	3D Visualization and Modulation	57
4.2.1	A comparative analysis of low and high color modulation	59
4.3	Contrast of hue and cold-warm contrast	60
4.3.1	Contrast of hue results on Itten's dataset	60
4.3.2	Contrast of hue results per artist	65
4.3.3	Cold-warm contrast results on Itten's dataset	69
4.3.4	Cold-warm contrast results per artist	73
4.3.5	Robustness	90
4.3.6	Discussion	99
5	Application of proposed methods on business documents	102
5.1	Business documents	102
5.2	Color in business documents	103
5.3	Analysis of contrasts in pie charts	104
5.4	Results	106
5.5	Discussion	110
6	Conclusion and future work	112
6.1	Conclusion	112
6.2	Future work	113
	Bibliography	115

List of Tables

Table 3.1	Conversion Table of RGB values to Cartesian coordinates in HSL Space	20
Table 4.1	Database of paintings described by Itten: artist name, painting name, source	58
Table 4.2	Artists who used <i>contrast of hue</i> : Botticelli, Fra Angelico, Franz Marc, Kandinsky, Macke	75
Table 4.3	Artists who used <i>cold-warm contrast</i> : Bonnard, Cézanne, Monet	85
Table 4.4	Artists who used <i>cold-warm contrast</i> : Pissaro, Renoir	86
Table 4.5	Images used for robustness test: ‘Entree du Village’ (<i>cold-warm contrast</i>) and ‘The singing fish’ (<i>contrast of hue</i>)	91
Table 4.6	Modulation measures for paintings shown in Figure 4.1 and Figure 4.2 on page 61-62	101
Table 5.1	Classification of pie charts in SAP business documents	105

List of Figures

Figure 2.1 Representative photographs from Photo.net [3] rated by online users. Photos are scored from 1 to 7, however most photographs were scored 5 or higher.	6
Figure 2.2 Relationship between high-level concepts and low-level features. High level concepts are listed in the center column. Edges connect high level concepts to low level features.	7
Figure 2.3 Rule of thirds- the eye of the bee is located at the top-right power point [4]	9
Figure 2.4 Blur and Depth of Field- a blurred background creates a low depth of field, thus creating a focus on the sharp robin [3] . . .	9
Figure 2.5 Photograph in color [3] and converted to grayscale, illustrating the impact of color on our attention.	10
Figure 2.6 Moon & Spencer model of color harmony, depicting areas of ‘identity’, ‘similarity’, ‘contrast’ and ‘ambiguity’ in the hue layer [43]. If all the colors in the image fall in the non-ambiguous areas, the color combination is harmonious.	12
Figure 2.7 Matsuda’s Harmonic Templates [8] are based on the relative distance between two colors. If all the colors in an image fall within the gray slice(s), the color combination is harmonious.	12
Figure 3.1 The Itten Color Sphere. Views of the surface	19
Figure 3.2 The HSL Cylinder	21
Figure 3.3 The Itten Twelve-Part Color Wheel depicting the relative position of hues	21
Figure 3.4 ‘Composition 1928’ by Mondrian. Top row: image and its color palette; Second and third row: red hue sector of color palette; red-orange hue sector of color palette; orange hue sector of color palette; blue sector of color palette.	25

Figure 3.5 ‘Cafe at evening’ by Van Gogh. Top row: image and its color palette; Bottom row: red hue sector of color palette; red-orange hue sector of color palette; orange hue sector of color palette; blue sector of color palette; Last row: mean and standard deviation of color distribution in top 4 most populated hue sectors.	26
Figure 3.6 Itten’s Twelve-Part Color Circle, depicting primary, secondary and tertiary colors.	27
Figure 3.7 Illustrating the building of a co-occurrence matrix. Image on the left, co-occurrence matrix to the right.	30
Figure 3.8 Co-occurrence matrix, C_{diag} featuring the 3-cell diagonal band. The blank cells contain adjacent co-occurrences.	33
Figure 3.9 (a) hue warmth values (b) look up table of warmth contrast strength values computed as the difference of warmth indices	34
Figure 3.10 A simple checkered example	38
Figure 3.11 C_{diag} and C_{adj} derived from C for checkered example	39
Figure 3.12 Normalized Homogeneous Regions N_{hom} and Adjacencies N_{adj} for the checkered example.	40
(a) Normalized Homogeneous Regions N_{hom}	40
(b) Normalized Adjacencies N_{adj}	40
Figure 3.13 Summary of results for checkered color image	41
Figure 3.14 Coronation of the Virgin	42
Figure 3.15 La Belle Verriere	43
Figure 3.16 Picasso paintings	44
Figure 3.17 Cézanne Paintings	46
Figure 3.18 Summary of normalized co-occurrences for ‘Coronation of the Virgin’	49
Figure 3.19 Summary of normalized co-occurrences for ‘La Belle Verriere’	50
Figure 3.20 Picasso Visualization- Contrast of hue results for homogeneous regions and 3D histogram of relative proportions of hue homogeneities.	51
Figure 3.21 Detailed results for ‘Apples and Oranges’ by Cézanne	52
Figure 3.22 Detailed results for ‘Full Bowl’ by Cézanne	53
Figure 3.23 Detailed results for ‘Montagne St. Victoire’ by Cézanne	54
Figure 3.24 Detailed results for ‘Card Players’ by Cézanne	55

Figure 3.25 Cézanne Visualization- Histogram of homogeneous regions with warmth indices and warmth contrast strengths for adjacencies listed in parentheses.	56
Figure 4.1 Paintings and their corresponding color palettes shown in incremental 120° rotations about the z axis. Column a) ‘Reclining Odalisque’ by Ingres; Column b) ‘Un Dimanche a la Grande Jatte’ by Seurat; Column c) ‘May Day excursion’ by Limbourg; Column d) ‘Houses of Parliament in fog’ by Monet	61
(a) Ingres	61
(b) Seurat	61
(c) Limbourg	61
(d) Monet	61
Figure 4.2 Paintings and their corresponding color palettes shown in incremental 120° rotations about the z axis. Column a) ‘Le Piano’ by Matisse; Column b) ‘Newborn Babe’ by de la Tour; Column c) ‘Apples and Oranges’ by Cézanne; Column d) ‘The Synagogue’ by Witz	62
Figure 4.3 Summary of normalized co-occurrences for ‘May-Day Excursion’	63
Figure 4.4 Summary of normalized co-occurrence for ‘Revelations de Saint Jean’	64
Figure 4.5 Summary of normalized co-occurrence for ‘Composition in Red II’	65
Figure 4.6 Fra Angelico-Tangere	66
Figure 4.7 Fra Angelico Visualization- Histogram of homogeneous regions .	67
Figure 4.8 Botticelli- The Madonna	68
Figure 4.9 Botticelli Visualization- Histogram of homogeneous regions . . .	69
Figure 4.10 Kandinsky-Church of St. Ursula	70
Figure 4.11 Kandinsky Visualization- Histogram of homogeneous regions .	71
Figure 4.12 Macke- Market in Algiers	72
Figure 4.13 Macke Visualization- Histogram of homogeneous regions	76
Figure 4.14 Franz Marc - Blue Horse	77
Figure 4.15 Franz Marc Visualization- Histogram of homogeneous regions .	78
Figure 4.16 Miro- The garden	79
Figure 4.17 Miro Visualization- Histogram of homogeneous regions	80
Figure 4.18 Summary of normalized co-occurrences for ‘Angel choir’	81

Figure 4.19 Summary of normalized co-occurrences for ‘Houses of Parliament’	82
Figure 4.20 Summary of normalized co-occurrences for ‘Le moulin de la galette’	83
Figure 4.21 Summary of normalized co-occurrences for ‘The Synagogue’ . .	84
Figure 4.22 Bonnard - Earthly Paradise	87
Figure 4.23 Bonnard Visualization- Histogram of homogeneous regions with warmth indices and warmth contrast strengths for adjacencies listed in parentheses.	88
Figure 4.24 Monet - Water Lillies	89
Figure 4.25 Monet Visualization- Paintings	92
Figure 4.26 Monet Visualization- Histogram of homogeneous regions with warmth indices and warmth contrast strengths for adjacencies listed in parentheses.	93
Figure 4.27 Pissaro - Entree du Village	94
Figure 4.28 Pissaro Visualization- Histogram of homogeneous regions with warmth indices and warmth contrast strengths for adjacencies listed in parentheses.	95
Figure 4.29 Renoir - The two sisters	96
Figure 4.30 Renoir Visualization - 3D histogram of homogeneous regions with warmth indices and warmth contrast strengths for adjacencies listed in parentheses.	97
Figure 4.31 Robustness Visualization for <i>contrast of hue</i> - 3D histogram of homogeneous regions	98
Figure 4.32 Robustness Visualization for <i>cold-warm contrast</i> - 3D histogram of homogeneous regions and adjacencies.	99
Figure 5.1 The values of hues. This diagram sows the relative values of hues at full intensity. The horizontal broken line corresponds to middle-value gray[16, p. 39]	104
Figure 5.2 3D Histograms of <i>contrast of hue</i> and <i>cold-warm contrast</i> in group 1 pie charts	106
Figure 5.3 3D Histograms of <i>contrast of hue</i> and <i>cold-warm contrast</i> in group 2 pie charts	107
Figure 5.4 3D Histograms of <i>contrast of hue</i> and <i>cold-warm contrast</i> in group 3 pie charts	108

Figure 5.5 3D Histograms of <i>contrast of hue</i> and <i>cold-warm contrast</i> in group 4 pie charts	109
Figure 5.6 3D Histograms of <i>contrast of hue</i> and <i>cold-warm contrast</i> in group 5 pie charts	110
Figure 5.7 3D Histograms of <i>contrast of hue</i> and <i>cold-warm contrast</i> in group 6 pie charts	111

ACKNOWLEDGEMENTS

I would like to acknowledge the following persons for being part of this journey with me:

Dr. Alexandra Branzan Albu, for providing me with the opportunity to do this degree, endless guidance, support and encouragement. Above and beyond all, thank you for being a wonderful person.

Dr. George Tzanetakis, for kindly accepting to be in my supervisory committee, reading my thesis, and providing me valuable feedback that helped bring this thesis to completion.

David Agahchen, my husband and friend for supporting me through all the highs, lows, frustrations, celebrating the small victories and turning mountains into mole hills. Thank you.

Sahara Agahchen, my daughter for being incredibly patient as she anxiously waited to celebrate the end of this thesis, and spend more time with her mom.

My labmates: Marzieh Mehrnejad, Aleya Gebali, Trevor Beugeling, Frederic Jean, Jeremy Svendsen, Kawthar Moria for the camaraderie, support and fun. Thank you for making this a memorable experience.

DEDICATION

I would like to dedicate this thesis to the following family members, as a token of my appreciation for their involvement and support in my educational and life journey:

Enayat Zarif Agah Tashkand

Shoghieh Marandize

Touraj Agah

Parvine Dokht Ziaee

Elham Hughes

Shane Hughes

Soozan MacDonald

Saeed Agah

Bill Warthe

Susan Duffell Warthe

Hendrik Jonker

Regina Jonker

Marco Jonker

Lee Chen

Yulenda Evans

David Agahchen

Sahara Agahchen

Sabella Agahchen

Chapter 1

Introduction

1.1 Motivation

In recent years, with the advances of social media and the high volume of photographs in personal and online libraries, the study of aesthetics for the classification of images has received increased attention from Computer Science, notably from areas such as Computer Vision, Computer Graphics and Visual Analytics. This is motivated in part by the overwhelming amount of visual data that we generate, share via downloading and uploading on social networks, and store on our personal computing devices. Tools are needed to make sense of such data, and to triage the meaningful, memorable, and beautiful from the irrelevant, forgettable, and ordinary.

The classification of large numbers of images is not the only motivation for the study of visual aesthetics from a computational perspective. Studying aesthetics from a computational perspective may reveal some hidden aspects of this rather elusive principle. The Oxford Advanced Learner's Dictionary defines 'aesthetic' as (1) 'concerned with beauty and art and the understanding of beautiful things' and (2) 'made in an artistic way and beautiful to look at'. Both definitions are vague and don't lead directly to explicit, quantifiable descriptions of aesthetic attributes.

Color is a common and powerful feature used in the assessment of aesthetic quality in images. However, knowledge of color-based aesthetic theories is limited among Computer Vision researchers, resulting in an analysis of color composition that does not necessarily differentiate well between images deemed as having high aesthetic quality and low aesthetic quality. We aim to bring to Computer Vision some understanding and computational modelling of color-based aesthetic theories, and expect

that the proposed models will improve the aesthetic classification of images.

‘*Color harmony*’ is a common topic of discussion in color aesthetics. Color harmony is a common feature that Computer Vision researchers assess to discriminate between high aesthetic quality and low aesthetic quality in images. Color harmony is typically defined as the effect afforded by a pleasing color combination. This pleasing effect has been the subject of debates for hundreds of years [61]. The state-of-the-art color harmony models employed in the aesthetic classification of images in Computer Vision are Moon & Spencer’s [41] and Matsuda’s [43]. Both models are based on limited empirical evidence gained from user studies, and do not offer a conceptual link between their model and any color theories. The following excerpt from Westland et al. [61] on the topic of color aesthetics shows the current disconnect between the ways scientists and artists treat color aesthetics and color harmony: ‘... *the recent scientific approaches seem to be increasingly disconnected from the context of art and design. Thus the preferences that are empirically determined in the laboratory may bear no resemblance to the preferences and choices made by art and design practitioners in the context of an expressive idea or in response to a design brief. The last hundred years have seen a divergence in view between artists and scientists on the topic of color aesthetics, and we suggest that this trend needs to be reversed if significant progress is to be made in terms of understanding colour harmony.*’ We therefore turn our attention to color theory to understand color aesthetics.

Our study is a guided attempt at ‘understanding beautiful things’ from the perspective of color-based aesthetic theories. Two sets of color theories are widely adopted: theories surrounding the traditional color wheel composed of three primary colors (red, yellow and blue) as described by Johannes Itten (1888-1967), and theories surrounding the modern color wheel composed of five primary colors (red, yellow, blue, green and purple) as described by Albert Munsell (1858-1918). Munsell focussed on the accuracy of color representation, and his works strongly influenced the creation of the CIE $L^*a^*b^*$ color space. Leading color theorist Birren(1900-1988) who was the editor of many books on the topic of color perception, wrote the foreword for Itten’s second book [22], and describes him as follows: “he [Itten] has a keen perception of the genius of the old masters and writes with rare enlightenment on their color expression”. Further Birren wrote: “Johannes Itten was considered one of the greatest teachers of the art of color of modern times ... His insistence on spontaneity and personal expression with color - supported by adequate knowledge, discipline and training - became renowned”[23]. As such, our proposed approach is

grounded in Itten’s formulation of color theory, which is detailed in his two books: ‘The art of color’ [22] and ‘The elements of color’ [23]. As one of the most influential theorists of color aesthetics in modern times, Itten taught at the Bauhaus School of Art, and formulated his color theories on the basis of perception. In his comprehensive framework, he specified seven color *contrasts*, a color harmony model, and discussed color *modulation*. According to Birren, the seven color contrasts are ”one of chief features of Itten’s contribution to the art of color”. In his first book [22], Itten provided examples of paintings that use the *contrasts* [22], and we use these examples as our ground truth.

We focus on three specific aspects of color usage in visual art, namely color *modulation*, *contrast of hue* and *cold-warm contrast*. *Modulation* is a concept Itten described as subtle variations in tones and chroma. Using his description, we have developed a computational model to measure and visualize *modulation*. From the list of seven contrasts, we selected *contrast of hue* and *cold-warm contrast* as a starting point for developing computational models that assess the contrasts in images. Further, Itten refers to specific artists for their stylistic use of the two contrasts, thus we developed computational models to explore the patterns of use of these contrasts in their paintings.

One of Itten’s contributions to art and design was ‘the idea that art could be functional’ [14]. One such functional use is the application of design principles to business documents. Business documents are communication tools for organizations, that are used for both internal and external purposes. These purposes vary: reporting, communicating new directions, providing instructions for new procedures, marketing strategies, advertising campaigns. Examples of business documents include financial reports, presentations, posters, letters, and magazines. Organizations place a significant amount of information in documents. Most of them focus on the completeness of the content at the expense of design considerations, leaving the reader to extract the pertinent messages from the document. Document designers work on creating document layouts that allow the reader to better understand the content of the document. Document design topics include typesetting, layout, color and messaging. We take first steps towards improving the aesthetics and readability of business documents by applying principles from color-based aesthetic theories. As such, we investigate the use of our computational models for analyzing color contrasts in business documents.

1.2 Overview of thesis

This thesis is structured as follows:

Chapter 2 presents an overview of visual features used in the aesthetic classification of images in Computer Vision. We investigate color-related features deeper than other features. We also link low-level features that are directly gleaned from pixel information to high-level concepts that are intended to better match human perception of aesthetics in images. This is presented in Chapter 2.

Chapter 3 presents our computational models for (1) *modulation*, (2) *contrast of hue*, (3) *cold-warm contrast*, (4) assessing patterns of *contrast of hue* in an artist's style, and (5) assessing patterns of *cold-warm contrast* in an artist's style. We include a detailed explanation of our methods and provide examples to illustrate the results.

Chapter 4 presents the databases on which we tested our computational models, our results and a detailed analysis of our computational models. The first database contains digital copies of paintings Itten discussed as examples illustrating the use of the contrasts. For the images from this database, we provide our results and a detailed analysis of our computational models for the two contrasts on selected images. The second database contains images from artists that Itten mentioned for the use of *contrast of hue* and the third database contains images from artists that Itten mentioned for the use of *cold-warm contrast*. We provide our results and a detailed analysis of our computational models for the exploration of the patterns of the contrasts in the works of these artists.

Chapter 5 presents an explanation of the importance of design principles and color in business documents. We further discuss the implementation details of our computational models which we use to analyze the *contrast of hue* and *cold-warm contrast* in business documents, our results and observations.

Chapter 6 presents a summary of the contributions of the thesis. We conclude by listing possible future projects that could extend our work.

Chapter 2

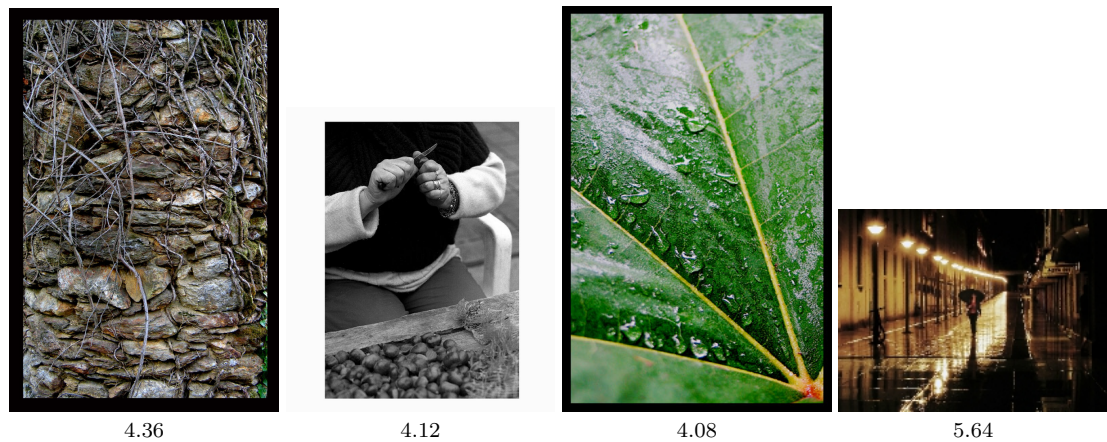
Related Work

The recent advances of social media and the high volume of photographs in personal and online libraries have motivated the study of aesthetics for the classification of images. The computer vision community has developed models to assess aesthetic image quality by discriminating between high quality and low quality images using features related to the whole image (global) and features related to regions of the image (local). Figure 2.1 shows representative images from Photo.net, an online peer-rated site for photographers.

Aesthetic judgement is highly qualitative, and is manifested as the viewer's subjective preference or emotional response towards an image [11][28][62]. Aesthetic judgement is also influenced by cultural and generational constructs. According to Marchesotti et al. [36], aesthetics and preference can be predicted using data-driven approaches such as mimicking the best practices of professional photographers. One of the photographic practices is to frame the image such that certain regions are intentionally noticed. When a region from an image 'pops out' and grabs the attention of the viewer, the region is salient. Saliency is caused by the 'effective contrast' between the region of interest and the rest of the image. Saliency is directly linked to bottom-up processes of visual attention [5], as the information at a salient location can be processed with less attention from the viewer [59]. The spotlight is a common metaphor for saliency: when a region is lit up with a spotlight, the spotlight effect allows 'for increased sensitivity and a more precise encoding of information from this spatial location' for the viewer [59]. Visual saliency influences human aesthetic judgement by causing the viewer to notice more detail from the salient regions at the expense of other regions. With this knowledge, the computer vision community has developed methods that bridge the gap between high level concepts and low level



(a) Photographs with average score 6.0 and above



(b) Photographs with average score below 6.0

Figure 2.1: Representative photographs from Photo.net [3] rated by online users. Photos are scored from 1 to 7, however most photographs were scored 5 or higher.

features.

The focus of our research in aesthetics is on the study of color *modulation* and contrasts in visual art. In the remainder of this chapter we will briefly describe visual features in aesthetics (section 2.1). Our discussion of visual features includes low level features (section 2.1.1), a discussion of color harmony models and connecting low level features to high level concepts in Computer Vision systems of aesthetic classification (section 2.1.2). We will also discuss the databases of images designed to test the performance of the features (section 2.2). Lastly, we will introduce our approach to the study of color *modulation* and *contrasts* (section 2.3).

2.1 Visual features in aesthetic classification

Low-level features such as spatial composition, texture, blur, depth of field and color are extracted directly from pixel information. Features for high level concepts are derived from a combination of low-level features, and are intended to better match human perception. The relationship between high level concepts and low-level features is depicted in Figure 2.2.

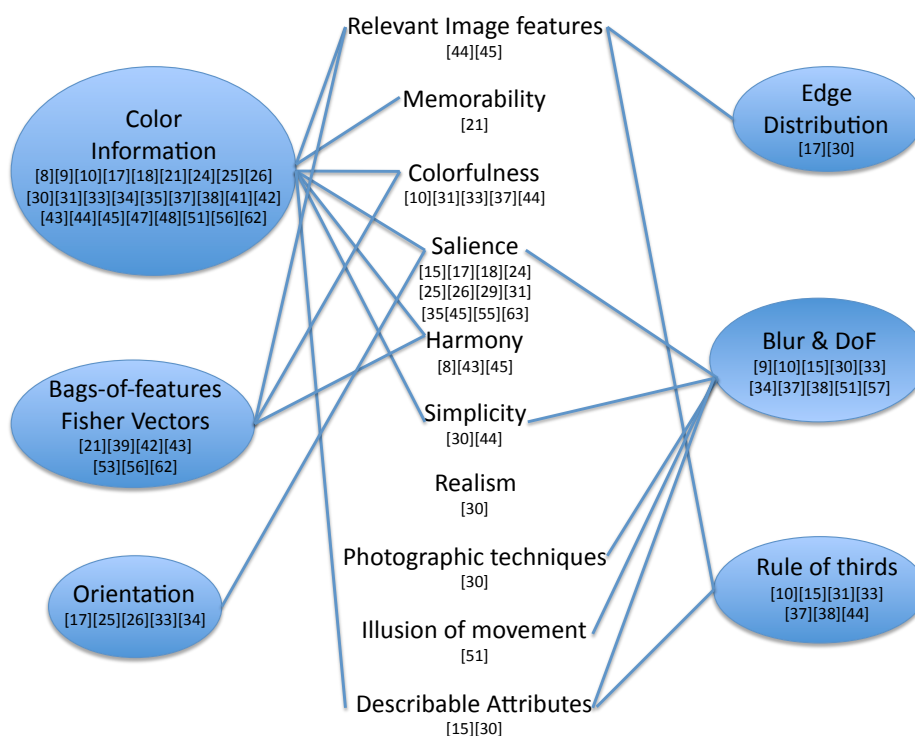


Figure 2.2: Relationship between high-level concepts and low-level features. High level concepts are listed in the center column. Edges connect high level concepts to low level features.

2.1.1 Low-level features

In 2006, Datta et al. [10] and Ke et al. [30] created some of the earliest systems for the aesthetic classification of photographs based on subjective preference. Datta et

al.’s low level features include color, blur, ‘rule of thirds’ and ‘depth of field’ (DoF). Ke et al.[30] proposed features that describe high level concepts and best practices from photography such as ‘*simplicity*’, [the lack of] ‘*realism*’ typically expressed by unusual poses, and ‘*basic photographic techniques*’; these high level features are linked to color information, blur, and depth of field. We will now discuss the advances in the field since Datta et al. [10] and Ke et al. [30].

Spatial composition

Spatial composition refers to the location and shape of certain regions in the image, as well as the spatial distribution of specific features. Spatial composition plays an important role in image aesthetics [50][44][31].

High quality photographs are assumed to have uniformly distributed edges, while low quality photographs have cluttered backgrounds. The edge distribution of an image is detected through image gradients that identify the strength of edges, followed by filtering high intensity edges and measuring their compactness. An ideally simple image is one whose high frequency edge distribution is compact and situated near the center of the image [30] .

The aspect ratio of an image is also a feature of interest. The aspect ratio refers to the ratio of the width and height. It is assumed that objects (or regions) whose aspect ratio is approximately equal to the golden ratio(1.618) are aesthetically pleasing [10]. The ‘rule of thirds’ is a simplification of the golden ratio, and is a guideline in photography that can be applied to the aesthetic classification of images [44]. If an image were divided into 3 equal vertical parts and 3 equal horizontal parts, the top-left and top-right intersections of the vertical and horizontal lines are power points (depicted in Figure 2.3). Power points are deemed to be locations where human attention is naturally directed [16]. An image that follows the ‘rule of thirds’ principle contains a region of interest near a power point. Li et al. [33] propose that the region enclosed by the two central vertical and horizontal lines is the ‘focus region’ of the image. Measures for spatial composition include center of mass, variance and skewness, average hue [15], average saturation [15] and average light [33][15].

Blur and DoF

Blur is typically an indicator of a low quality image [57]. An image with a blurred background and a focussed foreground however, is a photographic technique used in

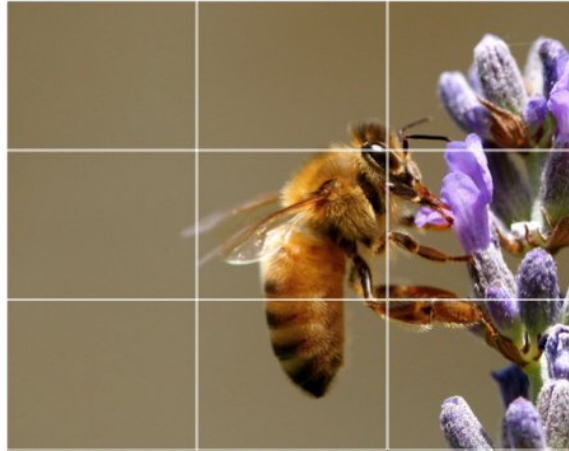


Figure 2.3: Rule of thirds- the eye of the bee is located at the top-right power point [4]

macro images featuring a contrast between ‘sharpness and unsharpness’ [51][30][33][38], as depicted in Figure 2.4. The contrast is measured by the ‘depth of field’(DoF) [10]. The lower the DoF, the higher the quality of the image. According to Peters et al. [51], blur is also an indicator of movement when the image is ‘unsharp in one direction’ and ‘the stronger the blur, the stronger the impression of speed’.



Figure 2.4: Blur and Depth of Field- a blurred background creates a low depth of field, thus creating a focus on the sharp robin [3]

Color

Color is a visual feature that focusses the attention of the viewer regardless of the position of the colored object [7]. “*The color of photos have a significant influence on their perceived quality*” [43], as depicted in Figure 2.5. Color is extracted in the early processing of visual stimuli [32], and is therefore seen before content [22]. Color also evokes emotional responses in viewers [22][23]. Ke et al. [30] learn the difference between the color palettes of professional images and snapshots through classification.



Figure 2.5: Photograph in color [3] and converted to grayscale, illustrating the impact of color on our attention.

Color information in digital images is in the RGB color space by default, thus each pixel contains three values that represent the amount of red, green and blue respectively. The intensity of light in pixels is easily interpreted from RGB values, however the range of color information humans perceive cannot be easily extracted from RGB. RGB images however can be converted to a perceptually relevant color space such as HSL (Hue, Saturation and Light), HSV (Hue, Saturation and Value), CIE Lab or CIE Luv. Ou et al. [48][47] propose a 3 dimensional color emotion space. The three ‘emotion’ channels are *color activity*, *color weight* and *color heat*.

Bags-of-features

Bags-of-features are representations that measure the statistics of a combination of low level features on small patches of the image. Statistics are aggregated on the bags-of-features for the whole image. These intermediate level representations are

needed to bridge low level features and high level concepts [36][62][21]. Solli [56] proposed a color-based-bags-of-emotion feature based on the emotion color space [48], where bags-of-emotions are used to retrieve images with similar ‘emotional’ content. Yanulevska et al. [62] propose clustering bags-of-visual words such that the center of the k-cluster is a visual word correlated with users’ ratings of positive or negative emotions.

Fisher vectors [39][53] are a generalization of bags-of-visual words, that also encodes local statistics. While bags-of-visual-words do not contain spatial information, the Fisher vector is computed on hierarchically divided regions, where local patches are extracted. The Fisher Vector looks at the distribution (2nd order statistics) of the local descriptors assigned to each visual word, thus resulting in a probabilistic visual vocabulary. The Fisher Vector describes patches as a continuous distribution.

2.1.2 High level concepts

Colorfulness

Colorfulness is measured by the contrast of color features between regions of interest, or between regions of interest and the full image. Features include luminance [10][31], clarity [37], chrominance [31], brightness [38][33], hue [33][30], saturation [33][9]. Luo et al. [37] propose a dark channel feature to capture the clarity and colorfulness of an area. A pixel is considered clear if it is not blurry. The dark channel feature is a combined measurement of clarity, saturation and hue composition. Luo et al. [37] found that their dark channel feature outperforms ‘clarity contrast’, blur, and other color related features in the aesthetic classification of images.

Color harmony

“Color harmony is a key factor in the various aspects that determine the perceived quality of a photo” [43]. The term ‘color harmony’ is often used to describe pleasing color combinations [61][50][47], however color harmony theories differ. Burchett [6] explains that *“the predominant understanding of color harmony ...[is frequently attributed]... to order, referring to uniformly spaced points in a color classification system.”* Moon & Spencer [41] introduced a quantitative model for color harmony, based on the relative distance between colors. Given a color in the hue layer, areas of ‘identity’, ‘similarity’, ‘contrast’, and ‘ambiguity’ are determined in the color wheel as

depicted in Figure 2.6. Any non-ambiguous combinations are harmonious. Although psychological experiments do not support the Moon & Spencer model, the computer vision and industrial design communities continue to use this model [20][61].

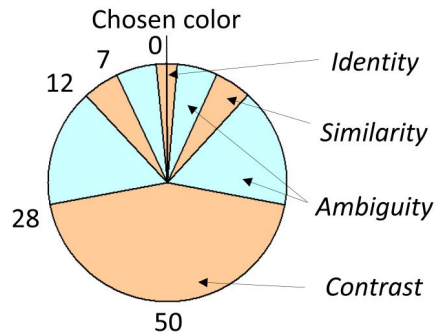


Figure 2.6: Moon & Spencer model of color harmony, depicting areas of ‘identity’, ‘similarity’, ‘contrast’ and ‘ambiguity’ in the hue layer [43]. If all the colors in the image fall in the non-ambiguous areas, the color combination is harmonious.

Matsuda developed harmonious templates for fabric design in the hue layer as well (depicted in Figure 2.7). He developed the templates based on the results of a user study. Similar to Moon & Spencer, Matsuda’s templates are based on the relative distance between two colors [43]. This model is also used in industrial design [58] and Computer Vision.

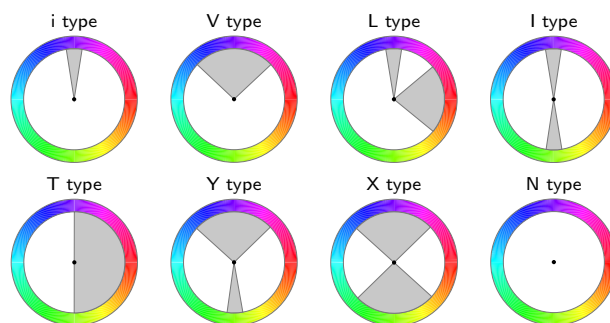


Figure 2.7: Matsuda’s Harmonic Templates [8] are based on the relative distance between two colors. If all the colors in an image fall within the gray slice(s), the color combination is harmonious.

Ou et al. [46] propose that color harmony is additive, thus images containing more harmonious features are preferred to images with fewer harmonious features. Nishiyama et al. [43] propose ‘bags-of-color-patterns’ by identifying the dominant color in the patch and applying the Moon & Spencer [41] measure of aesthetics. Thus, the color harmony score of a photograph is the sum of the color harmony of the patches.

Cohen-Or et al. [8] developed an algorithm to recolor an image to be more aesthetically pleasing by mapping all of the hues in an image to fit the regions in the eight harmonic templates depicted in Figure 2.7. This is done by identifying the dominant hue, then shifting all other hues to fit the closest hue region in the best fitting harmonic template.

Saliency

“Saliency is the distinct subjective perceptual quality which makes some items in the world stand out from their neighbors and immediately grab our attention” [24]. Humans perceive saliency because the region is distinguishable from the background [55][45][31][35]. Saliency makes the image memorable [21][52].

Itti et al. [24] proposed a computational framework where a topographical feature map is created for each of three features: color, intensity, orientation (to give the impression of motion). Each pixel’s saliency in the final map is determined by the maximum value afforded by color, orientation and intensity [25]. Color is an important feature in identifying salient regions in an image [29]. Color is assessed based on ‘double opponency’, a brain mechanism involved in processing color, where a color has a blue-yellow (BY) component and a red-green (RG) component [26]. Since warm colors attract attention [49], Gupta et al. [18] give the RG channel in double opponency a higher weight.

Zhao [63] learns a saliency map that associates weights with features that seem most promising for detecting saliency, by identifying where subjects (primates) will fixate their gaze on an image. They found that faces attract attention fastest, followed by orientation, then color and intensity.

Gopalakrishnan [17] measure the saliency among colors, by quantifying the ‘compactness’ and ‘isolation’ of various competing colors and probabilistically evaluate the saliency among them in the image. *Rarity* is measured by the distinctiveness of a color with respect to other colors in the space, and the rarity of the complexity of

orientations in the image space. *Compactness* is measured by the spatial confinement of the orientations.

Simplicity

Simplicity is a high-level ‘describable attribute’ of images. Simplicity is detected using the distribution of edges and assessing their compactness, the position of the region in the image, hue count, contrast of light between the object and the background [30].

Relevant Image Appeal features

A *relevant image appeal region* are features in an image that are relevant to easthetic appeal. According to Obrador et al. [44], a ‘relevant region’ is the region of a color-segmented object whose relevance value is above a certain theshhold. ‘Relevance’ is based on the principle of simplicity. An appeal map is constructed using colorfulness, relevance and visual balance. The measure of relevance of an object depends on the size of the object and its relative brightness. Further, the largest ‘non-relevant’ region is an ‘accent region’. Visual balance of the dominant regions is measured by computing the centroids and radii of relevant regions. Sharpness is also a contrasting region feature for image appeal [45]. The average distance between the centroids of the relevant regions, and the standard deviation of the distance are most predictive of aesthetic quality [44].

High-level describable attributes

High-level describable attributes are image cues that may be part of human-generated descriptions of high quality images [15]. Three groupings of ‘describable attributes’ are predictors of perceived aesthetic quality: ‘compositional attributes’, ‘content attributes’, and ‘sky-illumination attributes’. *Compositional Attributes* are characteristics related to how closely the image follows the rule of thirds. *Content attributes* are characteristics related to the presence of specific objects or categories of objects including faces, animals and scene types. *Sky-illumination attributes* are characteristics of the natural illumination present in a photograph.

Compositional attributes are detected using the ‘rule of thirds’, low depth-of-field and saliency [15]. ‘Rule of thirds’ measurements include the average hue, saturation and value of the region within the middle third of the image [10][45].

2.2 Databases

The performance of feature sets is tested on databases of images. The databases needed to assess the feature sets are built on the assumption of subjective preference. Images need to be annotated with descriptive labels to extract meaningful relationships between the feature set and the results. The challenge with annotating images for aesthetic judgement is the subjective nature of the aesthetic experience. Computer Vision researchers interested in assessing the perceptual quality of photographs have the opportunity of learning and testing features on images that are rated by online users. The inherent challenge of using social media ratings is the bias introduced when a person’s ratings are affected by their friends ratings, or the photographs are of a popular person or took place at a popular event or location [28].

Common databases are Photo.net [3][39][10][44], DPChallenge [1][30][43] [15][45], Flickr [2]. Photo.net [3] is a gallery of categorized photographs uploaded by photographers, and critiqued and rated by its members. Scores range from 1 to 7. In Figure 2.1, we showed sample images from Photo.net and the scores given by their members. Similarly, DPChallenge [1] is also a digital photography contest site where images are rated from 1 to 10. Flickr [2] is an online photo sharing application where users comment and rate the images based on ‘interestingness’ with scores ranging from 1 to 5. Dhar et al. [15] tested their feature sets on Flickr to capture interestingness, and on Photo.net [3] to assess aesthetic quality. Datta et al. [11] propose that Photo.net is the appropriate database for assessing aesthetics, and photographic skill while DPChallenge [1] is the appropriate database for assessing overall aesthetic quality of images categorized by topics and rated by the public. CUHK [10][39] is a database derived from DPChallenge. Some databases such as the Van Gogh Museum and the Kroller-Muller Museum [34][27] and ACQUINE [10] are not available to all researchers. Some researchers create a private database of their own images [33][37] and others combine their personal photographs and Flickr [31][38].

A recent advance in Computer Vision AVA [42], a database derived from DPChallenge, addresses the need for collection, annotation and distribution of ground truth data to help advance the research. AVA is a collection of images and meta-data derived from DPChallenge, with 255000 images from 1447 photographic challenges collapsed into 14 categories. Images selected contain aesthetic annotations which are scores given by amateur and professional photographers. 66 textual tags provide semantic annotations and manually selected challenges correspond to photographic

styles about light, color and composition. Murray et al. [42] found that aesthetic score distribution in AVA is largely gaussian, standard deviation is a function of mean score, and images with high variance are often non-conventional.

Marchesotti et al. [36] created a bag-of-words vector for each image based on textual annotations associated with images in the AVA dataset. For topics that were too vague to connect to attributes, they used unsupervised attribute discovery to attempt to correlate the vague topics to relevant attributes. Using attractiveness scores and supervised attribute discovery, they learn regression parameters, select discriminative textual features and attribute discriminability through clustering bigrams. They found that the unsupervised attribute discovery, followed by the supervised attribute discovery performed comparatively well to the generic image features of Fisher Vectors and Bags-of-Words from their previous work [39].

2.3 Discussion

The current Computer Vision techniques for extracting color information that match human perception are based on empirical results from various user studies, and the methods are not grounded in color-based aesthetic theories. Our research is grounded in Itten’s comprehensive color theories, as opposed to aesthetic rankings collected from on-line photography communities. Itten offers a comprehensive model composed of seven color contrasts, and techniques for achieving color harmony. His theories are based on perception. According to Itten, “The eye and the mind achieve distinct perception through comparison and contrast.” [23]

Itten’s significant contribution is his description of contrast where ‘visual perception is the result of seven specific methods of color contrast’: value (light), saturation, hue, extension, warm/cool, complements and simultaneous contrast. This idea of ‘simultaneous contrast encompasses contrasts of hue, brightness, and colorfulness and its ubiquitous phenomenon in color vision’ [61]. Itten’s color theories represent an unexplored data source for deriving computational descriptors for aesthetic analysis.

The aesthetics of photographs do not generalize well to paintings. Davey [12] explains that in a painting, ‘the subject matter is mediated through a sensibility. We see how something was perceived, not what was perceived.’ The chromatic distribution of a painting represents one of the main expressive tools for the artist painter. This is not valid for photographs, which are not ‘an interpretation of reality but a presentation of how something looked’ [12]. For instance, the ‘simplicity’ measure

proposed by Ke et al. [30] does not represent a valid measure of aesthetics in digital images of paintings, since there are numerous masterpieces with intricate, complex color schemes.

As a starting point, we created a visualization of a painting's color palette in the HSL color space. We also developed the following computational models:

- a computational model for the study of *modulation* within the color palette, our measure for *modulation* encompasses hue-specific non-spatial color relationships in a painting
- a computational model to measure the *contrast of hue* in paintings, this measure is spatially relevant
- a computational model to measure *cold-warm contrast* in a painting, this measure complements the measures of *modulation* and can be interpreted as a spatially relevant measure of inter-hue *modulation*
- we extrapolate both measures of *contrast of hue* and *cold-warm contrast* to analyze the styles of selected artists based on Itten's comments

Chapter 3

Proposed Approach

Our proposed approach is grounded in Johannes Itten’s formulation of color theory with a focus on perception, which is detailed in his two books: ‘The art of color’ [22] and ‘The elements of color’ [23]. Itten’s works have been widely cited in academic publications [6][8][50][61][19][9], including the fields of psychology, color science, graphics and aesthetics. Itten was recently cited in a ‘design management’ book as an influential master in the functional movement of art, with ‘the idea that art could be functional’ [14].

Our interest in Itten’s theories lies in developing computational models that measure and assess the use of color in images, as related to understanding the aesthetic experience. We chose Itten’s theories of color contrasts because his theories are translatable into computational models. In his own words, Itten asserts that “*The concept of color harmony should be removed from the realm of subjective attitude into that of objective principle*” [23, p. 19]. In his books, Itten formulates and provides examples for seven types of color contrasts. His use of geometric terminology and geometric shapes in describing the color contrasts have inspired the quantitative measurements and computational models we developed for two of the seven contrasts: *contrast of hue* and *cold-warm contrast*. For those two contrasts, we developed a visualization model to investigate the style of artists Itten refers to for *contrast of hue* and *cold-warm contrast*. Itten also discussed *modulation*, a concept he described as subtle variations in tones and chroma. Using his description, we have developed a computational model to measure and visualize *modulation*.

In this chapter, we first describe the main elements of Itten’s color theory used in our work. Next, we provide a detailed description of our proposed computational models for modulation and contrast.

3.1 A summary of Itten’s Color Theory

Color spaces can be defined as geometric frameworks for visualizing and understanding color relationships. Itten [22] [23] chooses to work with a spherical space because its symmetry ‘*serves to visualize the rule of complementaries, illustrates all fundamental relationships among colors, and between chromatic colors and black and white.*’

Itten’s color sphere (see Figure 3.1), contains six equally spaced parallel circles, parallel to the equatorial plane, which partition the sphere into seven zones. Twelve meridians uniting the two poles are orthogonal to these zones. The two zones between the white and equatorial zone are populated with evenly spaced tints (i.e. mixtures of pure hues with white) of each hue. Similarly, two evenly spaced shades (i.e. mixtures of pure hues with black) of each hue are found in the zones between the equatorial and black zone. Tones (i.e. mixtures of pure hues with grey) are distributed with radial symmetry inside the sphere.

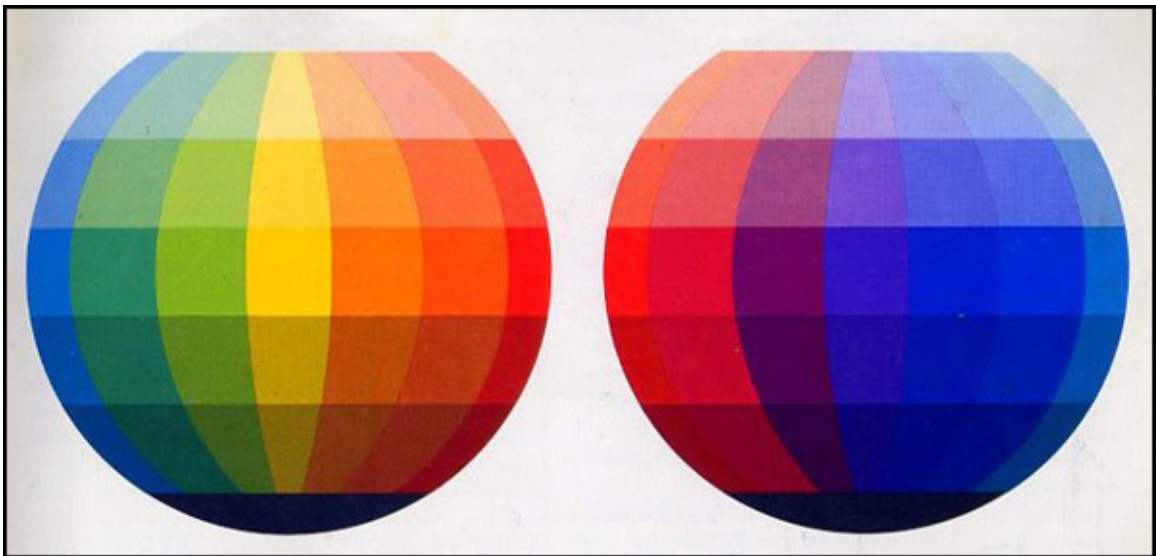


Figure 3.1: The Itten Color Sphere. Views of the surface

The Itten color sphere is not a valid metric space from a mathematical viewpoint, as it is designed for artistic purposes rather than for quantitative measurements. Our approach works with a metric color space that is closest to Itten’s sphere, namely the HSL (Hue-Saturation-Lightness) cylinder. In HSL, hues of maximal saturation are located in the middle of the cylinder (which is consistent with Itten’s colour sphere), whereas in other chromatic spaces, such as HSV, they are located at the

top. The HSL color space is the color space most consistent with Itten’s color sphere, allowing us to develop measures for *modulation* and *color contrasts* according to his theory. Itten’s framework is based on the notion that the color sphere contains every imaginable color, and each color has a unique coordinate position in the color sphere as displayed in Figure 3.1. Each color from Itten’s color sphere maps to a coordinate position composed of hue, saturation and light on the HSL color space. As the HSL color space is cylindrical, very light and very dark colors from Itten’s sphere can map to several coordinate positions at the top and bottom of the HSL color space; those pixels however do not affect our models and implementation as they do not contain chromatic information. The standardized representation of a color in the cylindrical HSL system is (r, θ, z) (Figure 3.2). For a given pixel, Table 3.1 describes the conversion of RGB values to the Cartesian coordinates within the HSL color space. The following paragraph describes each of the three coordinates in the HSL space.

Cartesian Coordinates in HSL Space	
Chroma	$M = \max(R, G, B)$ $m = \min(R, G, B)$ $C = M - m$
Hue	$H' = \begin{cases} \text{undefined}, & \text{if } C = 0 \\ \frac{G-B}{C} \pmod{6} & \text{if } M = R \\ \frac{B-R}{C} + 2 & \text{if } M = G \\ \frac{R-G}{C} + 4 & \text{if } M = B \end{cases}$ $H = H' * 60 \text{ deg}$
Saturation	$S = \begin{cases} 0, & \text{if } C = 0 \\ \frac{C}{1- 2L-1 } & \text{otherwise} \end{cases}$
Light	$L = \frac{M + m}{2}$
Cartesian Coordinates	$x = S * \cos(H)$ $y = S * \sin(H)$ $z = 2 * (L - 0.5)$

Table 3.1: Conversion Table of RGB values to Cartesian coordinates in HSL Space

Hue is what we typically refer to as color in every day language. In effect, hue h is the angular polar coordinate, $h = \theta, 0 \leq \theta \leq 2\pi$. The outer disk of the color sphere

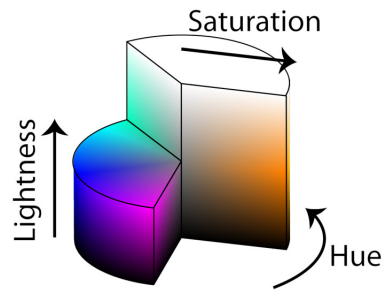


Figure 3.2: The HSL Cylinder

(Figure 3.3) represents the set of hues on Itten's color wheel, which is equivalent to the perimeter of the equatorial plane of the Itten sphere (Figure 3.1) or the equator of the sphere.

Saturation is the strength of the color, and is represented by the radial coordinate of the color inside the cylinder, $s = r, 0 \leq r \leq 1$. Along the equator of both the color sphere and the HSL color space, hues are fully saturated, with a saturation value 1. Along the vertical axis of the color sphere and the HSL color space, saturation is 0.

ranges between

Light values represent the darkness or dullness of a given color, along the vertical axis of the sphere. In the HSL cylindrical coordinate system, $l = z, 0 \leq z \leq 1$. The bottom of the sphere (black) is represented with light value $l = 0$, gradually increasing towards grey at the center of the sphere ($l = 0.5$) then white at the top of the sphere ($l = 1$).



Figure 3.3: The Itten Twelve-Part Color Wheel depicting the relative position of hues

The following examples describe the coordinate position for a few sample colors ($h = \theta, 0 \leq s \leq 1, 0 \leq l \leq 1$) in the HSL coordinate system (Figure 3.2) and the hue specified by the angle θ (Figure 3.3):

1. **Black** at the bottom of the sphere is represented by cylindrical coordinate $(\theta, s, 0)$ where $h = \theta$ and $0 \leq \theta \leq 2\pi$
2. **Neutral (or medium grey)** is represented by $(\theta, 0, 0.5)$, where $0 \leq \theta \leq 2\pi$
3. **White** at the top of the sphere is represented by cylindrical coordinate $(\theta, s, 1)$ where $0 \leq \theta \leq 2\pi$
4. **Fully saturated colors** are represented by $(\theta, 1, 0.5)$ where $0 \leq \theta \leq 2\pi$

3.2 Modulation

Itten defines *modulation* as the subtle, gradual, and local chromatic variation of color. The presence or absence of *modulation* has a direct effect on the perception of contrast, regardless of the type of contrast. Let's consider the *cold-warm contrast* as an example. A highly modulated *cold-warm contrast* involves the presence of cold and warm hues, with numerous, subtle intra-hue chromatic variations. These subtle variations will attract and hold the gaze of the viewer, focussing her attention onto the local details of the painting. According to Turner [60], '*[...] the meaning of modulation is that it embodies the transitional aspect of the experience, the feeling of our attention shifting from here to there.*' In contrast, a low modulated *cold-warm contrast* involves a limited number of hues, with bolder chromatic transitions between usually large homogeneous regions. This leads the viewer to perceive the image as a whole, and pay less attention to local detail.

Modulation is a defining element of an artist's style. For instance, Itten highlights the extensive use of *modulation* by Cézanne: '*To him [Cézanne], modulating a color meant varying it between cold and warm, light and dark, or dull and intense. Such modulation throughout the picture area accomplished new, vivid harmonies.*'[22, p. 15] On the other hand, '*Matisse refrained from modulation, to [...] express simple, luminous areas in subjective equilibrium.*'[22, p. 16].

We pose two questions with respect to *modulation*: (1) can we visualize modulation in the color space? (2) can we provide quantitative measures for modulation using this visualization? First, we propose a new visualization of the chromatic distribution of a given painting in the HSL space, called the 'color palette'. This 3D visualization isolates the chromatic information from spatial or structural information. In other words, we discard any shape-related information in order to focus only

on the color distribution in the color space. Second, we propose that the 3D visualization facilitates the study of color *modulation* and provides means for quantifying the *modulation* for every hue sector of the HSL space. Hue-specific *modulation* is measured via a set of three descriptors using first and second order statistics on the color distribution within the HSL space. Our visualization and measures on *modulation* are performed on a subset of the visual art exhibits discussed by Itten in [22] and [23]. We show that our measures on *modulation* are consistent with Itten’s color principles on *modulation* and *contrast*. Moreover, we claim that the proposed visualization offers valuable insight into the nuances and subtleties of color modulation expressed in a variety of painting styles.

3.3 Computational model for modulation

For a given painting, our proposed visualization maps all its unique color points in the HSL space, thus obtaining the 3D ‘color palette’ of the painting. Our approach works with digital reproductions of paintings that need to be converted from RGB to HSL (as in Table 3.1). Extrinsic Cartesian coordinates are preferred to intrinsic cylindrical ones for the purpose of manipulating (rotating) the proposed visualization about the z axis. It is worth mentioning that our color mapping in the HSL space preserves Itten’s partition of the sphere in twelve hue sectors.

3.3.1 Descriptors for modulation

We propose a set of simple quantitative descriptors for *modulation* that are consistent with Itten’s principles, definitions and descriptive comments. To measure the *modulation* for a given hue sector, we consider the set of unique color points in each hue sector of the HSL space. To focus on the chromatic range of colors, we avoid grey pixels by mapping only pixels with saturation range $s \geq 0.1$; we also avoid very dark and very dull pixels by mapping only pixels with light values falling within the center 75% of the light range, $0.125 \leq l \leq 0.875$.

For each of the 12 hue sectors we first compute the average Euclidian distance p_{dist} of each color point p to its 5 nearest neighbours located in the same hue sector.

$$p_{dist} = \sum_{i=1}^5 \frac{\sqrt{(p_{i_x} - p_x)^2 + (p_{i_y} - p_y)^2 + (p_{i_z} - p_z)^2}}{5} \quad (3.1)$$

Next, we compute the mean μ_{dist} of the distance p_{dist} ,

$$\mu_{dist} = \sum_{i=1}^N \frac{p_{dist}(i)}{N} \quad (3.2)$$

and the standard deviation σ_{dist} of the distance p_{dist} .

$$\sigma_{dist} = \sqrt{\frac{1}{N} \sum_{i=1}^N (p_{dist} - \mu_{dist})^2} \quad (3.3)$$

Modulation is therefore described via the set of three scalar descriptors:

- the average distance μ_{dist} of a color point to its five closest neighbours (see Equation 3.2). This is a measure of the spatial closeness of color points in a given hue sector. Low values for μ_{dist} indicate subtle color transitions and thus high *modulation*, whereas high values indicate more abrupt transitions, thus low *modulation*.
- the standard deviation σ_{dist} of the distance of a color point to its five closest neighbours (see equation 3.3). This is a measure of the variation of the spatial closeness across the hue sector, i.e. of how *modulation* varies inside the considered sector.
- the total number N of distinct color points within the hue sector. This is a global measure of *modulation*, and it is useful to provide context for the interpretation of μ_{dist} and σ_{dist} values. For instance, consider an extreme hypothetical case where a hue sector contains only five very close color points. In this case, μ_{dist} will be low (estimating high *modulation*) and σ_{dist} will be high (estimating uniform *modulation*). However, a low value for N is a stronger estimator for low *modulation*, and overrides the estimations of μ_{dist} .

We illustrate how these descriptors work with two examples of paintings discussed by Itten [22][23] that exhibit low and high *modulation* respectively:

Let us first consider ‘Composition 1928’ by Piet Mondrian[22, p. 44] [23, p. 36], shown in Figure 3.4. Mondrian’s painting style employs *contrast of hue*. He works with a very limited number of fundamental colors: yellow, red, blue, white and black. According to Itten, ‘[Mondrian’s] feeling for clean design leads him to an unadorned, visually strong, geometrical, elemental realism of form and color’[22, p. 44].

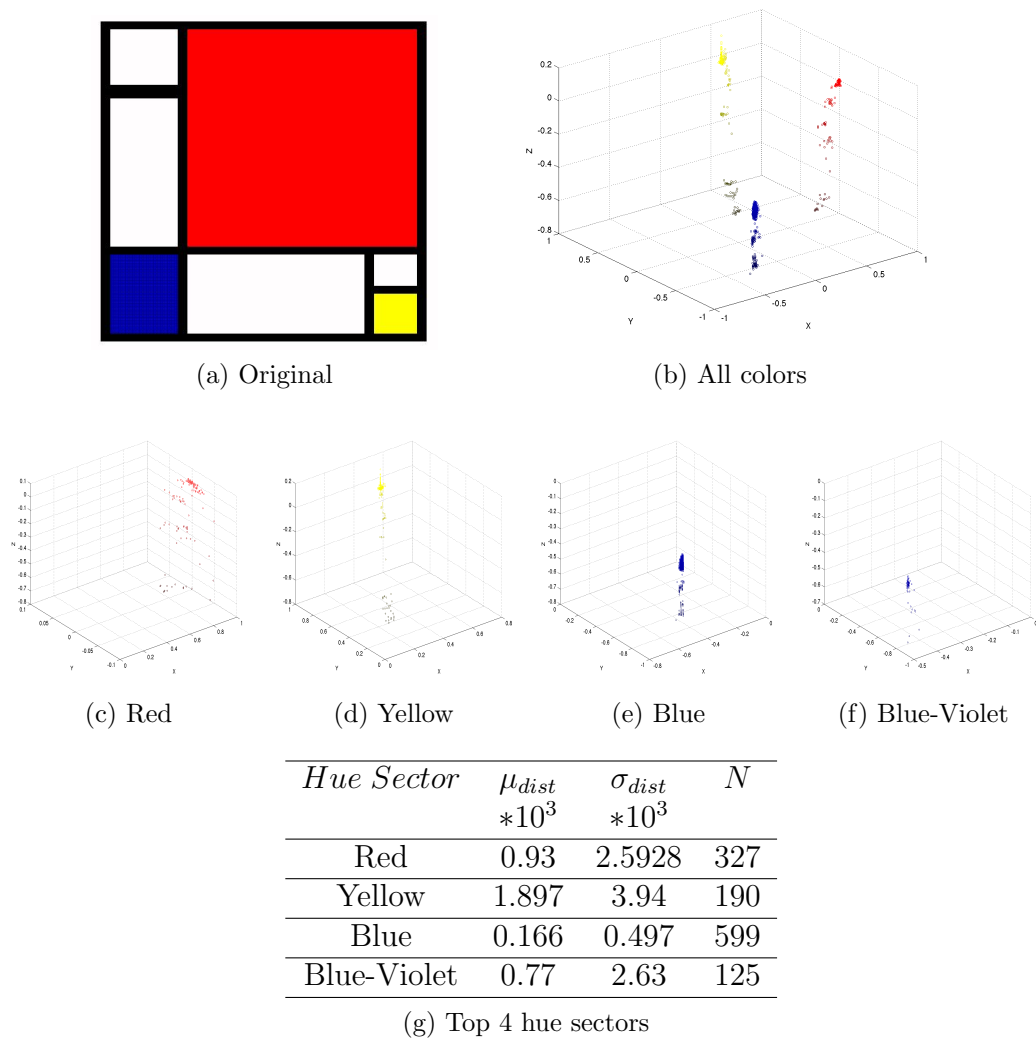


Figure 3.4: ‘Composition 1928’ by Mondrian. Top row: image and its color palette; Second and third row: red hue sector of color palette; red-orange hue sector of color palette; orange hue sector of color palette; blue sector of color palette.

Second, let us discuss ‘Cafe at Evening’ by Van Gogh[22, p. 94] [23, p. 54], shown in Figure 3.5. Van Gogh’s chromatic style features strong colors and *simultaneous contrast* between yellow-orange and blue-violet. Itten discusses Van Gogh’s preference for ‘*using texture as a means of rhythmicizing and intensifying colors*’[22, p. 94]. Textured colors are highly modulated.

As shown in Table 3.4, Mondrian’s minimalist style is reflected in high values for μ_{dist} (which estimate low *modulation*) in all hue sectors, except for blue, which is slightly textured. In contrast, we obtain much lower values for μ_{dist} for all hues in Van Gogh’s case. The number N of distinct color points per hue is also much higher

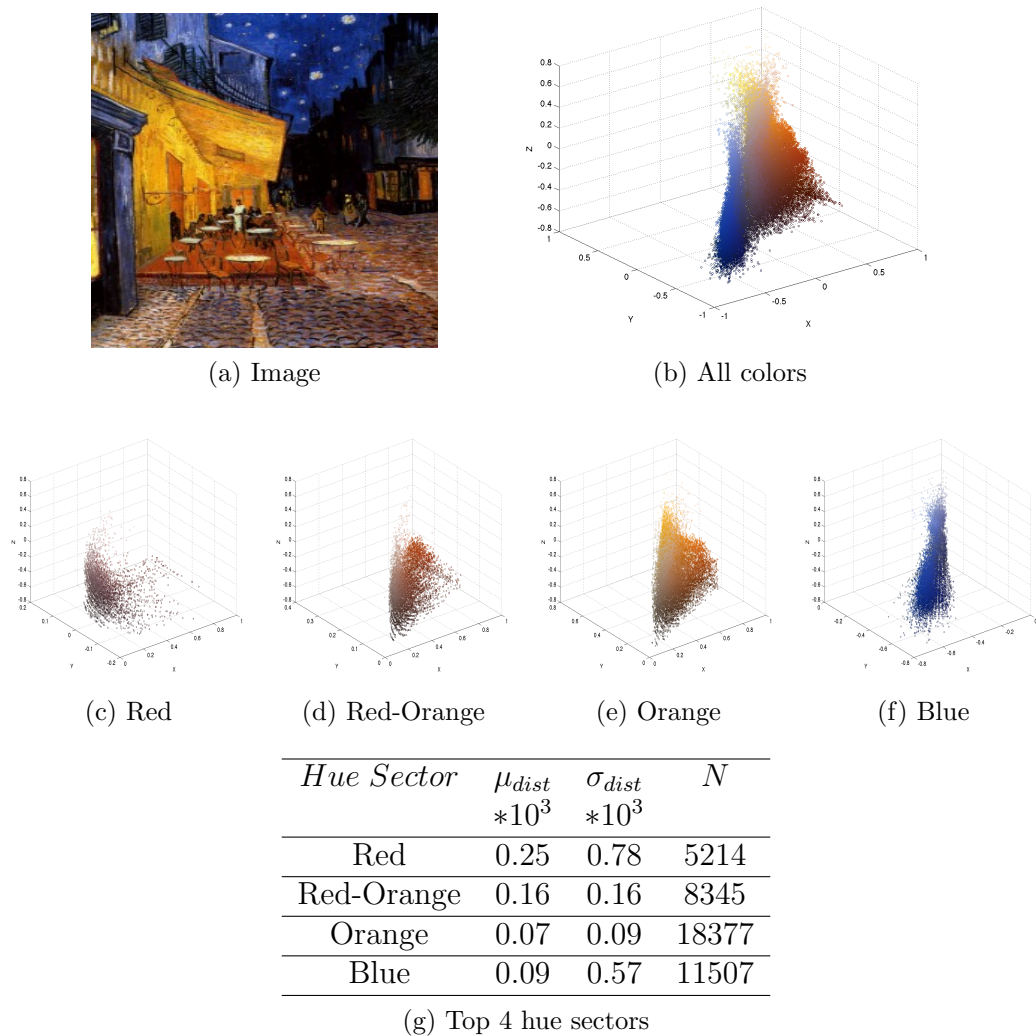


Figure 3.5: ‘Cafe at evening’ by Van Gogh. Top row: image and its color palette; Bottom row: red hue sector of color palette; red-orange hue sector of color palette; orange hue sector of color palette; blue sector of color palette; Last row: mean and standard deviation of color distribution in top 4 most populated hue sectors.

in Van Gogh than in Mondrian.

A visual comparison of the color palettes corresponding to the two paintings in Figures 3.4 and 3.5 reveals the sparseness of Mondrian’s palette in contrast with the compactness and continuity of Van Gogh’s palette. Intuitively, one may associate high *modulation* to a smooth, continuous 3D color palette, and low *modulation* to a sparse 3D palette.

3.4 Contrasts



Figure 3.6: Itten’s Twelve-Part Color Circle, depicting primary, secondary and tertiary colors.

Itten claims that contrast in color is what allows us to distinguish among colors, in the same way that we perceive differences in size, light, etc. In his exploration of color contrasts, he has identified seven categories. *“Each [contrast] is unique in character and artistic value, in visual, expressive, and symbolic effect; and together they constitute the fundamental resource of color design”* [23, p. 32]. We further summarize Itten’s description of the contrasts.

Contrast of hue is the perceptual effect achieved when an image is primarily composed of three fully saturated colors that are positioned on the vertices of an equilateral triangle inside the color sphere. While any three colors positioned on an equilateral triangle are contrasting, the effect of this contrast is strongest when the three colors are primary, and weakest when using tertiary colors. Figure 3.6 shows primary, secondary and tertiary hues. Itten states: *“Just as black-white represents the extreme of light-dark contrast, so yellow/red/blue is the extreme instance of [hue] contrast”*[23, p. 33]. For example, an image composed of yellow, red and blue is perceived as having a stronger contrast than an image composed of orange, green and violet. Further, such color combinations are also harmonious as the center of mass of the three vertices on an equilateral triangle on the equatorial disk of the color sphere coincides with medium-grey at the center of the sphere. In practice, Itten relaxes the requirement of seeing only 3 colors in the composition, but maintains the requirement that the colors making up the contrast are fully saturated.

Light-dark contrast is the perceptual effect achieved when different levels of brightness are used in an image. Light levels affect perception whether the image is achromatic, has a single hue or several hues. Small changes to light levels can change the

impression of an image, by making the colors significantly darker or dull.

Cold-warm contrast is the perceptual effect that some colors appear warm while others appear cool. The warmest color is red-orange and the coldest color is blue-green. Whether other colors in an image appear cold or warm depends on their relative position with respect to these extremes. “*Experiments have demonstrated a difference of five to seven degrees [Fahrenheit] in the subjective feeling of heat or cold between a workroom painted in blue-green and one painted red-orange.*”[23, p. 45] According to Itten, cold colors are also known to recede (appear as background), and warm colors to advance (appear as foreground). [23, p. 46]

Complementary contrast is the perceptual effect created when opposite pairs of color on the color wheel appear together. For each color, its complementary is located diagonally across the color sphere. When a color and its complement are placed next to each other, the combination is vivid. The combination of complimentary colors is considered harmonious because the midpoint of the two vertices where the colors are situated on the color circle coincides with medium grey. “*The rule of complementaries is the basis of harmonious design because its observance establishes a precise equilibrium in the eye*”[23, p. 49].

Simultaneous contrast is the perceptual effect where a viewer sees a color in an image, and that color is actually not present. “*Simultaneous contrast results from the fact that for any given color the eye simultaneously requires the complementary color, and generates it spontaneously if it is not already present*”[23, p. 52]. When simultaneous contrast occurs between a strong chromatic color and a grey, the grey becomes tinged with the color of the complementary. Simultaneous contrast also occurs between two hues that are not complementary, thus creating dynamic activity or disturbed stability. According to Marini and Rizzi[40], well known illusions are caused by simultaneous contrast as defined by Itten.

Contrast of saturation is the perceptual effect created when an intense (pure color) and its diluted form appear in the same image. Examples of this effect appear in faded, dull tones. “*Dull tones, most especially grays, live by virtue of the vivid ones surrounding them*”[23, p. 58]

Contrast of extension is the perceptual effect achieved by manipulating the proportion of colors in an image, based on the inherent luminosity of each color. The concept of *inherent luminosity* comes from Goethe (1749-1832) where each hue is assigned a value that reflects its natural brightness. For example, if pure yellow has the highest brightness value, and pure violet has the lowest brightness value. When

pure yellow and pure violet are placed next to each other, pure yellow will appear brighter than pure violet. To create a harmonious image, the proportion of the colors used should be the reciprocal of the inherent luminosity values.[23, p. 59]

We focus our work with contrasts on creating computational models for the study of *contrast of hue* and *cold-warm contrast* as a starting point.

3.5 Computational models for color contrasts

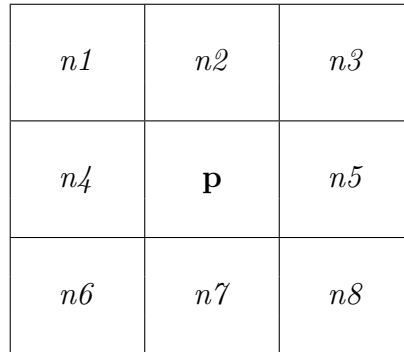
Images characterized by *contrast of hue* contain well defined homogeneous regions of color. Although complex color adjacencies may exist, the homogeneous regions take precedence in the visual field. Images characterized by *cold-warm contrast* display complex inter-hue relationships. Depending on the artist’s style and technique, *cold-warm contrast* is seen between homogeneous regions, as well as locally modulated adjacent regions.

To analyse *contrast of hue* and *cold-warm contrast* in a painting, we consider the relative local position of the colored pixels and confer information about homogeneous regions of color and regions of more complex color adjacencies. Co-occurrence matrices [13] are tools for estimating second-order statistics of the spatial distribution of image intensities as they represent the relationship of intensities among neighbouring pixels. Co-occurrence matrices are typically used in texture analysis. We propose a novel use of co-occurrence matrices in order to identify local patterns of *contrast of hue* and *cold-warm contrast*. We consider the adjacency relationship of the ‘isotropic 8 vertex neighbourhood of a pixel’ as shown in Figure 3.7(a) and build our co-occurrence matrix accordingly.

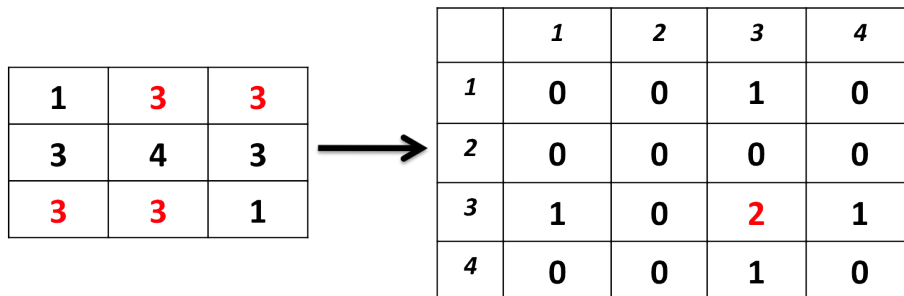
In Figure 3.7 (b), we show how a co-occurrence matrix is typically built with a pixel to the right ‘adjacency’ relationship. For the image on the left, the entries of the co-occurrence matrix correspond to the number of instances of co-occurring adjacencies in the image. For example, cell (3,3) of the co-occurrence matrix contains a 2, corresponding to the two pairs of 3’s in the image. When employing an ‘isotropic 8 pixel neighbourhood’, we consider the adjacencies between the center pixel and the surrounding pixels as shown in Figure 3.7(c). For instance, the value of cell (4,3) is 6 and corresponds to the number of adjacencies between the center pixel 4 and its neighbouring pixels of value 3.

In the next two sections, we will describe *contrast of hue* and *cold-warm contrast* in detail, as well as provide algorithms for our computational models. To focus on

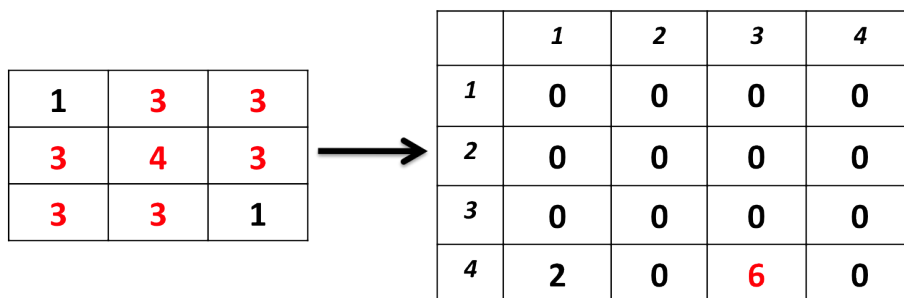
the chromatic color information, we avoid very dark and very dull pixels by requiring the pixels considered to be within the range $20 \leq (R, G, B) \leq 245$. We also avoid grey pixels by requiring the R,G and B values to have a minimum of 10% difference: $(\frac{R}{G}, \frac{R}{B}, \frac{B}{G}) \leq (0.9, 0.9, 0.9)$ or $(\frac{R}{G}, \frac{R}{B}, \frac{B}{G}) \geq (1.1, 1.1, 1.1)$.



(a) 8 vertex isotropic neighbourhood



(b) One pixel to the right adjacency



(c) Isotropic 8 pixel adjacency

Figure 3.7: Illustrating the building of a co-occurrence matrix. Image on the left, co-occurrence matrix to the right.

3.5.1 Contrast of hue

Since *contrast of hue* is ‘illustrated by the undiluted colors in their most intense luminosity’[23, p. 33], our goal is to generate a normalized co-occurrence matrix that verifies the presence of homogeneous regions with fully saturated hues. With 12 hues, we first generate a 12 x 12 co-occurrence matrix that counts the number of times H_P , the hue of pixel P is adjacent to H_N , the hue of its neighbouring pixels N . Since *contrast of hue* is characterized by fully saturated homogeneous regions, we impose the requirement that only fully saturated pixels are counted. In our experience, 80% of maximum saturation provides a robust way of handling artifacts and degradation, hence we require S_P (the saturation of the center pixel) and S_{Nj} (the saturation of the j^{th} neighbouring pixel) to both be ≥ 0.8 . In Algorithm 1 we describe how we generate N , a normalized co-occurrence matrix of homogeneous regions. We initially build a 12x12 matrix C where adjacent pixels of uniform saturation and light are counted. We also require that S_P and S_{Nj} , be within saturation range S_T while L_P and L_{Nj} (their light values) are within light range L_T . Next we extract $Cdiag$, a 12x12 matrix composed of the 3-cell diagonal band in C . In our experience, a homogeneous region is rarely composed of a single hue and usually contains pixels of the adjacent hue in the color wheel. For example, an orange region will contain red-orange pixels, as well as yellow-orange pixels. Since we are only interested in the homogeneous regions, we extract into $Cdiag$ the 3 cell diagonal band as shown in Figure 3.8. Finally, to compute N , we normalize $Cdiag$ by dividing each cell by the sum of all entries in $Cdiag$.

We therefore explore 3 ranges of saturation and light to identify which range is best suited to capture the relevant co-occurrences:

- Range 1: $S_T = 0, L_T = 0$. This range captures hue co-occurrences where S_P the saturation and light values of surrounding pixels are identical to the saturation and light values of the center pixel. This range is ideal for the study of *contrast of hue* since it will convey the most information about ideally homogeneous regions.
- Range 2: $S_T = 1/20, L_T = 1/7$. This range captures hue co-occurrences where the saturation values may differ up to 5%, and the light values are within one light zone (1/7th of the vertical space), as shown in Figure 3.1. In our experience, this range is sufficient for capturing 80% of the considered pixels in the image.

Data: Let $P=(H_P, S_P, L_P)$ be a pixel with color information given in (H,S,L) coordinates. Let N_j for $j = 1..8$ be the 8 neighbours of P .

Result: N, a normalized co-occurrence matrix of homogeneous regions

```
//Initialization;
C[12][12]=0;
Cdiag[12][12]=0;
N[12][12]=0;
//Build raw co-occurrence matrix C:
for each P do
  for j=1..8 do
    if  $S_P \geq 0.8$  and  $S_{N_j} \geq 0.8$  then
      if  $\|S_P - S_{N_j}\| \leq S_T$  and  $\|L_P - L_{N_j}\| \leq L_T$  then
        |  $C(H_P, H_{N_j}) = C(H_P, H_{N_j}) + 1;$ 
      end
    end
  end
end
//Put 3 cell diagonal band in Cdiag: for i=1..12 do
  for j=1..12 do
    if  $i=j$  or  $i=j+1$  or  $i=j-1$  then
      |  $Cdiag(i,j)=C(i,j);$ 
    end
  end
end
Diag_Total=sum(CDiag);
//Normalize diagonal band;
for i=1..12 do
  for j=1..12 do
    |  $N(i, j) = \frac{Cdiag(i,j)}{Diag\_Total};$ 
  end
end
end
```

Algorithm 1: Contrast of Hue

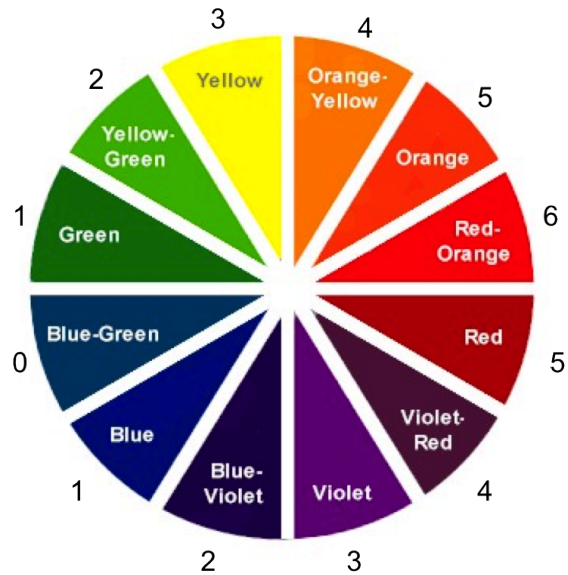
- Range 3: $S_T = 1/10, L_T = 1/7$. This range captures hue co-occurrences where S_P the saturation values of pixel P and the saturation level of surrounding pixels S_{N_j} may differ by up to 10% and the light values L_{N_j} are within one light zone (1/7th of the vertical space), as shown in Figure 3.1. In our experience, this range is sufficient for capturing 95% of the considered pixels in the image.

Adjacent contrasts with Saturation range S_T and Light range L_T												
	R	RO	O	YO	Y	YG	G	BG	B	BV	V	RV
R	R	*										
RO	*	RO	*									
O		*	O	*								
YO			*	YO	*							
Y				*	Y	*						
YG					*	YG	*					
G						*	G	*				
BG							*	BG	*			
B								*	B	*		
BV									*	BV	*	
V										*	V	*
RV											*	RV

Figure 3.8: Co-occurrence matrix, C_{diag} featuring the 3-cell diagonal band. The blank cells contain adjacent co-occurrences.

3.5.2 Cold-warm contrast

In *cold-warm contrast*, the perception of the heat contrast between hues is relative. Based on the notion of cold and warm poles [23, p. 45], red-orange is always warm and blue-green is always cool. ‘*The intermediate hues between them in the color circle may be either cold or warm according [to their contrast] with warmer and colder tones*’[23, p. 46]. We propose a uniform quantization of the 12 hues by assigning *warmth indices* of 0 to the coldest color (blue-green), and incrementally assigning higher indices to hues in the color wheel until red-orange (warmth index 6) as seen in Figure 3.9(a). We further propose measuring the strength of the *cold-warm contrast* for both the homogeneous regions and finer modulated regions by considering the *warmth contrast strength* as the absolute value of the difference between two *warmth indices*. A look up table as shown in Figure 3.9(b) indicates the strength of the contrast between hues. For example, red (warmth index 5) and orange (warmth index 5) offer no contrast in warmth when placed next to one another; however, either of them placed next to red-orange (warmth index 6) will appear mildly cooler. As a result, a red region adjacent to an red-orange region will have a *warmth contrast strength* of 1, while a red region adjacent to an orange region will have a *warmth contrast strength* of 0, computed as the difference between the *warmth indices* (see Figure 3.9).



(a) Warmth Index for hues

		R	RO	O	YO	Y	YG	G	BG	B	BV	V	RV
	Warmth Index	(5)	(6)	(5)	(4)	(3)	(2)	(1)	(0)	(1)	(2)	(3)	(4)
R	(5)	0	1	0	1	2	3	4	5	4	3	2	1
RO	(6)	1	0	1	2	3	4	5	6	5	4	3	2
O	(5)	0	1	0	1	2	3	4	5	4	3	2	1
YO	(4)	1	2	1	0	1	2	3	4	3	2	1	0
Y	(3)	2	3	2	1	0	1	2	3	2	1	0	1
YG	(2)	3	4	3	2	1	0	1	2	1	0	1	2
G	(1)	4	5	4	3	2	1	0	1	0	1	2	3
BG	(0)	5	6	5	4	3	2	1	0	1	2	3	4
B	(1)	4	5	4	3	2	1	0	1	0	1	2	3
BV	(2)	3	4	3	2	1	0	1	2	1	0	1	2
V	(3)	2	3	2	1	0	1	2	3	2	1	0	1
RV	(4)	1	2	1	0	1	2	3	4	3	2	1	0

(b) cold-warm contrast strengths for adjacent hues

Figure 3.9: (a) hue warmth values (b) look up table of warmth contrast strength values computed as the difference of warmth indices

Data: Let $P=(H_P, S_P, L_P)$ be a pixel with color information given in (H,S,L) coordinates. Let N_j for $j = 1..8$ be the 8 neighbours of P .

Result: N_{hom} , a normalized co-occurrence matrix of homogeneous regions

N_{adj} , a normalized co-occurrence matrix of hue adjacencies

//Initialization;

$C[12][12]=0$, $Cdiag[12][12]=0$, $Cadj[12][12]=0$, $Nhom[12][12]=0$, $Nadj[12][12]=0$;

//Build raw co-occurrence matrix C:

for each P do

for j=1..8 do

if $\frac{3}{7} \leq L_P \leq \frac{4}{7}$ and $\frac{3}{7} \leq L_{N_j} \leq \frac{4}{7}$ then

if and $\|S_P - S_{N_j}\| \leq S_T$ and $\|L_P - L_{N_j}\| \leq L_T$ then

$C(H_P, H_{N_j}) = C(H_P, H_{N_j}) + 1$;

end

end

end

end

//Put 3 cell diagonal band in Cdiag, and remaining cells in Cadj:

for i=1..12 do

for j=1..12 do

if i=j or i=j+1 or i=j-1 then

$Cdiag(i,j)=C(i,j)$;

else

$Cadj(i,j)=C(i,j)$;

end

end

end

$Diag_Total=\text{sum}(Cdiag)$;

$Adj_Total=\text{sum}(Cadj)$;

//Normalize diagonal band, normalize adjacencies:

for i=1..12 do

for j=1..12 do

$Nhom(i, j) = \frac{Cdiag(i,j)}{Diag_Total}$;

$Nadj(i, j) = \frac{Cadj(i,j)}{Adj_Total}$;

end

end

Algorithm 2: Cold-warm contrast

For *cold-warm contrast*, our goal is to generate two normalized co-occurrence matrices: N_{hom} that verifies the presence of homogeneous regions whose hues contrast in warmth, and N_{adj} that verifies the presence of contrasting adjacent hues. Since we have 12 hues, we first generate a 12 x 12 co-occurrence matrix that counts the number of times H_P , the hue of pixel P is adjacent to H_N , the hue of its neighbouring pixel N . Since *cold-warm contrast* is characterized by colors whose light values lie within the center light zone [23, p. 48], we only count adjacent pixels in the range $\frac{3}{7} \leq (L_P, L_N) \leq \frac{4}{7}$. To ensure that adjacent pixels counted are of uniform saturation and light, we also require that S_P and S_{Nj} , the saturations of the two pixels are within saturation range S_T while L_P and L_{Nj} , their light values are within light range L_T .

We therefore explore 3 ranges of saturation and light to identify which range is best suited to capture the relevant co-occurrences:

- Range 1: $S_T = 0, L_T = 0$. This range captures hue co-occurrences where the saturation and light values of surrounding pixels are identical to the saturation and light values of the center pixel. This range is ideal for the study of *Cold Warm Contrast* in homogeneous regions of good quality images.
- Range 2: $S_T = 1/20, L_T = 1/7$. This range captures hue co-occurrences where the saturation values may differ up to 5%, and the light values are within one light zone (1/7th of the vertical space), as shown in Figure 3.1. In our experience, this range is sufficient for capturing 80% of the considered pixels in the image.
- Range 3: $S_T = 1/10, L_T = 1/7$. This range captures hue co-occurrences where S_P the saturation values of pixel P and the saturation level of surrounding pixels S_{Nj} may differ by up to 10% and the light values are within one light zone (1/7th of the vertical space), as shown in Figure 3.1. In our experience, this range is sufficient for capturing 95% of the considered pixels in the image.

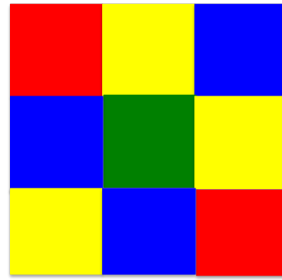
As discussed previously, a homogeneous region of one hue typically contains pixels of the adjacent hue in the color wheel. We extract into C_{diag} the 3 cell diagonal band as shown in Figure 3.8. We store the remaining cells into C_{adj} . Finally, to compute N_{hom} , we normalize C_{diag} by dividing each cell by the sum of all entries in C_{diag} . Since perceptually, there is no difference in the order of hue adjacencies for *cold-warm contrast* (for example orange-blue adjacencies are treated the same way as blue-orange adjacencies), we add the co-occurrence counts of equivalent hue adjacencies. To

compute N_{adj} , we normalize the cells in C_{adj} by dividing each cell of C_{adj} by Adj_Total , the sum of all adjacent hue co-occurrences. In our analysis of *cold-warm contrast* in an image, we assess the contrast in the homogeneous regions by considering the relative percentages in N_{hom} along with the *warmth index* in Figure 3.9(a); we also assess the strength of the contrast in hue adjacencies by considering the relative percentages in N_{adj} and look up the *warmth contrast strength* in Figure 3.9(b). All *warmth contrast strengths* range from 0 to 6. The strength of the contrast is computed as the difference of the *warmth indices* of two hues $CS(H_i, H_j) = |CWI(H_i) - CWI(H_j)|$. We interpret a *warmth contrast strength* of 0 to mean no contrast, 1 and 2 as low contrast, 3 and 4 medium, 5 and 6 as high contrast.

3.5.3 Worked example

Let us consider the checkered image in Figure 3.10 (a) to illustrate the computational steps in our algorithms. Figure 3.10(b) is the corresponding 6x6 pixel matrix representing the hues of the image. Let us also assume that all pixels in this image have saturation value 1, and light value 0.5. Since all pixels are uniform in saturation and light values, are fully saturated and the light values lie within the center zone, the image shows both *contrast of hue* and *cold-warm contrast*. The resulting co-occurrence matrices C_{diag} are the same for both Algorithms 1 and 2, N of Algorithm 1 is the same as N_{hom} of Algorithm 2 while N_{adj} in Algorithm 2 provides the normalized adjacencies count.

Traversing the image from left to right, and top to bottom, the raw co-occurrence matrix C in Figure 3.10(d) is computed based on the ‘isotropic 8 vertex neighbourhood’ adjacency. For example, consider the vertex at position (3,3) of green hue as shown in Figure 3.10 (c). We count the co-occurrences at pixel (3,3) as: G-R(1), G-Y(2), G-G(3) and G-B(2). Once the matrix C is computed, the co-occurrences along the diagonal band of C are extracted into C_{diag} , and the remaining cells of C are placed in C_{adj} . Both C_{diag} and C_{adj} are shown in Figure 3.11. To compute N_{diag} , we divide each cell of C_{diag} by $DiagTotal$, the sum of all the cells in C_{diag} . For example, the sum of all cells in C_{diag} is 112. The percentage of red-red co-occurrences in N_{diag} is computed at $\frac{24}{112} = 21\%$. To compute N_{adj} , we sum equivalent adjacencies and divide each cell of C_{adj} by $AdjTotal$, the sum of all the cells in C_{adj} . For example, the number of yellow-blue co-occurrences is 15, and the number of blue-yellow co-occurrences is also 15, and the sum of all hues adjacencies is 102. Since we do not differentiate between



(a) Image

<i>R</i>	<i>R</i>	<i>Y</i>	<i>Y</i>	<i>B</i>	<i>B</i>
<i>R</i>	<i>R</i>	<i>Y</i>	<i>Y</i>	<i>B</i>	<i>B</i>
<i>B</i>	<i>B</i>	<i>G</i>	<i>G</i>	<i>Y</i>	<i>Y</i>
<i>B</i>	<i>B</i>	<i>G</i>	<i>G</i>	<i>Y</i>	<i>Y</i>
<i>Y</i>	<i>Y</i>	<i>B</i>	<i>B</i>	<i>R</i>	<i>R</i>
<i>Y</i>	<i>Y</i>	<i>B</i>	<i>B</i>	<i>R</i>	<i>R</i>

(b) 6 x 6 pixel representation

<i>R</i>	<i>Y</i>	<i>Y</i>
<i>B</i>	<i>G</i>	<i>G</i>
<i>B</i>	<i>G</i>	<i>G</i>

(c) 8 vertex neighbourhood for pixel (3,3)

	R	RO	O	YO	Y	YG	G	BG	B	BV	V	RV
R	24	0	0	0	8	0	2	0	8	0	0	0
RO	0	0	0	0	0	0	0	0	0	0	0	0
O	0	0	0	0	0	0	0	0	0	0	0	0
YO	0	0	0	0	0	0	0	0	0	0	0	0
Y	8	0	0	0	38	0	9	0	15	0	0	0
YG	0	0	0	0	0	0	0	0	0	0	0	0
G	2	0	0	0	9	0	12	0	9	0	0	0
BG	0	0	0	0	0	0	0	0	0	0	0	0
B	8	0	0	0	15	0	9	0	38	0	0	0
BV	0	0	0	0	0	0	0	0	0	0	0	0
V	0	0	0	0	0	0	0	0	0	0	0	0
RV	0	0	0	0	0	0	0	0	0	0	0	0

(d) Raw co-occurrence matrix with uniform saturation and uniform light

Figure 3.10: A simple checkered example

	R	RO	O	YO	Y	YG	G	BG	B	BV	V	RV
R	24	0	0	0	0	0	0	0	0	0	0	0
RO	0	0	0	0	0	0	0	0	0	0	0	0
O	0	0	0	0	0	0	0	0	0	0	0	0
YO	0	0	0	0	0	0	0	0	0	0	0	0
Y	0	0	0	0	38	0	0	0	0	0	0	0
YG	0	0	0	0	0	0	0	0	0	0	0	0
G	0	0	0	0	0	0	12	0	0	0	0	0
BG	0	0	0	0	0	0	0	0	0	0	0	0
B	0	0	0	0	0	0	0	0	38	0	0	0
BV	0	0	0	0	0	0	0	0	0	0	0	0
V	0	0	0	0	0	0	0	0	0	0	0	0
RV	0	0	0	0	0	0	0	0	0	0	0	0

(a) C_{diag}

	R	RO	O	YO	Y	YG	G	BG	B	BV	V	RV
R	0	0	0	0	8	0	2	0	8	0	0	0
RO	0	0	0	0	0	0	0	0	0	0	0	0
O	0	0	0	0	0	0	0	0	0	0	0	0
YO	0	0	0	0	0	0	0	0	0	0	0	0
Y	8	0	0	0	0	0	9	0	15	0	0	0
YG	0	0	0	0	0	0	0	0	0	0	0	0
G	2	0	0	0	9	0	0	0	9	0	0	0
BG	0	0	0	0	0	0	0	0	0	0	0	0
B	8	0	0	0	15	0	9	0	0	0	0	0
BV	0	0	0	0	0	0	0	0	0	0	0	0
V	0	0	0	0	0	0	0	0	0	0	0	0
RV	0	0	0	0	0	0	0	0	0	0	0	0

(b) C_{adj} Figure 3.11: C_{diag} and C_{adj} derived from C for checkered example

yellow-blue and blue-yellow adjacencies, the percentage of yellow-blue co-occurrences in N_{adj} is $\frac{15+15}{102} = 29\%$.

To analyze this image for *contrast of hue*, we only need to look at N_{hom} , and see that yellow and blue each have 34% of the co-occurrences, red has 21% and green has 11%. We confirm by looking at the image that yellow and blue each occupy the same number of blocks and make up the largest proportion of the image, followed by red then green. To analyze the results for *cold-warm contrast*, we look at N_{hom} with the *warmth index* and N_{adj} with the *warmth contrast strength* (see Figure 3.9). The

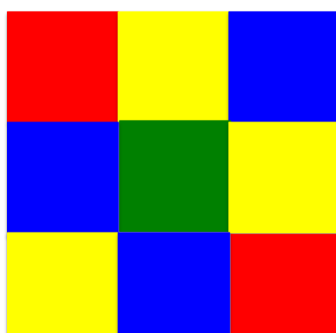
	R	RO	O	YO	Y	YG	G	BG	B	BV	V	RV
R	21%	0%	0%	0%	0%	0%	0%	0%	0%	0%	0%	0%
RO	0%	0%	0%	0%	0%	0%	0%	0%	0%	0%	0%	0%
O	0%	0%	0%	0%	0%	0%	0%	0%	0%	0%	0%	0%
YO	0%	0%	0%	0%	0%	0%	0%	0%	0%	0%	0%	0%
Y	0%	0%	0%	0%	34%	0%	0%	0%	0%	0%	0%	0%
YG	0%	0%	0%	0%	0%	0%	0%	0%	0%	0%	0%	0%
G	0%	0%	0%	0%	0%	0%	11%	0%	0%	0%	0%	0%
BG	0%	0%	0%	0%	0%	0%	0%	0%	0%	0%	0%	0%
B	0%	0%	0%	0%	0%	0%	0%	0%	34%	0%	0%	0%
BV	0%	0%	0%	0%	0%	0%	0%	0%	0%	0%	0%	0%
V	0%	0%	0%	0%	0%	0%	0%	0%	0%	0%	0%	0%
RV	0%	0%	0%	0%	0%	0%	0%	0%	0%	0%	0%	0%

(a) Normalized Homogeneous Regions N_{hom}

	R	RO	O	YO	Y	YG	G	BG	B	BV	V	RV
R	0%	0%	0%	0%	16%	0%	4%	0%	16%	0%	0%	0%
RO	0%	0%	0%	0%	0%	0%	0%	0%	0%	0%	0%	0%
O	0%	0%	0%	0%	0%	0%	0%	0%	0%	0%	0%	0%
YO	0%	0%	0%	0%	0%	0%	0%	0%	0%	0%	0%	0%
Y	0%	0%	0%	0%	0%	0%	18%	0%	29%	0%	0%	0%
YG	0%	0%	0%	0%	0%	0%	0%	0%	0%	0%	0%	0%
G	0%	0%	0%	0%	0%	0%	0%	0%	18%	0%	0%	0%
BG	0%	0%	0%	0%	0%	0%	0%	0%	0%	0%	0%	0%
B	0%	0%	0%	0%	0%	0%	0%	0%	0%	0%	0%	0%
BV	0%	0%	0%	0%	0%	0%	0%	0%	0%	0%	0%	0%
V	0%	0%	0%	0%	0%	0%	0%	0%	0%	0%	0%	0%
RV	0%	0%	0%	0%	0%	0%	0%	0%	0%	0%	0%	0%

(b) Normalized Adjacencies N_{adj} Figure 3.12: Normalized Homogeneous Regions N_{hom} and Adjacencies N_{adj} for the checkered example.

results are summarized in Figure 3.13. We see that a medium contrast of 4 occurs between the blue and red homogeneous regions, as well as green and red; however red and blue share more adjacencies than red and green, making the red and blue contrast more perceptually relevant. We also see that yellow offers a weak contrast of 2 with both green and blue. Since yellow-blue adjacencies are more common than yellow-green adjacencies, we conclude that the contrast of yellow with blue is more perceptually relevant for *cold-warm contrast*. Green is also adjacent to blue but offers



(a) Checkered Image

Hue	Percentage	Warmth Index
Yellow	34%	3
Blue	34%	1
Red	21%	5
Green	11%	1

(b) Homogeneous regions

Adjacent Hues	Percentage	Warmth Contrast
Yellow-Blue	29%	2
Yellow-Green	18%	2
Green-Blue	18%	0
Red-Blue	16%	4
Red-Green	4%	4

(c) Adjacencies

Figure 3.13: Summary of results for checkered color image

no contrast in warmth.

3.5.4 Analysis of paintings with the proposed computational models

Using our algorithm and comments from Itten, we use our algorithms to verify that they capture well the *contrast of hue* and *cold-warm contrast*. We also investigate the range of saturation and light appropriate for capturing the contrast in each painting. In this chapter, we limit our discussion to one painting for each contrast, and will discuss the remaining paintings in Chapter 4 (Results).

For *contrast of hue*, let us consider Charonton’s ‘The Coronation of the Virgin’ shown in Figure 3.14. “*In the composition of this monumental painting, Charonton used the colors gold, orange, red, blue, green, white and gray. At the top, he begins with yellow [...]. This condenses into darker orange [...]. Contrasting [...] is the red of the mantles of Father and Son*’ [22, p. 40]. Our results for this painting are sum-

marized in Figure 3.18 (page 49). Looking at the painting, we see large homogeneous regions of red, orange and blue, with some green and gold. We confirm that the homogeneous regions in this image are captured by our methods in range $S_T = 0, L_T = 0$, with the exception of blue represented by the least percentage of co-occurrences. Our algorithm mostly ignored the large dark-blue regions due to their very low light levels. The highly saturated blue in the image is interwoven with shades of dark grey and black, thus reducing the co-occurrences computed.

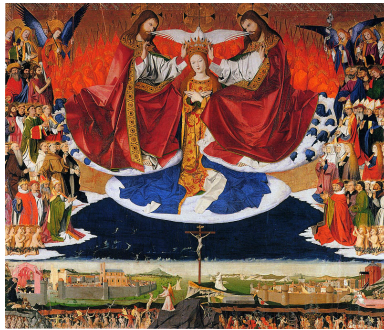


Figure 3.14: Coronation of the Virgin

For *cold-warm contrast*, let us consider ‘La Belle Verriere’, a famous stained glass painting in Chartres Cathedral (shown in Figure 3.15) . Itten describes this painting: ‘The blue of the dress appears against a red-orange ground, lending it a cold, radiant light. The ice blue and red-orange are intense cold-warm contrast’[22, p. 68]. Figure 3.19 (page 50) shows the painting, and summary of results. We note that in our digital copy of the image, some of the blue appears violet. In the first range of saturation and light $S_{T1} = 0, L_{T1} = 0$, we confirm that red, blue and red-orange homogeneous regions are dominant. We also note the medium *warmth contrast strength* of 4 between red and blue homogeneous regions, and high *warmth contrast strength* of 5 between red-orange and blue which confirms Itten’s statement about the intensity of the contrast. To correctly capture the adjacencies we see in the image, the second range $S_{T1} = 1/20, L_{T1} = 1/7$ is needed.

We therefore conclude that our algorithms capture *contrast of hue* and *cold-warm contrast* well.



Figure 3.15: La Belle Verriere

3.5.5 Analysis of artists' chromatic style

Itten briefly mentioned several artists for having used *contrast of hue* or *cold-warm contrast* in their work. To explore these contrasts in their works, we developed a computational model to visualize the contrasts in several paintings by the same artist. Our results on each painting consist of a list of normalized co-occurrences from N_{hom} and N_{adj} . We display the values in N_{hom} and N_{adj} in a 3D histogram. We represent the percentage of co-occurrences in homogeneous regions and adjacencies as bar graphs. The histogram of the homogeneous regions in each painting is $HIST_{hom}(image) = [N_{hom}(R), N_{hom}(RO), \dots, N_{hom}(V), N_{hom}(RV)]$ for each of the 12 hues, and $HIST_{adj}(image) = [N_{adj}(R - RO), N_{adj}(R - O), \dots, N_{adj}(V - RV)]$ for each of 55 hue adjacencies. To explore an artist's style, we analyze the normalized co-occurrences displayed side by side and vertically, resulting in a 3D histogram.

For *contrast of hue*, Itten mentioned Stefan Lochner, Fra Angelico, Botticelli, Mondrian, Picasso, Leger, Miro, and the early works of Franz Marc, Kandinsky and Macke. Our computational model displays the normalized co-occurrences in homogeneous regions for all of an artist's paintings sequentially. In this chapter, we explore Picasso's style by studying 5 of his paintings using our computational model. The styles of the remaining artists will be explored in Chapter 4 (Results).

In Figure 3.16, we display all 5 of Picasso's paintings. In Figure 3.20, we show the

percentage of co-occurrences in the homogenous regions for each painting and each of the three ranges of saturation and light. In figure 3.20(c), we plot the homogeneities over 12 hues, N_{hom} , grouped by range of saturation and light in a 3D histogram:

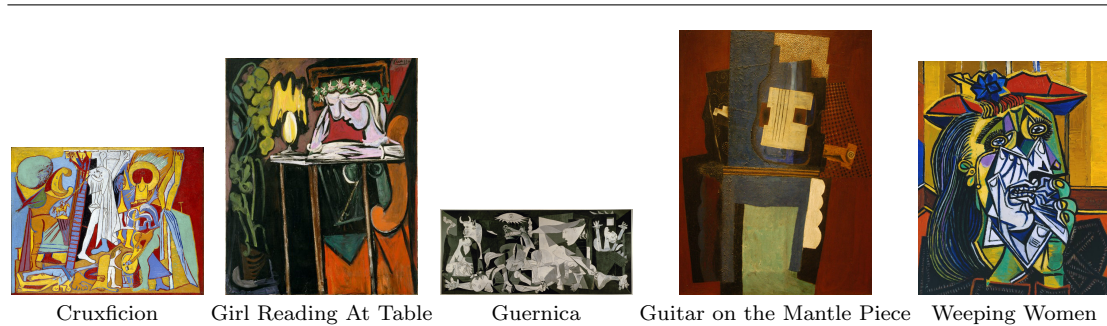


Figure 3.16: Picasso paintings

- *Crucifixion*. Our algorithm computes co-occurrences for fully saturated homogeneous regions. The first range $S_{T_1} = 0, L_{T_1} = 0$ identifies red has having 76% of co-occurrences, followed by orange at 12%, then yellow-orange at 8%. In the other two ranges, $S_{T_1} = 1/20, L_{T_1} = 1/7$ and $S_{T_1} = 1/10, L_{T_1} = 1/7$, red co-occurrences are still the majority, followed by yellow-orange then orange. For this painting, we conclude that the contrasting hues are red, orange and yellow-orange.
- *Girl Reading at Table*. Our algorithm identifies fully saturated homoneous regions in the order of orange followed by red-orange then yellow-orange and yellow in all three ranges. The orange and red-orange in the chair contrast with the yellow and yellow-orange of the lamp.
- *Guernica*. This painting has no chromatic information, therefore our algorithm has zeros for all hues co-occurrences. We include it only for completeness.
- *Guitar on the Mantle Piece*. Our algorithm computes that red-orange as the largest homogeneous regions, followed by orange in all three ranges. The first range $S_{T_1} = 0, L_{T_1} = 0$ also brings in red as only 1% of the co-occurrences.
- *Weeping Women*. Our algorithm computes that the homogeneous regions are primarily yellow-orange, followed by orange, red-orange, and red in the first range ($S_{T_1} = 0, L_{T_1} = 0$). The other two ranges detect a small amount of

yellow as well, however the yellow homogeneous regions are not fully saturated. We conclude that the first range is sufficient for detecting the fully saturated homogeneous regions: yellow-orange, orange, red, and red-orange.

The first 3D histogram in Figure 3.20(c) shows the normalized co-occurrences of the homogeneous regions for all 5 paintings in the range $S_{T1} = 0, L_{T1} = 0$. The first column of the 3D Histogram (in black) is a plot of the homogenous values of the painting ‘Cruxificion’ shown in Figure 3.20(b) for the range $S_{T1} = 0, L_{T1} = 0$. Each column plots the percentage of homogeneities for 12 hues, from red (R) at the bottom to red-violet (RV) at the top. The lengths of the bars are proportional to the percentages listed in Figure 3.20(b). Similarly, the second column (in dark grey) is a plot of the homogenous values of ‘Girl Reading At Table’ in the same saturation and light range. Therefore the first 3D Histogram in Figure 3.20(c), is a plot of all homogeneities from all 5 of Picasso’s paintings in the range $S_{T1} = 0, L_{T1} = 0$. The second and third 3D histograms, plot the homogeneities in the second range $S_{T1} = 1/20, L_{T1} = 1/7$ and third range $S_{T1} = 1/10, L_{T1} = 1/7$ respectively, while maintaining the order of the paintings.

By looking at the 3D histograms of Picasso’s paintings, we see that his use of *contrast of hue* is focussed on hues between red and yellow-orange. Although he uses blues and greens, these hues do not satisfy the requirement of being fully saturated. We also see that the ranges $S_{T1} = 1/20, L_{T1} = 1/7$ and $S_{T1} = 1/10, L_{T1} = 1/7$ do not provide us with significantly different information about paintings, therefore the first range $S_{T1} = 0, L_{T1} = 0$ is sufficient for our analysis of Picasso’s 5 chosen paintings. We see from this example that the 3D histograms are valuable, as they allow us to identify the dominant colors in an artist’s palette.

For *cold-warm contrast*, Itten mentioned Bonnard, Cézanne, Monet, Pissaro and Renoir. Our computational model displays the normalized co-occurrences in homogeneous regions as well as adjacencies for all of an artist’s paintings sequentially. In this chapter, we explore the works of Cézanne for *cold-warm contrast* as shown in Figure 3.17. We will first explore each of the images in detail, then explore the 3D histograms of the normalized co-occurrences for homogeneous regions and adjacencies as shown in Figure 3.25 on page 56. The styles of the remaining artists will be explored in Chapter 4 (Results).

We will describe our results for four paintings (shown in Figure 3.17):

- *Apples and Oranges*. In this painting, Cézanne employs yellow, orange, blue,

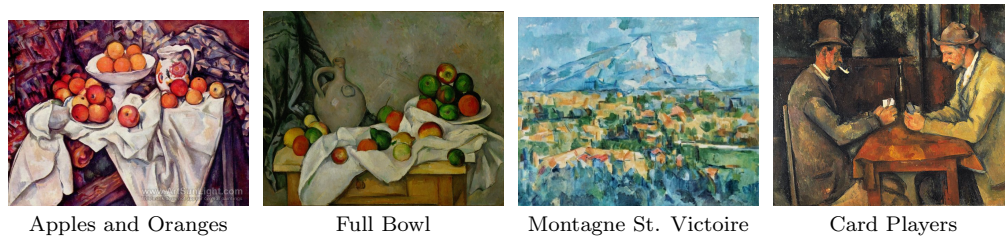


Figure 3.17: Cézanne Paintings

violet and pink. Our digital copy of the image shows more blue and violet for the regions that appear green in the physical copy of the image [22], and yellow fruits appear orange. Itten says: *‘In the still life “Apples and Orange”, all hues of the color circle are employed ... The four principal colors [red, green, blue, orange] are distributed throughout the surface in diversely modulated patches.’* Further he says: *‘The pictorial expression of the work results from modulations in cold-warm contrast ... For this he uses colors of equal brilliance, taking their chromatic sequence from the color circle. Yellow, green, blue, violet, pink and light orange succeed each other. These cold-warm modulations produce the enchantment of the objective world which Cézanne was striving for’*[22, p. 75]. The painting and our results are displayed in Figure 3.21. Our results for homogeneous regions confirm the presence of almost all hues, with the exception of yellow and green which appear orange and violet in the digital image. We also observe a contrast of warm hues (red, orange and red-orange) with cooler hues (blue, blue-violet and violet). In the adjacencies, we see each hue adjacent to red-violet which is the prevalent color of the background in the digital copy of the image. Since Cézanne varies the saturation of the colors, we need the third range to get an accurate computation of the co-occurrences. We note the *warmth contrast strengths* in the third range of light and saturation show a high contrast between homogeneous regions, but a weak and mild contrast in the adjacencies. In general, all three ranges provide similar information.

- *Full Bowl*. Itten did not comment about this painting. The painting and our results are displayed in Figure 3.22. We observe from the painting a green background with hints of yellow and red. The fruits in the foreground are red, yellow, orange and green, placed over a yellow and yellow-orange table. The relative proportion of co-occurrences in the homogeneous regions remains the

same for all three contrasts, however the third range is needed to capture the red-orange and yellow adjacencies with moderate *warmth contrast strength* 3.

- *La Montagne St. Victoire*. Itten’s analysis of this painting is focused on *modulation* and the use of complementary contrast. Our analysis will focus on the elements of *cold-warm contrast*. Itten says of the chromatic construction: ‘*The four colors principally used are set in the three separate planes. In the foreground there is dusky brown-violet. In the middle distance, yellow-green and orange predominate, and in the background blue*’. He also says: ‘*Thus on beholding this landscape, one clearly discerns an organization into three horizontal planes*’[22, p. 84]. The painting and our results are displayed in Figure 3.23. Unfortunately, the digital copy of this image does not do justice to the organization of hues Itten describes. In the digital image, the dark blue of the mountain appears of the same color as the blue-green of the sky, and the dusky brown-violet is also blue-green. Our algorithm therefore detects blue-green as having the largest percentage of the homogeneous regions. The orange, yellow-orange, yellow and green in the middle plane are in small connected patches, which appears in the adjacencies of the second and third range, weak *warmth contrast strength*, yet significantly warmer than the blue regions on the background and foreground. The yellow and green captures in all three ranges is indicative of the high modulated regions in the middle ground of the image.
- *Card Players*. Itten did not comment about this painting. The painting and our results are displayed in Figure 3.24. We observe in the painting the orange table, the player on the right with a yellow-orange coat, and the red-orange wall in the background. In contrast, the player on the left has yellow-green interspersed with yellow on his coat; yellow and yellow-green are also interspersed in the background above the brown wall. The homogeneous regions are well captured in all three ranges, and the adjacencies are captured in the second and third ranges of saturation and light.

In Figure 3.25, we display the digital copies of the paintings in the top half of the figure. In the second half, we display the 3D histograms of the homogeneous regions for all three ranges, as well as the histogram of the adjacencies to allow us to analyze the artist’s style. Let us consider the first row of Figure 3.25(b). In the first 3D histogram, we plot the normalized percentages of the homogeneous hue regions of the 4 paintings over 12 hues, in the order the images appear in Figure 3.25(a). All

hues are listed from red at the bottom, to red-violet at the top. Each hue has its *warmth index* in parentheses. The first column (displayed in black) corresponds to the homogeneous regions of ‘Apples and Oranges’ and the length of the bars corresponds to the results in Figure 3.21 for the range $S_{T1} = 0, L_{T1} = 0$. For example, we see longer bars in the red, red-orange and orange hues (warmer hues), and shorter bars for blue-violet, violet and red-violet (cooler hues). The second column (displayed in dark grey) corresponds to the homogeneous regions of ‘Full Bowl’, for which we see the tallest bar at yellow, corresponding to the results in Figure 3.22. The third column (displayed in light grey) corresponds to the homogeneous regions of ‘La Montagne St. Victoire’, for which we see the tallest bar at blue-green, corresponding to our results in Figure 3.23. The last column (displayed in white) corresponds to the homogeneous regions of the painting ‘Card Players’, for which we see the tallest bars at yellow and yellow-orange, corresponding in turn to the results in Figure 3.24.

The next three 3D histograms display the results of 55 hue adjacencies ranging from R-O to O-Y. To better visualize these results, we separated the adjacencies into three groups: 1) R-O to O-Y displayed in the second 3D histogram, 2) O-YG to Y-RV displayed in the third 3D histogram, and 3) YG-GB to BV-RV displayed in the last 3D histogram. Each hue adjacency has its *warmth contrast strength* value in parentheses. For example, a bar at Y-G(2) indicates the percentage of co-occurrences captured by our algorithm for regions of yellow adjacent to green. Yellow has a *warmth index* of 3 and green has a *warmth index* of 1, resulting in a low *warmth contrast strength* of 2. The columns are also listed for each painting in the order the paintings appear in Figure 3.25(a). Similarly, the length of the bars corresponds to the normalized hue adjacency results for each painting. Further, the next two rows of 3D histograms display the results for the ranges $S_{T1} = 1/20, L_{T1} = 1/7$ and $S_{T1} = 1/10, L_{T1} = 1/7$ respectively. Looking at the 3D histogram results for Cézanne’s four paintings, we see that the homogeneous regions of his paintings are well saturated, as expanding the range of saturation and light does not change the relative proportion of co-occurrences. In the hue adjacencies however, the second and third range captured different proportions of co-occurrences than the first. Therefore the third range $S_{T1} = 1/10, L_{T1} = 1/7$ is needed to accurately capture the hue adjacencies.

We also conclude that our algorithm captures *cold-warm contrast* well in Cézanne’s paintings.



(a) Coronation of the Virgin

Chromatic Ground Truth: Orange, blue, red, gold, green
(Blue-green in original image appears blue in digital image)

$S_{T_1} = 0, L_{T_1} = 0$ Percentage	$S_{T_1} = 1/20, L_{T_1} = 1/7$ Percentage	$S_{T_1} = 1/10, L_{T_1} = 1/7$ Percentage
RO 42%	RO 26%	RO 23%
R 16%	O 18%	O 20%
O 12%	R 16%	R 16%
YO 5%	B 1%	YO 2%
Y 2%		B 1%
YG 1%		
B 1%		

(b) Homogeneous Regions

Figure 3.18: Summary of normalized co-occurrences for ‘Coronation of the Virgin’



(a) La Belle Verriere

Chromatic ground truth: ice-blue and red-orange
Some blue from original image appears violet in digital image

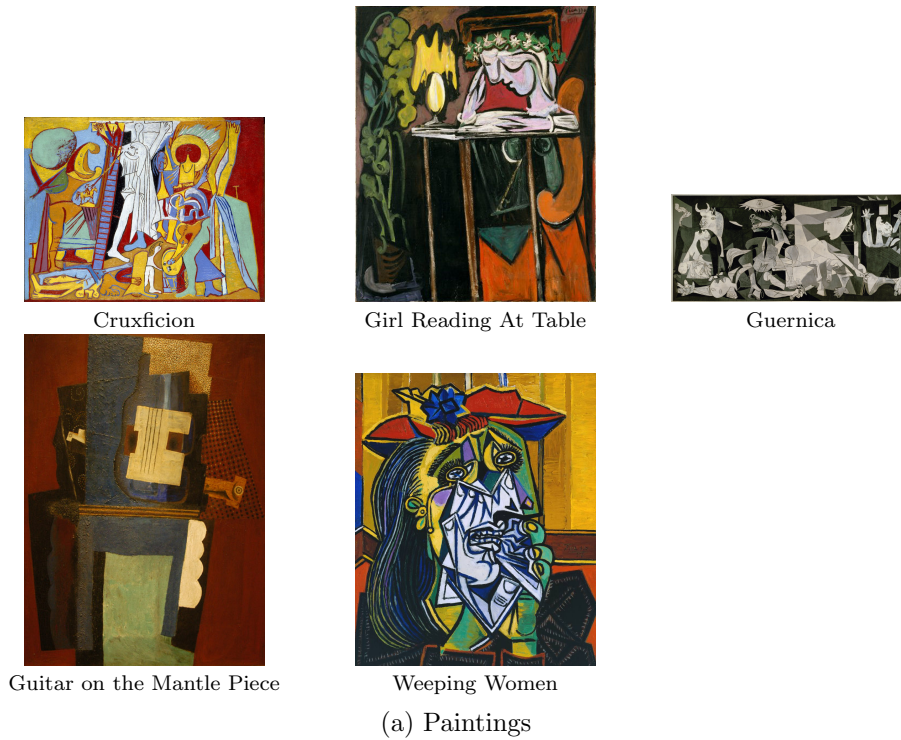
$S_{T_1} = 0, L_{T_1} = 0$	Warmth Index	$S_{T_1} = 1/20, L_{T_1} = 1/7$	Warmth Index	$S_{T_1} = 1/10, L_{T_1} = 1/7$	Warmth Index
R(49%)	5	B(30%)	1	B(32%)	1
B(18%)	1	R(22%)	5	R(20%)	5
RO(6%)	6	BG(7%)	0	BG(7%)	0
O(6%)	5	BV(6%)	2	BV(6%)	2
BV(4%)	2	O(5%)	5	O(4%)	5
BG(3%)	0	RO(4%)	6	RO(3%)	6
G(2%)	1	G(3%)	1	G(3%)	1
Y(1%)	3	Y(1%)	3	Y(1%)	3
YG(1%)	2	YG(1%)	2	YG(1%)	2

(b) Homogeneous Regions

$S_{T_1} = 0, L_{T_1} = 0$	Warmth Strength	$S_{T_1} = 1/20, L_{T_1} = 1/7$	Warmth Strength	$S_{T_1} = 1/10, L_{T_1} = 1/7$	Warmth Strength
R-V(9%)	2	R-RV(6%)	1	R-O(6%)	0
R-RV(9%)	1	R-O(6%)	0	R-RV(5%)	1
RO-V(5%)	3	R-V(5%)	2	R-V(5%)	2
O-V(5%)	2	B-V(3%)	2	G-B(3%)	0
YO-V(5%)	1	BV-RV(3%)	2	B-V(3%)	2
Y-V(5%)	0	G-B(3%)	0	BV-RV(3%)	2
YG-V(5%)	1	O-RV(3%)	1	O-RV(3%)	1
G-V(5%)	2	B-RV(3%)	3	B-RV(3%)	3
BG-V(5%)	3	RO-RV(3%)	2	RO-RV(3%)	2
B-V(5%)	2	G-BV(3%)	1	G-RV(2%)	3

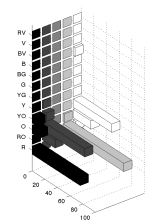
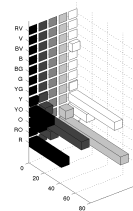
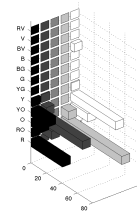
(c) Adjacencies

Figure 3.19: Summary of normalized co-occurrences for ‘La Belle Verriere’



Painting	Range	R	R-O	O	Y-O	Y	Y-G	G	B-G	B	B-V	V	R-V
Cruxifixion	$S_T = 0, L_T = 0$	76%	1%	12%	8%	1%	0%	0%	0%	0%	0%	0%	0%
	$S_T = 1/20, L_T = 1/7$	42%	1%	13%	23%	2%	0%	0%	0%	0%	0%	0%	0%
	$S_T = 1/10, L_T = 1/7$	41%	2%	13%	22%	2%	0%	0%	0%	0%	0%	0%	0%
Girl Reading At Table	$S_T = 0, L_T = 0$	0%	20%	67%	6%	1%	0%	0%	0%	0%	0%	0%	0%
	$S_T = 1/20, L_T = 1/7$	0%	15%	55%	8%	1%	0%	0%	0%	0%	0%	0%	0%
	$S_T = 1/10, L_T = 1/7$	0%	14%	54%	7%	1%	0%	0%	0%	0%	0%	0%	0%
Guernica	$S_T = 0, L_T = 0$	0%	0%	0%	0%	0%	0%	0%	0%	0%	0%	0%	0%
	$S_T = 1/20, L_T = 1/7$	0%	0%	0%	0%	0%	0%	0%	0%	0%	0%	0%	0%
	$S_T = 1/10, L_T = 1/7$	0%	0%	0%	0%	0%	0%	0%	0%	0%	0%	0%	0%
Guitar on the Mantle Piece	$S_T = 0, L_T = 0$	1%	96%	2%	0%	0%	0%	0%	0%	0%	0%	0%	0%
	$S_T = 1/20, L_T = 1/7$	0%	80%	9%	0%	0%	0%	0%	0%	0%	0%	0%	0%
	$S_T = 1/10, L_T = 1/7$	0%	79%	10%	0%	0%	0%	0%	0%	0%	0%	0%	0%
Weeping Women	$S_T = 0, L_T = 0$	4%	4%	28%	61%	0%	0%	0%	0%	3%	0%	0%	0%
	$S_T = 1/20, L_T = 1/7$	4%	4%	23%	59%	1%	0%	0%	0%	4%	0%	0%	0%
	$S_T = 1/10, L_T = 1/7$	4%	4%	22%	58%	1%	0%	0%	0%	4%	0%	0%	0%

(b) Percentage of Co-occurrences in Homogeneous Regions computed for all 5 paintings

 $S_T = 0, L_T = 0$  $S_T = 1/20, L_T = 1/7$  $S_T = 1/10, L_T = 1/7$

(c) 3D Histograms Visualizing Homogeneous regions in all 5 paintings, grouped by range of light and saturation

Figure 3.20: Picasso Visualization- Contrast of hue results for homogeneous regions and 3D histogram of relative proportions of hue homogeneities.



(a) Painting

 Chromatic ground truth: yellow, blue, orange, violet and pink

Homogeneous regions

$S_{T1} = 0, L_{T1} = 0$	Warmth Index	$S_{T1} = 1/20, L_{T1} = 1/7$	Warmth Index	$S_{T1} = 1/10, L_{T1} = 1/7$	Warmth Index
R(32)	5	R(33)	5	R(32)	5
O(25)	5	O(20)	5	O(19)	5
RO(21)	6	RO(16)	6	RO(15)	6
V(8)	3	V(3)	3	V(3)	3
YO(2)	4	YO(1)	4	YO(1)	4
BV(2)	2	BV(1)	2	BV(1)	2
RV(2)	4	RV(1)	4	RV(1)	4
B(1)	1	B(1)	1	B(1)	1

Adjacencies

$S_{T1} = 0, L_{T1} = 0$	Contrast Strength	$S_{T1} = 1/20, L_{T1} = 1/7$	Contrast Strength	$S_{T1} = 1/10, L_{T1} = 1/7$	Contrast Strength
R-RV(14)	1	R-RV(13)	1	R-RV(13)	1
BV-RV(8)	2	BV-RV(6)	2	R-V(7)	2
RO-RV(7)	2	RO-RV(6)	2	RO-RV(6)	2
O-RV(7)	1	O-RV(6)	1	O-RV(6)	1
YO-RV(7)	0	YO-RV(6)	0	YO-RV(6)	0
Y-RV(7)	1	Y-RV(6)	1	Y-RV(6)	1
YG-RV(7)	2	YG-RV(6)	2	YG-RV(6)	2
G-RV(7)	3	G-RV(6)	3	G-RV(6)	3
BG-RV(7)	4	B-RV(6)	3	BV-RV(6)	2
B-RV(7)	3			B-RV(6)	3

(b) Normalized co-occurrences

Figure 3.21: Detailed results for ‘Apples and Oranges’ by Cézanne



(a) Painting

 Chromatic ground truth: none available

Homogeneous regions

$S_{T_1} = 0, L_{T_1} = 0$		$S_{T_1} = 1/20, L_{T_1} = 1/7$		$S_{T_1} = 1/10, L_{T_1} = 1/7$	
	Warmth Index		Warmth Index		Warmth Index
Y(62)	3	Y(44)	3	Y(44)	3
YO(16)	4	YO(12)	3	YO(12)	3
YG(14)	2	YG(11)	2	YG(11)	2
G(2)	1	G(2)	1	G(2)	1
O(1)	5	O(1)	5	O(1)	5

Adjacencies

$S_{T_1} = 0, L_{T_1} = 0$		$S_{T_1} = 1/20, L_{T_1} = 1/7$		$S_{T_1} = 1/10, L_{T_1} = 1/7$	
	Contrast Strength		Contrast Strength		Contrast Strength
O-Y(100)	2	YO-YG(65)	2	YO-YG(60)	2
		O-Y(26)	2	O-Y(29)	2
		Y-G(9)	2	Y-G(10)	2
				RO-Y(2)	3

(b) Normalized co-occurrences

Figure 3.22: Detailed results for ‘Full Bowl’ by Cézanne



(a) Painting

Chromatic ground truth: blue, orange, violet and yellow-green					
Homogeneous regions					
$S_{T_1} = 0, L_{T_1} = 0$		$S_{T_1} = 1/20, L_{T_1} = 1/7$		$S_{T_1} = 1/10, L_{T_1} = 1/7$	
	Warmth Index		Warmth Index		Warmth Index
BG(72)	0	BG(49)	0	BG(48)	0
G(13)	1	G(14)	1	G(14)	1
O(3)	5	O(6)	5	O(6)	5
YO(3)	4	YO(5)	4	YO(4)	4
B(3)	1	B(2)	1	B(2)	1
Y(1)	3	Y(2)	3	Y(2)	3
YG(1)	2	YG(2)	2	YG(2)	2

Adjacencies					
$S_{T_1} = 0, L_{T_1} = 0$		$S_{T_1} = 1/20, L_{T_1} = 1/7$		$S_{T_1} = 1/10, L_{T_1} = 1/7$	
	Contrast Strength		Contrast Strength		Contrast Strength
Y-G(100)	2	Y-G(23)	2	Y-G(22)	2
		YO-YG(12)	2	YO-YG(17)	2
		O-Y(6)	2	YO-G(6)	3
		YG-BG(5)	2	O-Y(6)	2
		YO-G(4)	3	YG-BG(4)	2
		R-O(3)	0	R-O(3)	0
		Y-BG(3)	3	O-YG(2)	3
		YO-BG(3)	4	Y-BG(2)	3
		R-B(3)	4	YO-BG(2)	4
		G-B(3)	0	R-B(2)	4

(b) Normalized co-occurrences

Figure 3.23: Detailed results for ‘Montagne St. Victoire’ by Cézanne



(a) Painting

Chromatic ground truth: none available					
Homogeneous regions					
$S_{T_1} = 0, L_{T_1} = 0$	Warmth Index	$S_{T_1} = 1/20, L_{T_1} = 1/7$	Warmth Index	$S_{T_1} = 1/10, L_{T_1} = 1/7$	Warmth Index
O(54)	5	O(47)	5	O(46)	5
YO(32)	4	YO(25)	4	YO(25)	4
RO(8)	6	RO(6)	6	RO(6)	6
Y(2)	3	Y(2)	3	Y(2)	3
G(1)	1	YG(1)	2	YG(1)	2

Adjacencies					
$S_{T_1} = 0, L_{T_1} = 0$	Contrast Strength	$S_{T_1} = 1/20, L_{T_1} = 1/7$	Contrast Strength	$S_{T_1} = 1/10, L_{T_1} = 1/7$	Contrast Strength
		O-Y(13)	2	O-Y(19)	2
		YO-YG(11)	2	YO-YG(12)	2
		R-O(8)	0	R-O(9)	0
		G-B(6)	0	Y-G(4)	2
		Y-G(5)	2	G-B(4)	0
		R-BV(4)	3	O-YG(4)	3
		O-YG(3)	3	O-G(3)	4
		O-G(3)	4	YO-B(3)	3
		YO-B(3)	3	YG-B(3)	1
		YG-B(3)	1	R-BV(3)	3

(b) Normalized co-occurrences

Figure 3.24: Detailed results for ‘Card Players’ by Cézanne



(a) Paintings

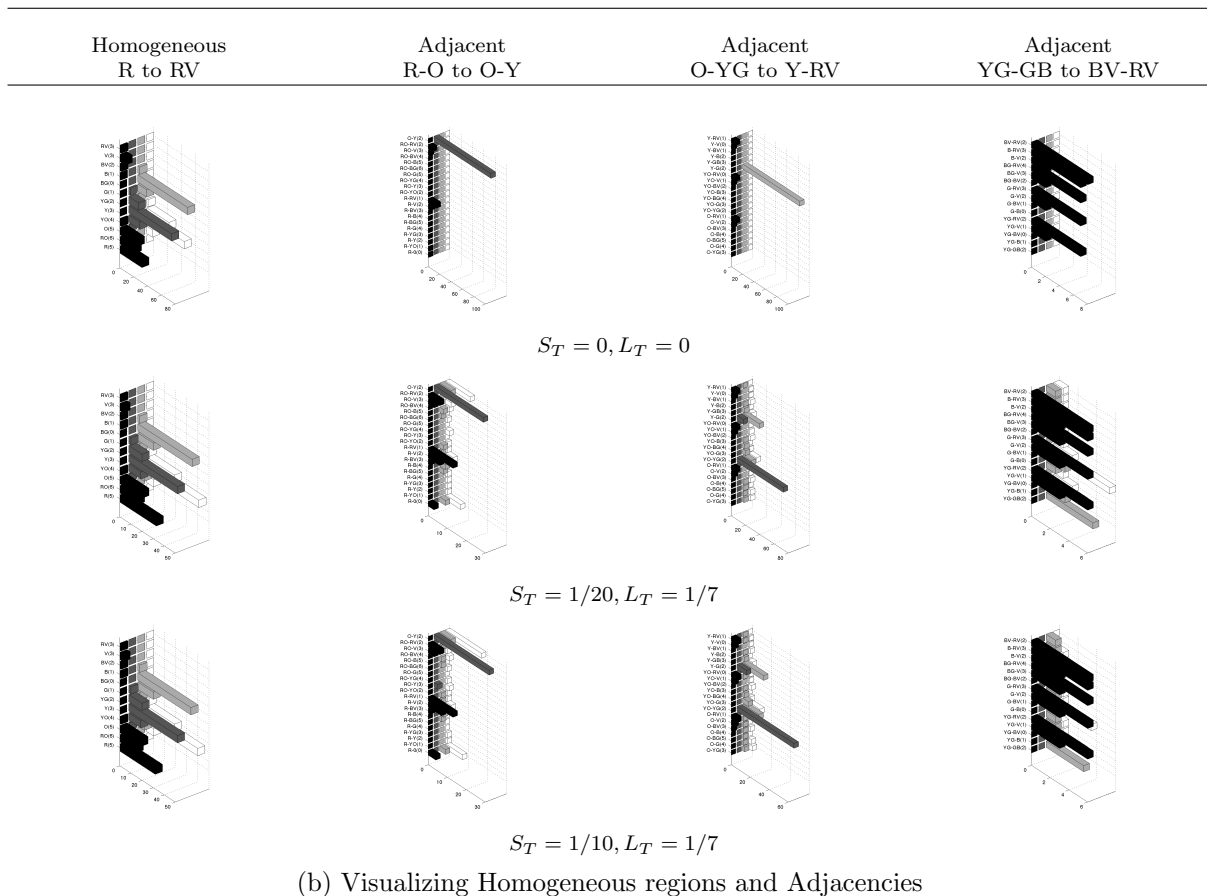


Figure 3.25: Cézanne Visualization- Histogram of homogeneous regions with warmth indices and warmth contrast strengths for adjacencies listed in parentheses.

Chapter 4

Experiments

4.1 Database

The collection of images upon which we test our computational models for *modulation*, *contrast of hue* and *cold-warm contrast* are images displayed and discussed in Itten's book 'The Art of Color'[22]. Table 4.1 shows the database of these 23 images. In this chapter, we discuss the results obtained by the proposed computational models for *modulation*, *contrast of hue* and *cold-warm contrast*. We test our computational models for analyzing artist styles on a collection of paintings from artists whom Itten mentioned for *contrast of hue* (see Table 4.2 on page 75) and *cold-warm contrast* (see Table 4.3 on page 85 and Table 4.4 on page 86). We also test the robustness of our algorithms on different digital versions of two selected paintings (see Table 4.5 on page 91).

4.2 3D Visualization and Modulation

The proposed measures for color *modulation*, as well as the color palette visualization were applied to a subset of 10 out of the 28 paintings discussed by Itten in [22] and [23], as a means to validate our computational models and the proposed color palette visualization with respect to *modulation*.

The 3D visualization of the color palette in the HSL color space requires the image to be converted from RGB to HSL, as explained in Chapter 3. HSL values range from 0 to 1. Hue values of 0 to 1 correspond to 0 to 360°, representing the hue circle. To focus on the chromatic range of colors in the image and to get a

Artist	Painting	Size in pixels	Source
Manuscript Apocalypse de Saint Sever	Revelations de Saint Jean	439 x 585	http://www.encyclopedie.bseditions.fr/
Enguerrand Charonton	Coronation of the Virgin	812 x 685	http://en.wikipedia.org/wiki/Enguerrand_Quarton
Paul de Limbourg	May day excursion	798x857	http://en.wikipedia.org/wiki/Tr%C3%A8s_Riches_Heures_du_Duc_de_Berry
Piet Mondrian	Composition in Red II	396x 470	http://www.anthroposophie.net/bibliothek/kunst/malerei/mondrian/bib_mondrian.htm
Francisco de Zurbaran	Lemons Oranges and rose	800 x 443	http://oldpainting.tumblr.com/post/6213971975/francisco-de-zurbaran-still-life-with-lemons
Rembrandt	Man in Golden Helmet	441 x 600	http://en.wikipedia.org/wiki/Rembrandt
Picasso	Guitar on a mantle piece	436 x 600	http://www.pbase.com/bmcmorrow/image/101087544/medium
Chartres	La Belle Verriere	366x 1331	http://commons.wikimedia.org/wiki/File:Chartres_-_Notre-Dame-de-la-Belle-Verri%C3%A8re.JPG
Grunewald	Angel choir Isenheim altarpiece	162 x 256	http://en.wikipedia.org/wiki/Isenheim_Altarpiece
Renoir	Le moulin de la galette (detail)	103 x 156	http://en.wikipedia.org/wiki/Pierre-Auguste_Renoir
Claude Monet	Houses of parliament	1164 x 1024	http://pictify.com/347016/claude-monet-london-houses-of-parliament-the-sun-shining-through-the-fog
Paul Cézanne	Apples and Oranges	600 x 463	http://en.wikipedia.org/wiki/Apples_and_oranges
Jan van Eyck	Madonna of the Chancellor Rolin	470 x 500	http://en.wikipedia.org/wiki/Madonna_of_Chancellor_Rolin
Piero della Francesca	Solomon Receiving the Queen Sheba	464 x 341	http://www.clivestratford.com/tag/piero-della-francesca/
Paul Cézanne	La Montagne Sainte-Victoire	417 x 327	http://album.aufeminin.com/album/668204/peintures-15850439.html
Manuscript Apocalypse de Saint Sever	Satan and the locusts	383 x 497	http://www.mmlab2.rlc.dcccd.edu/artc1353n03/assignments/unit1/Color.html
El Greco	Stripping of Christ	714 x 1211	http://www.ibiblio.org/wm/paint/auth/greco/
Vincent van Gogh	Café at Evening	232 x 300	http://www.bandagedear.com/product/cafe-terrasse-in-the-evening-by-vincent-van-gogh
Georges de la Tour	Newborn babe	1010 x 829	http://www.wga.hu/frames-e.html?/html/1/la_tour/georges/2/08newbo.html
Henri Matisse	Le Piano	319 x 370	http://www.moma.org/collection/object.php?object_id=78908
Konrad Witz	The synagogue	833 x 940	http://padraigrooney.com/blog/?p=42
Seurat	Un dimanche a la Grande Jatte	1249 x 834	http://nl.wikipedia.org/wiki/Dimanche_d'%C3%A9t%C3%A9_%C3%A0_la_Grande_Jatte
Ingres	Reclining Odalisque	849 x 476	http://en.wikipedia.org/wiki/Grande_Odalisque

Table 4.1: Database of paintings described by Itten: artist name, painting name, source

proportionally accurate visualization, we map the HSL values such that the color pixels are placed in their correct position in the HSL cylinder, centered with medium gray at position (0,0,0). We discard pixels that are very dark ($-1 \leq l \leq -0.75$), very dull ($0.75 \leq l \leq 1$), and gray ($s \leq 0.1$).

4.2.1 A comparative analysis of low and high color modulation

The results obtained on the Van Gogh and Mondrian paintings have been already discussed in Chapter 3. The remaining 8 visualizations are shown in Figures 4.1 and Figure 4.2, while the corresponding measures of *modulation* are given in Table 4.6 on page 101. The remainder of this section will discuss, for each analyzed painting, the results yielded by our computational model for *modulation* in light of Itten's comments. Images will be repeated when appropriate to support readability.

'Reclining Odalisque' by Ingres has a simple color composition that sustains the principal curves in the image. In Table 4.6, our measures correspond to high *modulation* for blue-violet, orange, yellow-orange, and blue. These sectors are characterized by low values for μ_{dist} and high values for N . Our findings support Itten's explanations: 'The color composition is very simple. Blue, orange, brown, and yellow are pure colors, modulated with black, white, and gray.'

'Un Dimanche a la Grande Jatte' by Seurat yields the highest *modulation* values in the yellow-green, green, and blue-violet hue sectors. Blue-violet colors the dress of the lady standing at the right, and the grass and the trees are mixtures of yellow, green, and yellow-green. All these areas are highly modulated, according to Itten: 'None of these areas are painted in homogeneously mixed colors; each consists of many distinguishable notes, meeting as smooth textures only in the eye of the observer.'

For 'May-Day Excursion' by Limbourg, we have computed high *modulation* values in yellow-green and green, which are hues expressive of spring and lend the scene a joyous and lively expression. Interestingly, despite the obvious differences in style between Seurat (impressionist) and Limbourg (Dutch medieval miniaturist painter), the two paintings convey the same enjoyment of spring via *modulation* in green hues.

'Houses of Parliament in fog' by Monet results are highly modulated in blue, blue-violet, and red. Warm (red) modulating tones are used for the last rays of the setting sun, which contrasts with cold (blue and blue-violet) tones of the foggy buildings and water. According to Itten '[Monet] meant to portray the shimmer of light in the air and over warm fields, color refractions in cloud and mist, highlights of flowing, undulant water, and the alternation of sunny and shady green in the foliage of trees'.

'Le Piano' by Matisse is an example of the use of low *modulation* in all hues except red, green, and blue (see Table 4.2). The painting contains large areas of quasi-homogenous color. The contrast is bold and unmodulated. According to Itten,

‘Over many years of activity, Matisse increasingly negated local color and modeling in light and shade. His paintings became more and more flat and abstract.’

Computed *modulation* measures for ‘Newborn Babe’ by de la Tour show high *modulation* only in the red hues. All other hue sectors are low-modulated. Some of the hue sectors are not populated at all, leading to zero-values. Low *modulation* in all populated hue sectors except red results in an introverted, meditative mood as indicated by Itten.

‘Apples and Oranges’ by Cézanne is a good example of modulated *cold-warm contrast*, as results show that red is the highest modulated hue, followed by blue-violet and violet. One may note that ‘Apples and Oranges’ and ‘Houses of Parliament in fog’ employ the same modulated cold-warm contrast. However, the two paintings convey a very different message and mood. This is due to differences in other aesthetic elements such as shape and composition, and relative ratios of green colors.

‘The Synagogue’ by Witz employs high *modulation* in the orange contrasting to high modulation in violet. Orange corresponds to portions of the lady’s dress, which is transformed into ‘a living, vibrant chord of simultaneous resonance.’

4.3 Contrast of hue and cold-warm contrast

In Chapter 3, we illustrated our computational model for *contrast of hue* by discussing the results on ‘The Coronation of the Virgin’, and our computational model for *cold-warm contrast* by discussing our results on ‘La belle verriere’. We also illustrated our computational models for analyzing artists’ styles for *contrast of hue* by discussing our results on a collection of Picasso’s paintings, and *cold-warm contrast* by discussing our results on Cézanne’s paintings. In this section, we will discuss the remainder of the paintings that Itten discussed and analyze the styles of artists he mentions with respect to both contrasts.

4.3.1 Contrast of hue results on Itten’s dataset

Contrast of hue occurs when a painting contains only a few fully saturated hues. Although adjacencies exist, they are few and do not represent the focus of the painting. In this section we will analyze in detail the remaining three paintings that Itten discussed as examples for showing *contrast of hue*:

- Limbourg’s ‘May-Day Excursion’

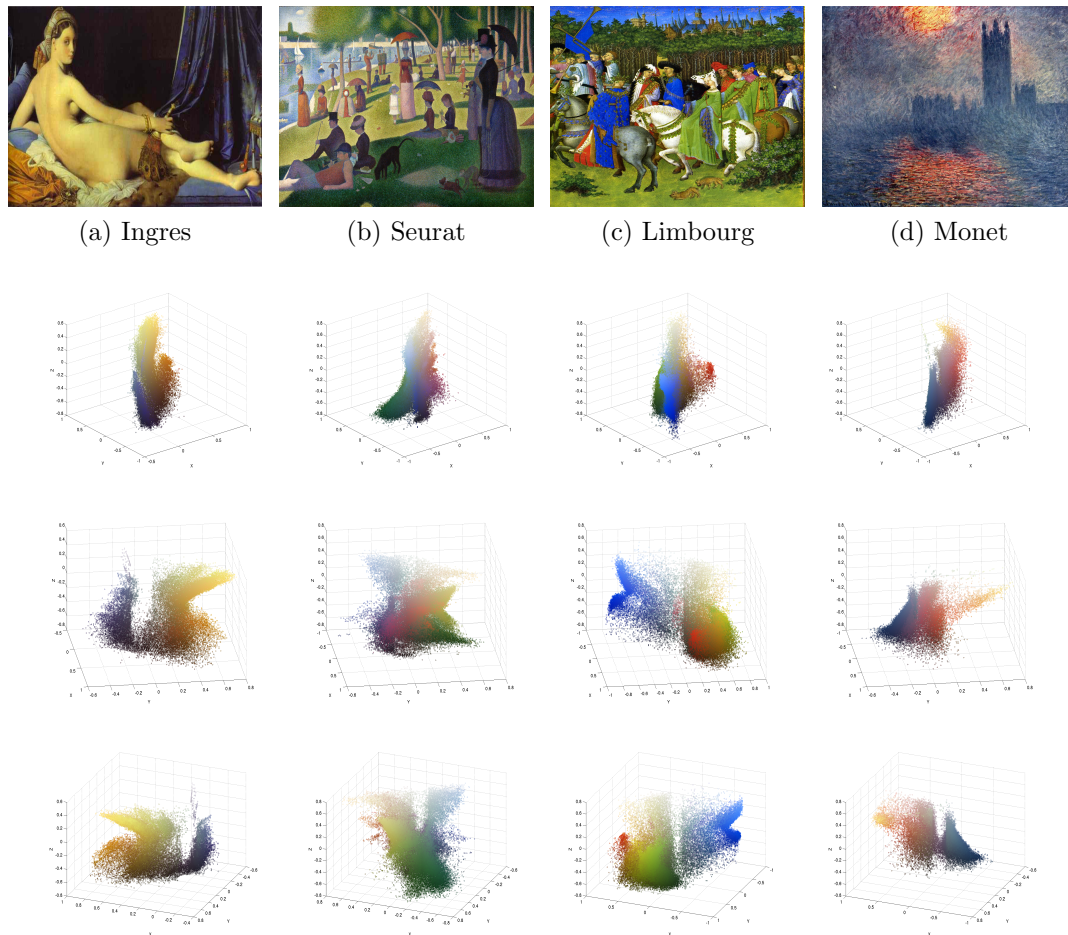


Figure 4.1: Paintings and their corresponding color palettes shown in incremental 120° rotations about the z axis. Column a) ‘Reclining Odalisque’ by Ingres; Column b) ‘Un Dimanche a la Grande Jatte’ by Seurat; Column c) ‘May Day excursion’ by Limbourg; Column d) ‘Houses of Parliament in fog’ by Monet

- ‘L’eglise d’Ephese’ found in a manuscript Apocalypse de Saint Sever. Although we were not able to find the image Itten has in his book, we used ‘Revelations de Saint Jean’ (see Figure 4.4), a different image from the same manuscript as he explicitly states that all images in the manuscript use *contrast of hue*.
- Mondrian’s ‘Composition in Red II’ - in place of Mondrian’s Composition 1928 due to the difficulty in finding a good quality version of Composition 1928. Yet, according to Itten, Mondrian’s artistic style is based on the use of *contrast of hue*.

Itten refers to Limbourg’s ‘May-Day Excursion’ as a perfect example *contrast of hue*[22]. Figure 4.3 shows the image, and the summary of the *contrast of hue*



Figure 4.2: Paintings and their corresponding color palettes shown in incremental 120° rotations about the z axis. Column a) ‘Le Piano’ by Matisse; Column b) ‘Newborn Babe’ by de la Tour; Column c) ‘Apples and Oranges’ by Cézanne; Column d) ‘The Synagogue’ by Witz

co-occurrence results in the homogeneous regions that are captured within the three ranges we measured. The *contrast of hue* takes place between blue, orange and yellow-orange which are fully saturated and are detected in the first range of parameters ($S_T = 0, L_T = 0$). The large patch of green is not fully saturated, and shows some variation in the light and saturation, and as such is detected in the second range of parameters ($S_T = 1/20, L_T = 1/7$). For this image, the first range $S_T = 0, L_T = 0$ is sufficient for capturing the hues involved in the *contrast of hue*.

Itten discussed the painting ‘L’eglise d’Ephese’ from the manuscript of Saint Sever as an example of *contrast of hue*. We were unable to find a digital copy of the image and therefore ran our algorithm on ‘Revelations de Saint Jean’, another painting



Chromatic ground truth: blue, red, green and some yellow-gold (brownish)

$S_{T1} = 0, L_{T1} = 0$ Percentage	$S_{T1} = 1/20, L_{T1} = 1/7$ Percentage	$S_{T1} = 1/10, L_{T1} = 1/7$ Percentage
B 81%	B 68%	B 65%
O 3%	YG 5%	YG 6%
YO 3%	O 4%	O 4%
YG 3%	RO 3%	YO 4%
RO 2%	YO 3%	Y 4%
Y 2%	R 3%	RO 3%
R 1%	R 1%	R 1%
		G 1%

Figure 4.3: Summary of normalized co-occurrences for ‘May-Day Excursion’

from the same manuscript. According to Itten, the whole manuscript employs the *Contrast of Hue*. Figure 4.4 displays the image, and the percentage of co-occurrences in the homogeneous regions. All three ranges of parameters capture YO, O, RO and Y. The third range of parameters ($S_{T1} = 1/10, L_{T1} = 1/7$), however, accurately captures orange and red-orange as having the largest co-occurrences. This is likely due to discoloration in the image, caused by the aging of the manuscript.

Mondrian’s ‘Composition in Red II’ is another example of *contrast of hue*, in the same theme as his ‘Composition 1928’ mentioned by Itten. Figure 4.5 displays the image, and the percentage of co-occurrences in the homogeneous regions. Blue having less co-occurrences than yellow in the first range ($S_{T1} = 0, L_{T1} = 0$), and appearing

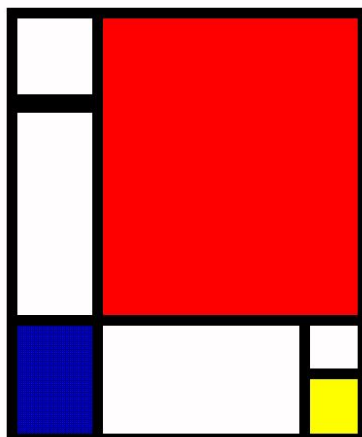


Homogeneous regions					
$S_{T_1} = 0, L_{T_1} = 0$	Percentage	$S_{T_1} = 1/20, L_{T_1} = 1/7$	Percentage	$S_{T_1} = 1/10, L_{T_1} = 1/7$	Percentage
YO	32%	O	24%	O	24%
O	27%	YO	21%	RO	19%
RO	22%	RO	19%	YO	19%
Y	5%	Y	2%	Y	2%

Figure 4.4: Summary of normalized co-occurrence for ‘Revelations de Saint Jean’

correctly in the second range is an unexpected result. This is due to the vertical and horizontal lines in the blue region that break up the homogeneity of the region. These lines are seen when we zoom into the image. This effect is likely an artifact of the digital copy rather than the original painting. As such, the range $S_{T_1} = 0, L_{T_1} = 0$ is sufficient for capturing the *contrast of hue*.

We thus confirm that the first range is sufficient in capturing the *contrast of hue* when the image quality is good. Otherwise, broadening the range is necessary.



Homogeneous regions					
$S_{T_1} = 0, L_{T_1} = 0$	Percentage	$S_{T_1} = 1/20, L_{T_1} = 1/7$	Percentage	$S_{T_1} = 1/10, L_{T_1} = 1/7$	Percentage
R	95%	R	88%	R	88%
Y	3%	Y	3%	Y	3%
B	2%	B	9%	B	9%

Figure 4.5: Summary of normalized co-occurrence for ‘Composition in Red II’

4.3.2 Contrast of hue results per artist

We applied our algorithm for *contrast of hue* on a collection of paintings from artists to whom Itten referred for the use of *contrast of hue*: Fra Angelico, Botticelli, Kandinsky, Macke, Franz Marc and Miro. Table 4.2 on page 75 displays our database of images for the *contrast of hue*.

An example of Fra Angelico’s painting is ‘Tangere’. In this image, the *contrast of hue* occurs between the dress of the kneeling saint, the yellow and yellow-orange halo around both saints as well as the golden fence in the background. Figure 4.6 shows the image and the co-occurrence patterns in the homogeneous regions. The chromatic range is captured in the first range of parameters ($S_{T_1} = 0, L_{T_1} = 0$). Both of Fra Angelico’s painting in our database and the 3D histograms to visualize the *contrast of hue* co-occurrence patterns in the homogeneous regions of the results are shown in Figure 4.7 (page 67). Our observations of the paintings and the co-occurrence results in the homogeneous regions are that Fra Angelico used orange as the dominant hue and kept the contrasting colors in the range of red to yellow-orange in the color wheel.

An example of Botticelli’s painting is ‘The Madonna’. Figure 4.8 (page 68) shows

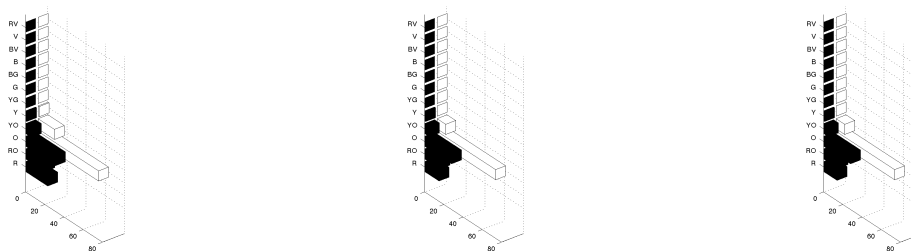
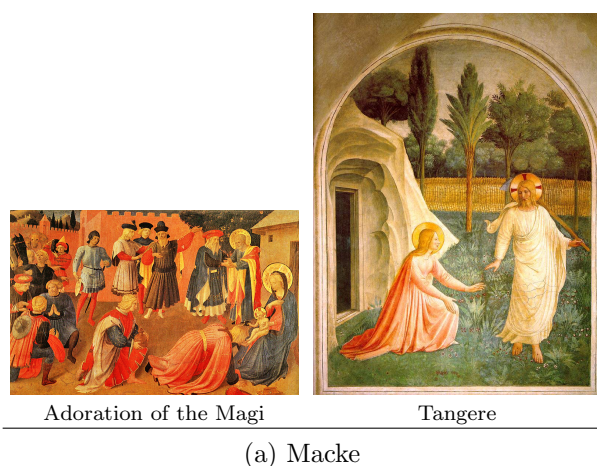


Homogeneous regions					
$S_{T1} = 0, L_{T1} = 0$		$S_{T1} = 1/20, L_{T1} = 1/7$		$S_{T1} = 1/10, L_{T1} = 1/7$	
O	63%	O	61%	O	61%
Y-O	17%	Y-O	9%	Y-O	9%
R-O	4%	R-O	6%	R-O	5%
R	1%	R	1%	R	1%
Y	1%				

Figure 4.6: Fra Angelico-Tangere

the image and the co-occurrence patterns in the homogeneous regions. In this image, the *contrast of hue* occurs between the red, orange and dark clothing at the bottom left of the image. This chromatic range is captured in the first range of parameters ($S_{T1} = 0, L_{T1} = 0$). The remainder of Botticelli's paintings and the 3D histograms to visualize the *contrast of hue* co-occurrence patterns in the homogeneous regions are shown in Figure 4.9 (page 69). Our observations of Botticelli's paintings is that homogeneous regions have a similar color scheme with one dominant hue and one or more secondary hues.

An example of Kandinsky's painting is 'Church of St. Ursula'. Figure 4.10 (page 70) shows the image and the co-occurrence patterns in the homogeneous regions. The *contrast of hue* occurs between the saturated patches of color: yellow green, orange, blue-violet, yellow. The first range of parameters captures the co-occurrences of the homogeneous regions more accurately than the second range of parameters, as the blue-violet sky has more co-occurrences than the yellow patches. Both of Kandinsky's paintings in our database, and the 3D histograms to visualize the *contrast of hue*



$$S_T = 1/10, L_T = 1/7$$

(b) 3D Visualization of homogeneous regions

Figure 4.7: Fra Angelico Visualization- Histogram of homogeneous regions

co-occurrence patterns in the homogeneous regions are shown in Figure 4.11 (page 71). Our observations of Kandinsky's paintings are that he uses no more than three principal hues, which is in line with *contrast of hue*.

An example of Macke's painting is 'Market in Algiers'. Figure 4.12 (page 72 shows the image and the *contrast of hue* co-occurrence patterns in the homogeneous regions. The *contrast of hue* occurs between the saturated regions of color such as red, orange, yellow, green. The second range of parameters ($S_T = 1/20, L_T = 1/7$) produces more accurate results, due to mild variations in the light and saturation. The remainder of Macke's paintings and the 3D histograms to visualize the *contrast of hue* co-occurrence patterns in the homogeneous regions are shown in Figure 4.13 (page 76). We observe that Macke uses few dominant hues in the contrasting homogeneous regions and these hues are adjacent in the color wheel.

An example of Franz Marc's painting is 'Blue Horse'. Figure 4.14 (page 77)



Homogeneous regions					
$S_{T_1} = 0, L_{T_1} = 0$		$S_{T_1} = 1/20, L_{T_1} = 1/7$		$S_{T_1} = 1/10, L_{T_1} = 1/7$	
YO	43%	O	20%	O	31%
O	27%	YO	25%	YO	23%
R	14%	R	15%	R	15%
RO	8%	RO	7%	RO	7%
Y	3%	Y	2%	Y	2%

Figure 4.8: Botticelli- The Madonna

shows the image and the co-occurrence patterns in the homogeneous regions. In this image, the *contrast of hue* occurs primarily between the blue, red-orange and yellow as captured in the first range of parameters. The remainder of Franz Marc's paintings and the 3D histograms to visualize the *contrast of hue* co-occurrence patterns in the homogeneous regions are shown in Figure 4.15 (page 78). We observe that Franz Marc tends to use one dominant hue, as detected in the first range of parameters ($S_{T_1} = 0, L_{T_1} = 0$).

An example of Miro's painting is 'The Garden'. Figure 4.16 (page 79) shows the image and the co-occurrence patterns in the homogeneous regions. In this image, saturated patches of many contrasting colors compete over the light blue background. The range of colors is well captured in the first range of parameters. The remainder of Miro's paintings and the 3D histograms to visualize the *contrast of hue* co-occurrence patterns in the homogeneous regions are shown in Figure 4.17 (page 80). We observe that Miro uses few dominant hues and these hues are adjacent in the color wheel.

We conclude as such that our computational model for exploring the *contrast of hue* patterns in an artist's style is valuable.

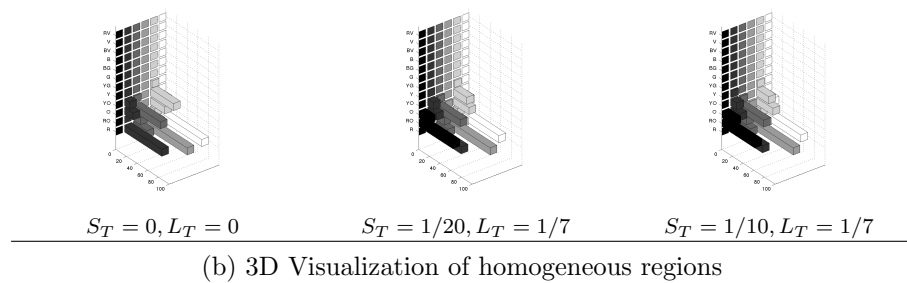
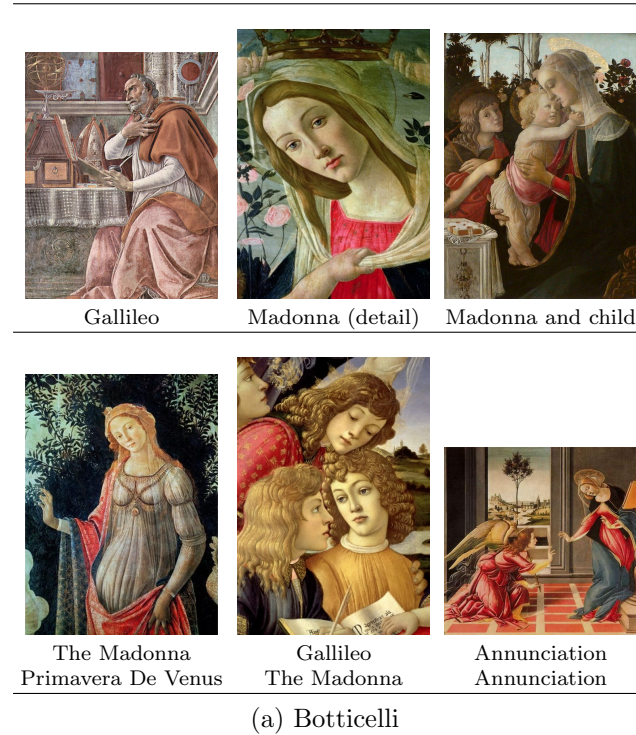
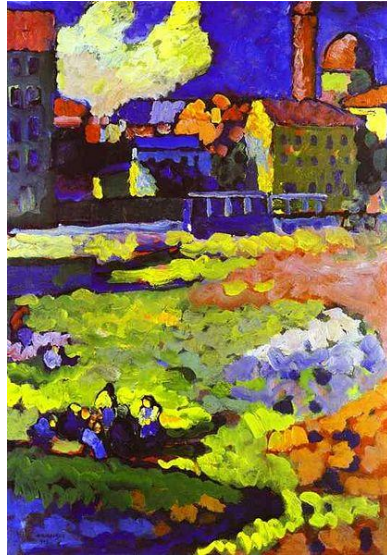


Figure 4.9: Botticelli Visualization- Histogram of homogeneous regions

4.3.3 Cold-warm contrast results on Itten's dataset

Cold-warm contrast is achieved by contrasting the warmth of the homogeneous regions, as well as the more subtle interplay of the hues within medium light range, and no light changes. There is no requirement for the saturation to remain unchanged, however, in the pure sense of the use of *cold-warm contrast*, it is best to assume that *contrast of saturation* is not at play. Our discussion in Chapter 3 includes an analysis of the *warmth indices* for the hues, and the *warmth contrast strength* in the adjacencies, and a detailed analysis of three of the seven paintings Itten discussed: Cézanne's 'Apples and Oranges', Cézanne's 'La Montagne St.Victoire' and 'La belle verriere'.



Homogeneous regions					
$S_{T1} = 0, L_{T1} = 0$		$S_{T1} = 1/20, L_{T1} = 1/7$		$S_{T1} = 1/10, L_{T1} = 1/7$	
YG	31%	YG	36%	YG	36%
O	17%	O	19%	O	18%
BV	16%	Y	9%	Y	9%
Y	10%	BV	8%	BV	8%
RO	7%	RO	5%	RO	5%
G	3%	YO	3%	YO	3%
YO	3%	R	1%	R	1%
R	1%	G	1%	R	1%
		B	1%	B	1%

Figure 4.10: Kandinsky-Church of St. Ursula

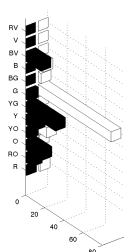
Warmth contrast strengths are mild (1,2), medium (3,4) and strong (5,6). We will now analyze the remaining four paintings that Itten described as showing *cold-warm contrast*:

- Grunewald's 'Angel Choir'
- Monet's 'Houses of Parliament'
- Renoir's 'Le Moulin de la Galette (Detail)'
- Witz' 'The Synagogue'

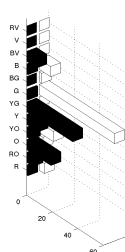
Grunewald's 'Angel Choir' is a portion of a larger painting: 'The Eisenheim Altarpiece'. According to Itten, the bright angel in the front is painted in light cold-warm



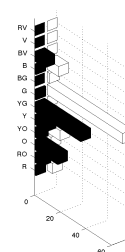
(a) Kandisky



$$S_T = 0, L_T = 0$$



$$S_T = 1/20, L_T = 1/7$$



$$S_T = 1/10, L_T = 1/7$$

(b) 3D Visualization of homogeneous regions

Figure 4.11: Kandinsky Visualization- Histogram of homogeneous regions

modulation of cool red and warm orange and gold, the soloist in the middle is ‘clad in hues from cool red to warm orange’ contrasting with the yellow-green halo of the angel in the back. Figure 4.18 (page 81) displays the image, the *cold-warm contrast* results in the homogeneous regions and adjacencies. The second range of parameters ($S_{T1} = 1/20, L_{T1} = 1/7$) is needed to capture the homogeneous regions as well as adjacencies. The homogeneous regions show that we have a generally warm image with a *warmth index* range of 4 to 6, and the adjacencies show a mild to medium *warmth contrast strength*.

Monet’s ‘Houses of Parliament’ imparts a strong feeling of *cold-warm contrast* as the sun breaks through the fog. According to Itten, ‘Monet uses the cold-warm contrast orange/blue-violet’[22, p. 74]. Figure 4.19 (page 82) displays the image, the



Homogeneous regions					
$S_{T_1} = 0, L_{T_1} = 0$		$S_{T_1} = 1/20, L_{T_1} = 1/7$		$S_{T_1} = 1/10, L_{T_1} = 1/7$	
YG	46%	YG	25%	YG	25%
R	24%	R	25%	R	25%
RO	7%	O	11%	O	11%
O	6%	YO	10%	YO	10%
YO	6%	RO	9%	RO	9%
Y	5%	Y	4%	Y	3%
G	1%	G	1%	G	1%

Figure 4.12: Macke- Market in Algiers

cold-warm contrast results in the homogeneous regions and adjacencies. The results show that the second range of parameters ($S_{T_1} = 1/20, L_{T_1} = 1/7$) captures the co-occurrences in the homogeneous regions, as well as the *modulations* reflected in the adjacencies. The sharpest warmth contrast occurs between red-orange (*warmth index 6*) and the small bit of blue-green (*warmth index 0*).

In describing the cold-warm effect of Renoir's 'Le Moulin de la galette', Itten only discusses the portion with the face of the woman in the center of the image. Figure 4.20 (page 83) displays the image, the *cold-warm contrast* results in the homogeneous regions and adjacencies. According to Itten "The colors in this painting all have a semblance of reflection [...] This effect is owing to cold-warm contrast" [22, p. 72]. The results show that the third range of parameters ($S_{T_1} = 1/10, L_{T_1} = 1/7$) captures the co-occurrences in the homogeneous regions, as well as the *modulations* of yellow and green reflected in the adjacencies. The warmth index captures the warmth of the image (*warmth index 4 and 5*) with a mild contrast in the adjacencies.

In his discussion of ‘The Synagogue’, Itten highlights that the yellow dress is modulated with violet tones of a similar brilliance and warm shadow tones seen in the red-orange of the sleeves. Figure 4.21 (page 84) displays the image, the *cold-warm contrast* results in the homogeneous regions and adjacencies. The third range of parameters ($S_{T1} = 1/10, L_{T1} = 1/7$) is needed to capture BV-RV adjacencies in the image. The high percentage of co-occurrences in the homogeneous regions that have a high warmth index (4-6) is indicative of the overall warmth of the image. The adjacencies reflect *modulations* with mild and medium *contrast strength*.

We conclude as such that our computational model is a valuable tool in analyzing *cold-warm contrast* in paintings. The second range of parameters is needed to capture the contrast, and the third range is needed for lower quality images.

4.3.4 Cold-warm contrast results per artist

In Chapter 3, we used our computational model to assess the use of *cold-warm contrast* in Cézanne’s paintings grounded in Itten’s comments and descriptions. Itten also mentioned that the following artists use *cold-warm contrast* in their work: Bonnard, Monet, Pissaro and Renoir. Table 4.3 on page 85 and Table 4.4 on page 86 show the database of images we used to test our computational model.

An example of Bonnard’s painting is ‘Earthly Paradise’. Figure 4.22 (page 87) displays the image, and the *cold-warm contrast* results for the homogeneous regions and adjacencies. This painting is highly modulated. In the second range of parameters ($S_{T1} = 1/20, L_{T1} = 1/7$), we see that that the *warmth index* of the homogeneous regions ranges from 0 to 6. In the adjacencies, the *warmth contrast strength* values show a pattern of mild contrast. Both of Bonnard’s paintings in our database, and the 3D histograms to visualize the *cold-warm contrast* co-occurrence patterns in both the homogeneous regions and the adjacencies are displayed in Figure 4.23 (page 88). In the second row of 3D histograms ($S_{T1} = 1/20, L_{T1} = 1/7$), we observe that the homogeneous regions in Bonnard’s paintings are mostly warm with a peak at orange (*warmth index 5*). We also observe that the peaks in the adjacencies are of mild and medium *warmth contrast strength*.

An example of Monet’s painting is ‘Water Lilies’. Figure 4.24 (page 89) displays the image, the *cold-warm contrast* results for the homogeneous regions and adjacencies. For this painting, we need the third range of parameters ($S_{T1} = 1/10, L_{T1} = 1/7$) as the quality is poor. We see a mostly cool image with homogenous regions having

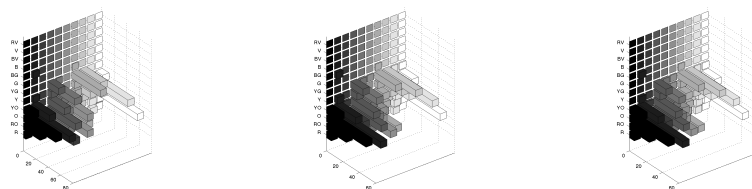
a warmth index of 1 and 0, contrasted with small amount of cooler hues. We also see highly modulated mild to medium contrasts in the adjacencies. The remainder of Monet's paintings are displayed in Figure 4.25 (page 92). The 3D histograms to visualize the *cold-warm contrast* co-occurrence patterns in both the homogeneous regions and the adjacencies are displayed in Figure 4.26 (page 93). We see a pattern where the highest percentage of co-occurrences is clustered around one peak in the homogeneous regions, as captured by the second range of parameters ($S_{T1} = 1/20, L_{T1} = 1/7$). This result corresponds to our observation that Monet painted many portraits with a landscape in the background. Some of his paintings are primarily warm, some are primarily cold, while others have both warm and cold hues. The peaks in the adjacencies have a mild *warmth contrast strength*.

Artist	Painting	Size in pixels	Source
Sandro Botticelli	Annunciation	600 x 587	http://historylink101.com/art/Sandro_Botticelli/pages/26_Annunciation_jpg.htm
Sandro Botticelli	Gallileo	350 x 450	http://www.theguardian.com/science/gallery/2009/mar/12/galileo-exhibition-florence-strozzi
Sandro Botticelli	Madonna and child	578 x 800	http://www.artcyclopedia.com/artists/botticelli_sandro.html
Sandro Botticelli	Madonna (detail)	417 x 585	http://botticellipaintings.com/
Sandro Botticelli	Primavera de Venus	431 x 585	http://www.artble.com/artists/sandro_botticelli/paintings/primavera
Sandro Botticelli	The Madonna	285 x 411	http://www.canvasreplicas.com/Botticelli.htm
Fra Angelico	Adoration of the Magi	859 x 550	http://englishclass.jp/reading/topic/Fra_Angelico
Fra Angelico	Tangere	781 x 1034	http://en.wikipedia.org/wiki/Noli_me_tangere
Franz Marc	Blue Horse	337 x 450	http://franzmarcpaintings.com/
Franz Marc	Fighting Forms 1914	1102 x 771	http://franzmarcpaintings.com/
Franz Marc	Fox	338 x 450	http://franzmarcpaintings.com/
Franz Marc	Mandrill	900 x 608	http://reproarte.com/de/bilder/der-mandrill-detail
Franz Marc	The enchanted mill 1913	821 x 1169	http://www.wikiart.org/en/franz-marc/the-enchanted-mill-1913
Franz Marc	The first animals 1913	1077 x 918	http://www.wikiart.org/en/franz-marc/the-first-animals-1913
Kandinsky	Church of St.Ursula	416 x 599	http://www.wikiart.org/en/wassily-kandinsky/munich-schwabing-with-the-church-of-st-ursula-1908
Kandinsky	Reiter	500 x 366	http://en.wikipedia.org/wiki/Wassily_Kandinsky
Macke	A Street	376 x 500	http://www.augustmacke.org
Macke	Children at the pump	470x x 401	http://www.augustmacke.org
Macke	Colored Composition	370 x 500	http://www.augustmacke.org
Macke	Colored Forms II	404 x 500	http://www.augustmacke.org
Macke	Farbige Formen III	408 x 500	http://www.augustmacke.org
Macke	Garden Gate	146 x 180	http://www.augustmacke.org
Macke	Market in Algier	376 x 500	http://www.augustmacke.org
Macke	Tegernsee Landscape	460 x 500	http://www.augustmacke.org
Macke	Turkish Caf	344 x 500	http://www.augustmacke.org
Macke	Vegetable Fields	470 x 370	http://www.augustmacke.org
Miro	Dona 3	398 x 571	http://joanmiro.com
Miro	Dutch Interiors	481 x 637	http://metmuseum.org
Miro	Dutch	474 x 593	http://utopiadystopiawwi.wordpress.com/surrealism/joan-miro/dutch-interior/
Miro	Plage de Mont Roig	500 x 407	http://catalogue.successiomiro.com/
Miro	Portrait Oil	425 x 539	http://www.abs-art.com/
Miro	Self Portrait	607 x 734	http://joanmiro.com
Miro	The farm	700 x 599	http://www.ebuypainting.com/
Miro	The garden	334 x 425	http://www.ebuypainting.com/
Miro	The Red Sun	382 x 500	http://www.ebuypainting.com/
Miro	There was a little Magpie	640 x 640	http://www.ebuypainting.com/
Miro	The singing fish	510 x 640	http://www.ebuypainting.com/
Miro	The village Prades	423 x 374	http://www.ebuypainting.com/
Picasso	Cruxificion	731 x 561	http://www.statveritas.com.ar/Arte/CPA-06.htm
Picasso	Girl Reading At Table	446 x 549	http://www.reproduction-gallery.com/oil_painting/details/copy_artist/1069414354/masterpiece/Pablo_Picasso/museum_quality/Girl_Reading_at_a_Table_1934.xhtml
Picasso	Guernica	758 x 339	http://arts-wallpapers.com/wallpaper/guernica/
Picasso	Guitar on the Mantle Piece	436 x 600	http://www.pbase.com/bmcmorrow/image/101087544
Picasso	Weeping Woman	870 x 1058	http://www.pablopicasso.org/the-weeping-woman.jsp

Table 4.2: Artists who used *contrast of hue*: Botticelli, Fra Angelico, Franz Marc, Kandinsky, Macke



(a) Macke



$$S_T = 1/10, L_T = 1/7$$

(b) 3D Visualization of homogeneous regions

Figure 4.13: Macke Visualization- Histogram of homogeneous regions

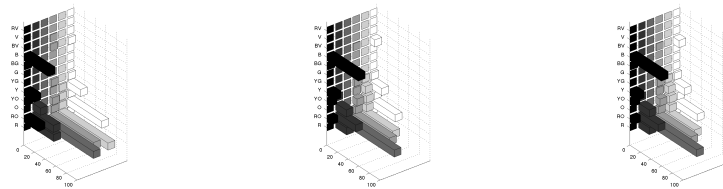


Homogeneous regions					
$S_{T1} = 0, L_{T1} = 0$		$S_{T1} = 1/20, L_{T1} = 1/7$		$S_{T1} = 1/10, L_{T1} = 1/7$	
B	46%	B	59%	B	59%
RO	27%	Y	14%	Y	14%
Y	19%	RO	8%	RO	7%
YO	4%	YO	6%	YO	6%
BG	2%	BG	2%	BG	2%

Figure 4.14: Franz Marc - Blue Horse



(a) Franz Marc



$$S_T = 1/10, L_T = 1/7$$

(b) 3D Visualization of homogeneous regions

Figure 4.15: Franz Marc Visualization- Histogram of homogeneous regions

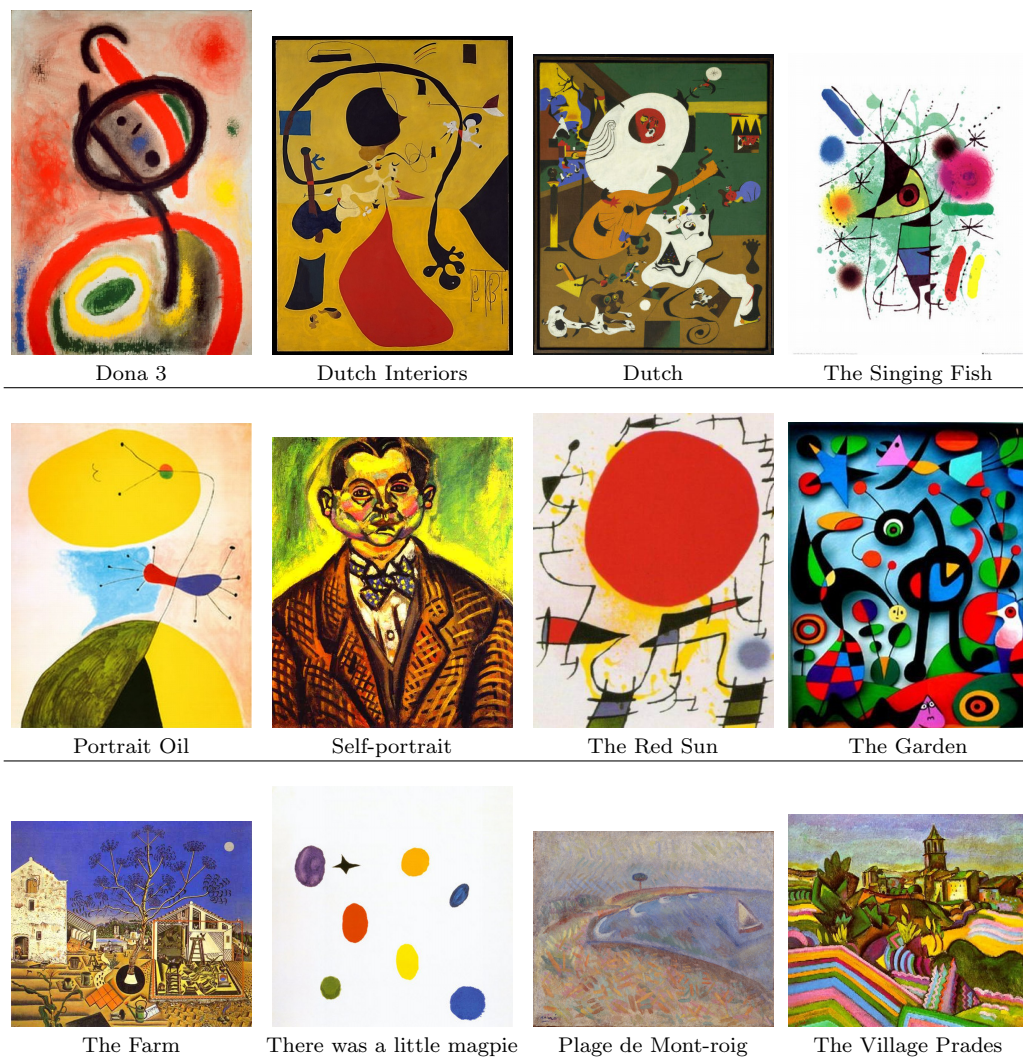


Homogeneous regions

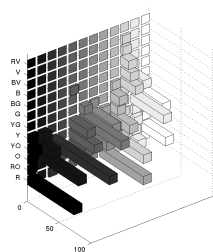
$S_{T_1} = 0, L_{T_1} = 0$ $S_{T_1} = 1/20, L_{T_1} = 1/7$ $S_{T_1} = 1/10, L_{T_1} = 1/7$

R	36%	R	26%	R	26%
G	23%	G	19%	G	19%
BG	16%	B	19%	B	19%
B	13%	BG	15%	BG	15%
BV	4%	BV	3%	O	3%
V	3%	O	3%	V	2%
RO	1%	RO	2%	RO	2%
O	1%	V	2%	YO	1%
YO	1%	YO	1%	Y	1%

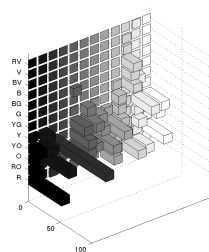
Figure 4.16: Miró- The garden



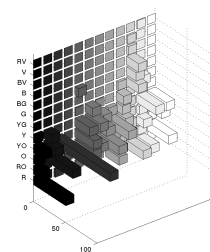
(a) Miró



$$S_T = 0, L_T = 0$$



$$S_T = 1/20, L_T = 1/7$$



$$S_T = 1/10, L_T = 1/7$$

(b) Visualizing Homogeneous regions and Adjacencies

Figure 4.17: Miró Visualization- Histogram of homogeneous regions



Homogeneous regions

$S_{T_1} = 0, L_{T_1} = 0$	Warmth Index	$S_{T_1} = 1/20, L_{T_1} = 1/7$	Warmth Index	$S_{T_1} = 1/10, L_{T_1} = 1/7$	Warmth Index
O(47%)	5	O(45%)	5	O(45%)	5
RO(37%)	6	RO(22%)	6	RO(21%)	6
R(11%)	5	R(8%)	5	R(8%)	5
YO(4%)	4	YO(2%)	4	YO(2%)	4

Adjacencies

$S_{T_1} = 0, L_{T_1} = 0$	Contrast Strength	$S_{T_1} = 1/20, L_{T_1} = 1/7$	Contrast Strength	$S_{T_1} = 1/10, L_{T_1} = 1/7$	Contrast Strength
		R-O(50%)	1	R-O(38%)	1
		O-Y(21%)	2	O-Y(38%)	2
		O-YG(7%)	3	YO-YG(10%)	2
		YO-YG(7%)	2	O-YG(5%)	3
		YO-G(7%)	3	YO-G(5%)	3
		R-RV(7%)	1	R-RV(5%)	1

Figure 4.18: Summary of normalized co-occurrences for ‘Angel choir’



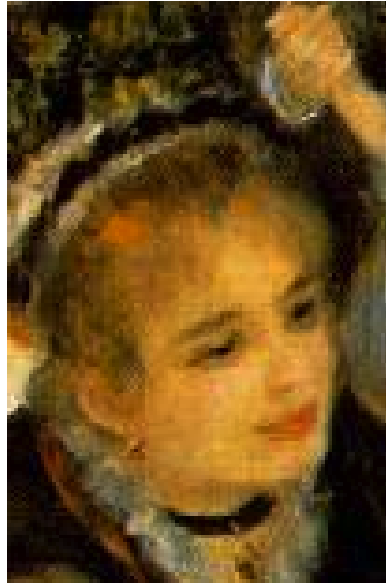
Homogeneous Regions

$S_{T_1} = 0, L_{T_1} = 0$	Warmth Index	$S_{T_1} = 1/20, L_{T_1} = 1/7$	Warmth Index	$S_{T_1} = 1/10, L_{T_1} = 1/7$	Warmth Index
B(58%)	1	B(38%)	1	B(38%)	1
R(12%)	5	R(18%)	5	R(18%)	5
BV(9%)	2	BV(6%)	2	BV(6%)	2
V(4%)	3	RO(6%)	6	RO(6%)	6
RO(4%)	6	O(4%)	5	O(4%)	5
RV(1%)	4	V(3%)	3	V(3%)	3
YO(1%)	4	G(1%)	1	G(1%)	1
G(1%)	1	BG(1%)	0	BG(1%)	0
BG(1%)	0				

Adjacencies

$S_{T_1} = 0, L_{T_1} = 0$	Contrast Strength	$S_{T_1} = 1/20, L_{T_1} = 1/7$	Contrast Strength	$S_{T_1} = 1/10, L_{T_1} = 1/7$	Contrast Strength
R-RV(11%)	1	R-RV(8%)	1	R-RV(8%)	1
B-RV(8%)	3	R-V(6%)	2	R-V(6%)	2
Y-RV(6%)	1	BV-RV(5%)	1	BV-RV(5%)	2
G-RV(6%)	3	O-RV(4%)	1	O-RV(4%)	1
RO-RV(6%)	2	RO-RV(4%)	2	RO-RV(4%)	2
O-RV(6%)	1	G-RV(4%)	3	G-RV(4%)	3
YO-RV(6%)	0	Y-RV(4%)	1	Y-RV(4%)	1
YG-RV(6%)	2	YO-RV(4%)	0	YO-RV(4%)	0
BG-RV(6%)	4	BG-RV(4%)	4	BG-RV(4%)	4

Figure 4.19: Summary of normalized co-occurrences for ‘Houses of Parliament’



Homogeneous Regions					
$S_{T_1} = 0, L_{T_1} = 0$	Warmth Index	$S_{T_1} = 1/20, L_{T_1} = 1/7$	Warmth Index	$S_{T_1} = 1/10, L_{T_1} = 1/7$	Warmth Index
O(100%)	5	O(87%) YO(6%)	5 4	O(87%) YO(5%)	5 4
Adjacencies					
$S_{T_1} = 0, L_{T_1} = 0$	Contrast Strength	$S_{T_1} = 1/20, L_{T_1} = 1/7$	Contrast Strength	$S_{T_1} = 1/10, L_{T_1} = 1/7$	Contrast Strength
		Y-G(100%)	2	O-Y(50%) Y-G(50%)	2 2

Figure 4.20: Summary of normalized co-occurrences for ‘Le moulin de la galette’



Homogeneous Regions					
$S_{T1} = 0, L_{T1} = 0$	Warmth Index	$S_{T1} = 1/20, L_{T1} = 1/7$	Warmth Index	$S_{T1} = 1/10, L_{T1} = 1/7$	Warmth Index
O(43%)	5	O(40%)	5	O(40%)	5
YO(20%)	4	YO(16%)	4	YO(16%)	4
R(13%)	5	R(9%)	5	R(9%)	5
RO(4%)	6	RO(4%)	6	RO(4%)	6
Y(3%)	3	Y(2%)	3	Y(2%)	3
V(3%)	3	B(2%)	1	B(2%)	1
RV(3%)	4	V(2%)	3	V(2%)	3
G(2%)	1	YG(1%)	2	YG(1%)	2
BG(2%)	0	G(1%)	1	G(1%)	1
BV(2%)	2	BG(1%)	0	BG(1%)	0
YG(1%)	2	BV(1%)	2	BV(1%)	2
		RV(1%)	4	RV(1%)	4

Adjacencies					
$S_{T1} = 0, L_{T1} = 0$	Contrast Strength	$S_{T1} = 1/20, L_{T1} = 1/7$	Contrast Strength	$S_{T1} = 1/10, L_{T1} = 1/7$	Contrast Strength
R-RV(9%)	1	R-RV(8%)	1	R-RV(8%)	1
R-V(8%)	2	R-V(7%)	2	R-V(7%)	2
B-RV(6%)	3	R-O(6%)	0	R-O(6%)	0
G-RV(5%)	3	BV-RV(5%)	2	BV-RV(5%)	2
RO-RV(5%)	2	O-RV(4%)	1	O-RV(4%)	1
O-RV(5%)	1	B-RV(4%)	3	B-RV(4%)	3
YO-RV(5%)	0	RO-RV(4%)	2	RO-RV(4%)	2
Y-RV(5%)	1	YO-RV(4%)	0	YO-RV(4%)	0
YG-RV(5%)	2	Y-RV(3%)	1	Y-RV(3%)	1
BG-RV(5%)	4	G-RV(3%)	3	YG-RV(3%)	2

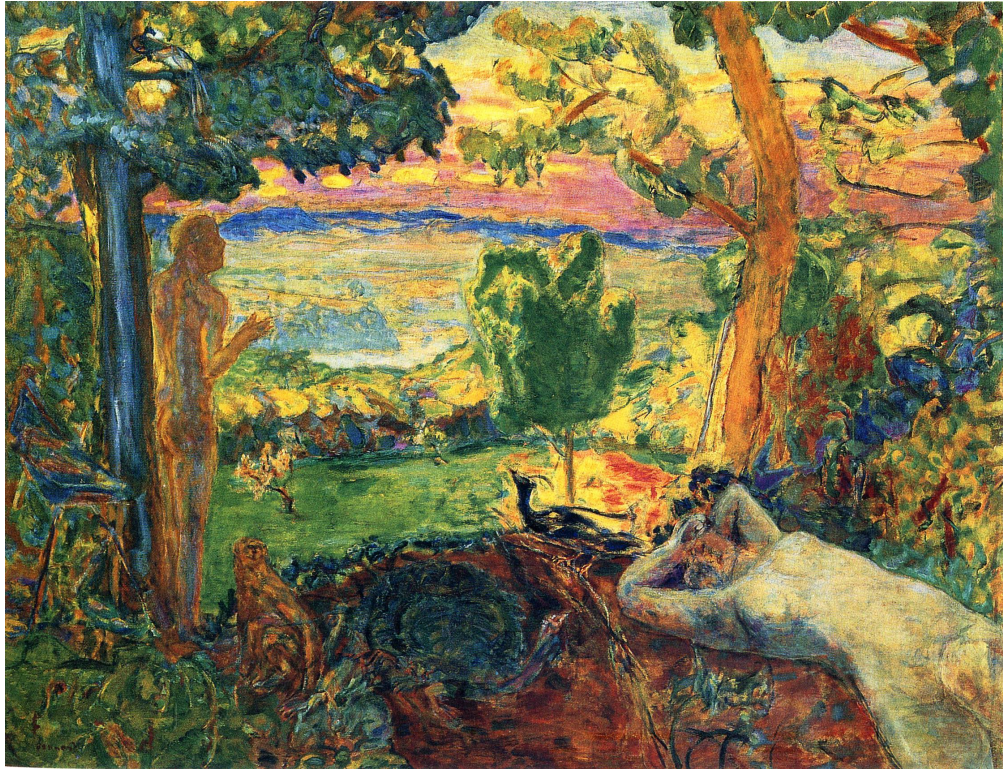
Figure 4.21: Summary of normalized co-occurrences for ‘The Synagogue’

Artist	Painting	Size in pixels	Source
Bonnard	Earthly Paradise	2240 x 1717	http://www4.ncsu.edu/~tjarmst3/gallery/edenic_scenes1.html
Bonnard	The breakfast room	302 x 420	http://www.moma.org/collection/object.php?object_id=79604
Paul Cézanne	Card players	696 x 584	http://nl.wikipedia.org/wiki/De_kaartspelers_(C%C3%A9zanne)
Paul Cézanne	Full bowl	740 x 600	http://s644.photobucket.com/
Claude Monet	Argenteuil	550 x 461	http://www.monetpainting.net/paintings/redboats.php
Claude Monet	Bridge over a pond of water lillies	112 x 140	http://www.metmuseum.org/collection/the-collection-online/search/437127
Claude Monet	Camille au metier	509 x 599	http://www.artistdaily.com/blogs/oilblog/archive/2011/10/24/he-was-rejected-over-and-over.aspx
Claude Monet	Camille Monet on a garden bench	800 x 595	http://www.metmuseum.org/collection/the-collection-online/search/438003
Claude Monet	Dejeuner sur l'herbe	220 x 256	http://en.wikipedia.org/wiki/Claude_Monet
Claude Monet	Grain Stack	762 x 600	http://www.wikiart.org/en/claude-monet/grainstack-at-sunset
Claude Monet	Houses of parliament	1164 x 1024	http://pictify.com/347016/claude-monet-london-houses-of-parliament-the-sun-shining-through-the-fog
Claude Monet	Jardin a Sainte Adresse	792 x 599	http://www.metmuseum.org/collection/the-collection-online/search/437133
Claude Monet	Jean Monet on his hobby horse	730 x 599	http://www.metmuseum.org/collection/the-collection-online/search/438435
Claude Monet	La maison du pecheur	762 x 600	http://commons.wikimedia.org/wiki/File:Claude_Monet_029.jpg
Claude Monet	le bateau Atelier	500 x 600	http://commons.wikimedia.org/wiki/File:Claude_Monet_Le_bateau_atelier.jpg
Claude Monet	Madame Monet en costume Japonais	359 x 600	http://en.wikipedia.org/wiki/Claude_Monet
Claude Monet	Mouth of the Seine	800 x 571	http://en.wikipedia.org/wiki/Claude_Monet
Claude Monet	Poppies Blooming	800 x 576	http://en.wikipedia.org/wiki/Claude_Monet
Claude Monet	Renoir	220 x 269	http://pixels.com/featured/claude-monet-reading-a-newspaper-pierre-auguste-renoir.html
Claude Monet	Rue Montorgueil	36 x 600	http://en.wikipedia.org/wiki/Rue_Montorgueil
Claude Monet	Sea Roses	800 x 372	http://www.canvasreplicas.com/Monet320.htm
Claude Monet	Seine Bassin	780 x 600	http://www.impressionism.org/teachimpress/browse/lesson1.htm
Claude Monet	Soleil Levant	304 x 234	http://www.fotopedia.com/wiki/Impression,_Sunrise#/items/flickr-9607515361
Claude Monet	Spring Time	784 x 600	http://en.wikipedia.org/wiki/File:Claude_Monet_-_Springtime_-_Google_Art_Project.jpg
Claude Monet	Sunshine and Snow	800 x 577	http://www.apollo-magazine.com/gallery-making-colour-at-the-national-gallery-london/
Claude Monet	The artist garden at Vetheuil	467 x 599	http://www.claudemonetgallery.org/The-Artist's-Garden-at-Vetheuil--1880.html
Claude Monet	The artist house a Argenteuil	738 x 600	http://en.wikipedia.org/wiki/Claude_Monet
Claude Monet	Train in the snow	795 x 599	http://commons.wikimedia.org/wiki/File:Claude_Monet_-_Train_in_the_Snow.jpg
Claude Monet	Water Lillies	140 x 140	http://en.wikipedia.org/wiki/Water_Lilies
Claude Monet	Weeping Willow	600 x 497	http://en.wikipedia.org/wiki/Claude_Monet
Claude Monet	Woman in a garden	740 x 599	http://en.wikipedia.org/wiki/Claude_Monet
Claude Monet	Woman with Parasol	394 x 600	http://en.wikipedia.org/wiki/Claude_Monet
Claude Monet	Les Tilleuls a Poissy	478 x 599	http://elblogdetuico.blogspot.ca/2013/07/tuico-y-la-pintura.html

Table 4.3: Artists who used *cold-warm contrast*: Bonnard, Cézanne, Monet

Artist	Painting	Size in pixels	Source
Pissaro	Boulevard Montmartre	724 x 600	http://gizgaleri.blogspot.ca/2014/04/camille-pissaro.html
Pissaro	Entree du Village	713 x 600	http://authorherstorianparent.blogspot.ca/2011_11_01_archive.html
Pissaro	Landscape at Pointoise	220 x 162	http://www.impressionismus-gemaelde.de/Pissarro/Landschaft-bei-Pontoise.jpg.php
Pissaro	Le Verger	730 x 600	http://totallyhistory.com/camille-pissarro/
Pissaro	The church at Eragny	497 x 600	http://en.wikipedia.org/wiki/Camille_Pissarro
Pissaro	The Harvest	800 x 444	http://en.wikipedia.org/wiki/Camille_Pissarro
Pissaro	Washer Woman	162 x 199	http://en.wikipedia.org/wiki/Camille_Pissarro
Pissaro	Hay Harvest at Eragny	619 x 515	http://en.wikipedia.org/wiki/Camille_Pissarro
Renoir	Dance a Bougival	1576 x 2971	http://www.impressionismus-gemaelde.de/Renoir/Der-Tanz-in-Bougival.jpg.php
Renoir	Girl Braiding her hair	489 x 600	http://en.wikipedia.org/wiki/Pierre-Auguste_Renoir
Renoir	Girls at Piano	220 x 297	http://en.wikipedia.org/wiki/Pierre-Auguste_Renoir
Renoir	Le Balancoire	466 x 599	http://en.wikipedia.org/wiki/Pierre-Auguste_Renoir
Renoir	Les Baigneuses	736 x 599	http://en.wikipedia.org/wiki/Pierre-Auguste_Renoir
Renoir	Lise Sewing	491 x 600	http://en.wikipedia.org/wiki/Pierre-Auguste_Renoir
Renoir	The two sisters	220 x 273	http://en.wikipedia.org/wiki/Pierre-Auguste_Renoir
Renoir	Le Moulin de la galette	103 x 156	http://en.wikipedia.org/wiki/Pierre-Auguste_Renoir

Table 4.4: Artists who used *cold-warm contrast*: Pissaro, Renoir



(a) Painting

Homogeneous regions

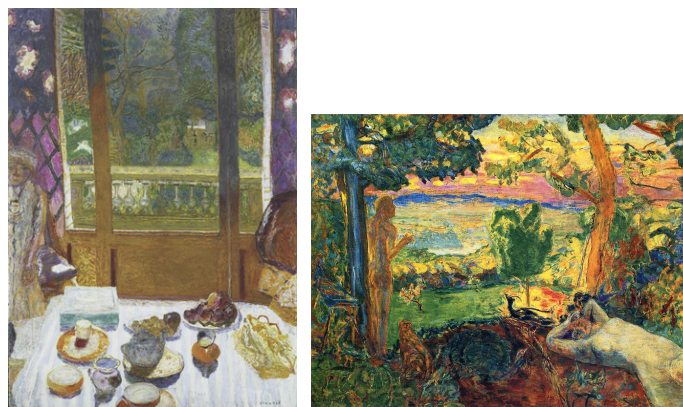
$S_{T_1} = 0, L_{T_1} = 0$		Warmth Index	$S_{T_1} = 1/20, L_{T_1} = 1/7$		Warmth Index	$S_{T_1} = 1/10, L_{T_1} = 1/7$		Warmth Index
YO(26%)	4		O(21%)	5		O(21%)	5	
O(21%)	5		YO(18%)	4		YO(18%)	4	
Y(18%)	3		Y(10%)	3		Y(10%)	3	
G(9%)	1		G(9%)	1		G(9%)	1	
YG(6%)	2		YG(7%)	2		YG(7%)	2	
RO(3%)	6		RO(3%)	6		RO(3%)	6	
R(2%)	5		R(2%)	5		R(2%)	5	
BG(2%)	0		BG(2%)	0		BG(2%)	0	
B(2%)	1		B(2%)	1		B(2%)	1	

Adjacencies

$S_{T_1} = 0, L_{T_1} = 0$		Contrast Strength	$S_{T_1} = 1/20, L_{T_1} = 1/7$		Contrast Strength	$S_{T_1} = 1/10, L_{T_1} = 1/7$		Contrast Strength
R-RV(16%)	1		R-RV(7%)	1		YO-YG(7%)	2	
G-RV(9%)	3		YO-YG(6%)	2		R-RV(7%)	1	
RO-RV(8%)	2		O-Y(4%)	2		R-O(5%)	0	
O-RV(8%)	1		R-O(4%)	0		O-Y(5%)	2	
YO-RV(8%)	0		R-V(4%)	2		R-V(4%)	2	
Y-RV(8%)	1		BV-RV(4%)	2		Y-G(4%)	2	
YG-RV(8%)	2		O-RV(4%)	1		BV-RV(4%)	2	
BG-RV(8%)	4		RO-RV(4%)	2		O-RV(4%)	1	
B-RV(8%)	3		Y-G(4%)	2		B-RV(4%)	3	
BV-RV(8%)	2					RO-RV(3%)	2	

(b) Normalized co-occurrences

Figure 4.22: Bonnard - Earthly Paradise

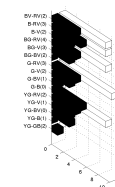
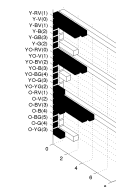
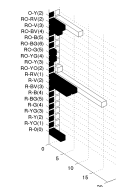
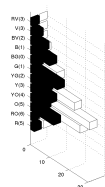


Breakfast Room

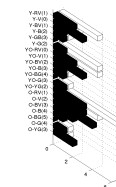
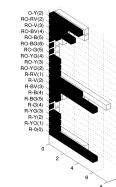
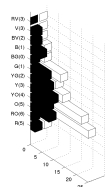
Earthly Paradise

(a) Bonnard

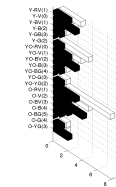
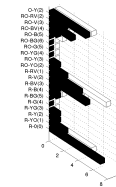
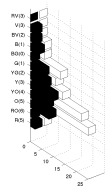
Homogeneous R to RV	Adjacent R-O to O-Y	Adjacent O-YG to Y-RV	Adjacent YG-GB to BV-RV
------------------------	------------------------	--------------------------	----------------------------



$$S_T = 0, L_T = 0$$



$$S_T = 1/20, L_T = 1/7$$



$$S_T = 1/10, L_T = 1/7$$

(b) Visualizing Homogeneous regions and Adjacencies

Figure 4.23: Bonnard Visualization- Histogram of homogeneous regions with warmth indices and warmth contrast strengths for adjacencies listed in parentheses.



(a) Painting

Homogeneous regions					
$S_{T_1} = 0, L_{T_1} = 0$		Warmth	$S_{T_1} = 1/20, L_{T_1} = 1/7$		Warmth
		Index			Index
B(56%)	1	B(38%)	1	B(37%)	1
G(16%)	1	G(10%)	1	G(10%)	1
BG(5%)	0	BG(4%)	0	BG(4%)	0
R(5%)	5	R(3%)	5	V(3%)	3
Y(3%)	3	BV(3%)	2	R(2%)	5
YG(3%)	2	O(2%)	5	YG(2%)	2
BV(3%)	2	YG(2%)	2	O(1%)	5
		V(1%)	3	Y(1%)	3
				V(1%)	3

Adjacencies					
$S_{T_1} = 0, L_{T_1} = 0$		Contrast	$S_{T_1} = 1/20, L_{T_1} = 1/7$		Contrast
		Strength			Strength
YO-YG(50%)	2	R-V(6%)	2	G-B(7%)	0
RO-BV(50%)	4	G-B(5%)	0	R-V(6%)	2
		R-RV(5%)	1	O-V(5%)	2
		O-V(4%)	2	B-V(4%)	2
		B-V(4%)	2	RO-V(4%)	3
		R-BV(3%)	3	R-RV(3%)	1
		RO-V(3%)	3	R-O(3%)	0
		R-O(3%)	0	R-BV(3%)	3
		G-RV(3%)	3	YO-V(3%)	1
		G-BV(3%)	1	Y-V(3%)	0

(b) Normalized co-occurrences

Figure 4.24: Monet - Water Lilies

An example of Pissarro's painting is 'Entree du Village'. Figure 4.27 (page 94) displays the image and the *cold-warm contrast* results for the homogeneous regions and adjacencies. In this painting, there is a clear and strong contrast in the homogeneous regions captured by the second range of parameters ($S_{T_1} = 1/20, L_{T_1} = 1/7$). The

largest percentage of co-occurrences occurs in the cold blue-green grass (warmth index 0), the next highest percentage of co-occurrences takes place in the orange trees, paths and rooftops (*warmth index 5*). The *warmth contrast strength* of the homogeneous regions is high (*warmth contrast strength 5*). The adjacencies range in *warmth contrast strength* 0 to 4. The remainder of Pissaro’s paintings, and the 3D histograms to visualize the *cold-warm contrast* co-occurrence patterns in both the homogeneous regions and the adjacencies are displayed in Figure 4.28 (95). We observe that Pissaro uses several hues in the homogeneous regions, causing some of the paintings to be primarily warm, primarily cold, or have a contrast between the cold and the warm homogeneous regions. Notable peaks in the adjacencies have *warmth contrast strengths* of 0,1 and 2.

An example of Renoir’s painting is ‘The two sisters’. Figure 4.29 (page 96) displays the image, the *cold-warm contrast* results for the homogeneous regions and adjacencies. The second range of parameters ($S_{T1} = 1/20, L_{T1} = 1/7$) captures the *cold-warm contrast* between the homogeneous regions where green has the highest percentage of co-occurrences, and contrasts with orange at a *warmth contrast strength* of 4. In the adjacencies, the strongest contrast of warmth occurs between orange and green. The image is also highly modulated between green and blue, both of which are cold hues that do not contrast in warmth. The remainder of Pissaro’s paintings, and the 3D histograms to visualize the *cold-warm contrast* co-occurrence patterns in the homogeneous regions and the adjacencies is displayed in Figure 4.30 (page 97). In the homogeneous regions, we note that Renoir uses one or two dominant hues, which we confirm by observation. We do not observe a particular pattern in the adjacencies.

Our computational model for capturing the *cold-warm contrast* in images is a valuable tool for assessing the presence of the contrast. The first range of parameters ($S_{T1} = 0, L_{T1} = 0$) is not an appropriate choice, as the range does not allow for any variation in saturation and light. In our experience, *cold-warm contrast* in good quality images can be detected in the second range of parameters ($S_{T1} = 1/20, L_{T1} = 1/7$), still capturing co-occurrences of colors with similar light and saturation values. The third range is generally needed for poor quality images.

4.3.5 Robustness

To test the robustness of our algorithms, we applied our algorithms and visualization for artist styles to three different copies of the same image, and analyze the results.

For *contrast of hue*, we applied Algorithm 1 to three different copies of Miro’s ‘The singing fish’. The images and the results are shown in Figure 4.31 on page 98. We found that our algorithm is consistent for detecting homogeneous regions for all three images and all three ranges. For *cold-warm contrast*, we applied Algorithm 2 to three different copies of Pissaro’s ‘Entree du Village’. The images and the results are shown in Figure 4.32 on page 99. We found that our algorithm is consistent in detecting homogeneous regions in all three copies of the image. In the adjacencies, we found that the set of adjacencies detected in images with lower resolution are a subset of adjacencies detected in the high resolution image. This result is expected as a higher resolution reflect more modulations, and as a result more adjacencies. We conclude as such that our algorithm is consistent for detecting adjacencies in images, and sensitive to resolution.

Artist	Painting	Size in pixels	Source
Pissaro	Entree du Village	713 x 600	http://authorherstoriantparent.blogspot.ca/2011_11_01_archive.html
Pissaro	Entree du Village	520 x 437	http://www.oilpaintings-sales.com/oil-paintings/camille-pissarro-entree-du-village-de-voisins-1872-78664.html
Pissaro	Entree du Village	2024 x 1702	http://en.wikipedia.org/wiki/Camille_Pissarro
Miro	The singing fish	510 x 640	http://www.ebuypainting.com/
Miro	The singing fish	500 x 627	http://stringvisions.ovationpress.com/2011/06/amazing-singing-fish/
Miro	The singing fish	759x 960	http://paintingandframe.com/uploadpic/joan_miro/big/the_singing_fish.jpg

Table 4.5: Images used for robustness test: ‘Entree du Village’ (*cold-warm contrast*) and ‘The singing fish’ (*contrast of hue*)

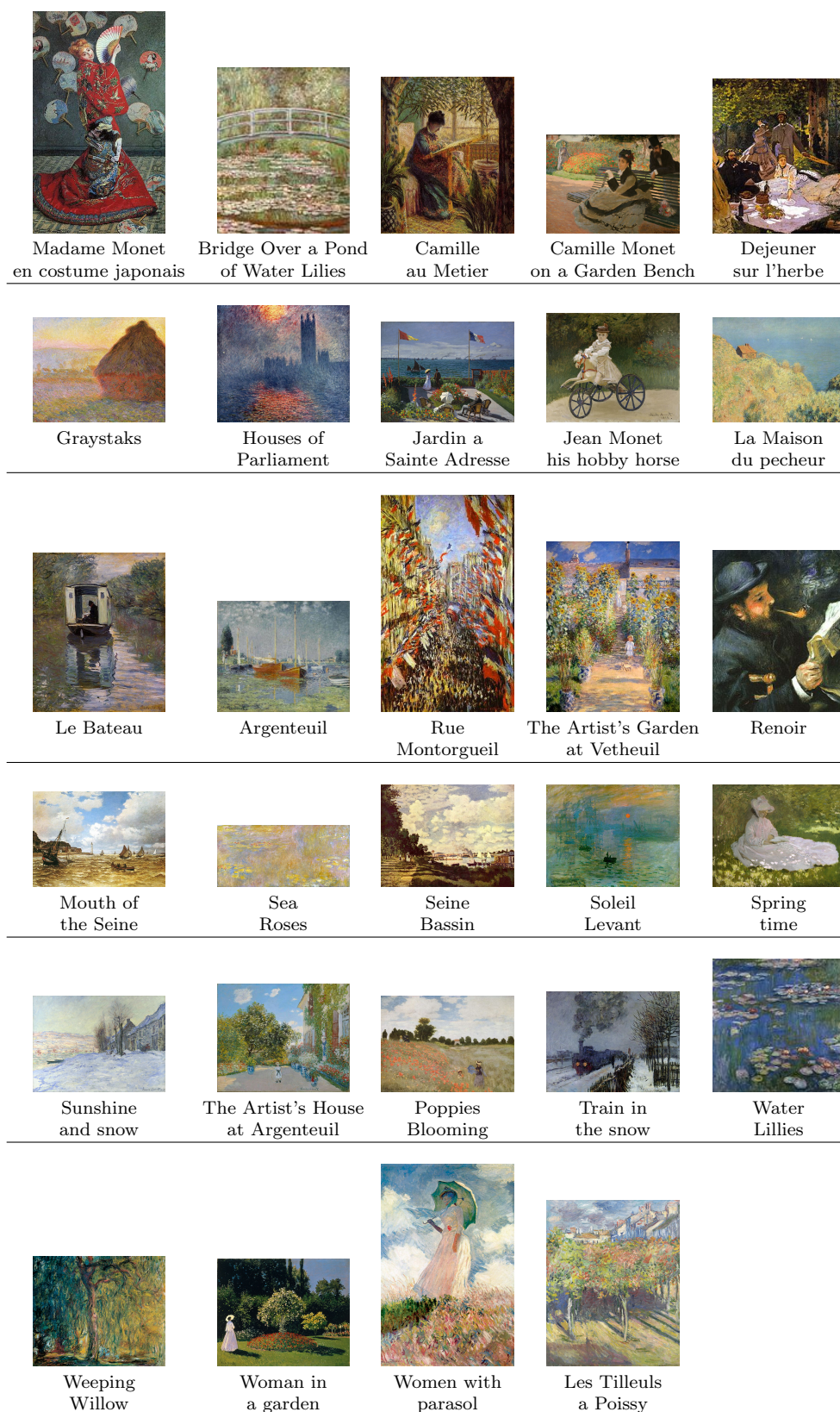


Figure 4.25: Monet Visualization- Paintings

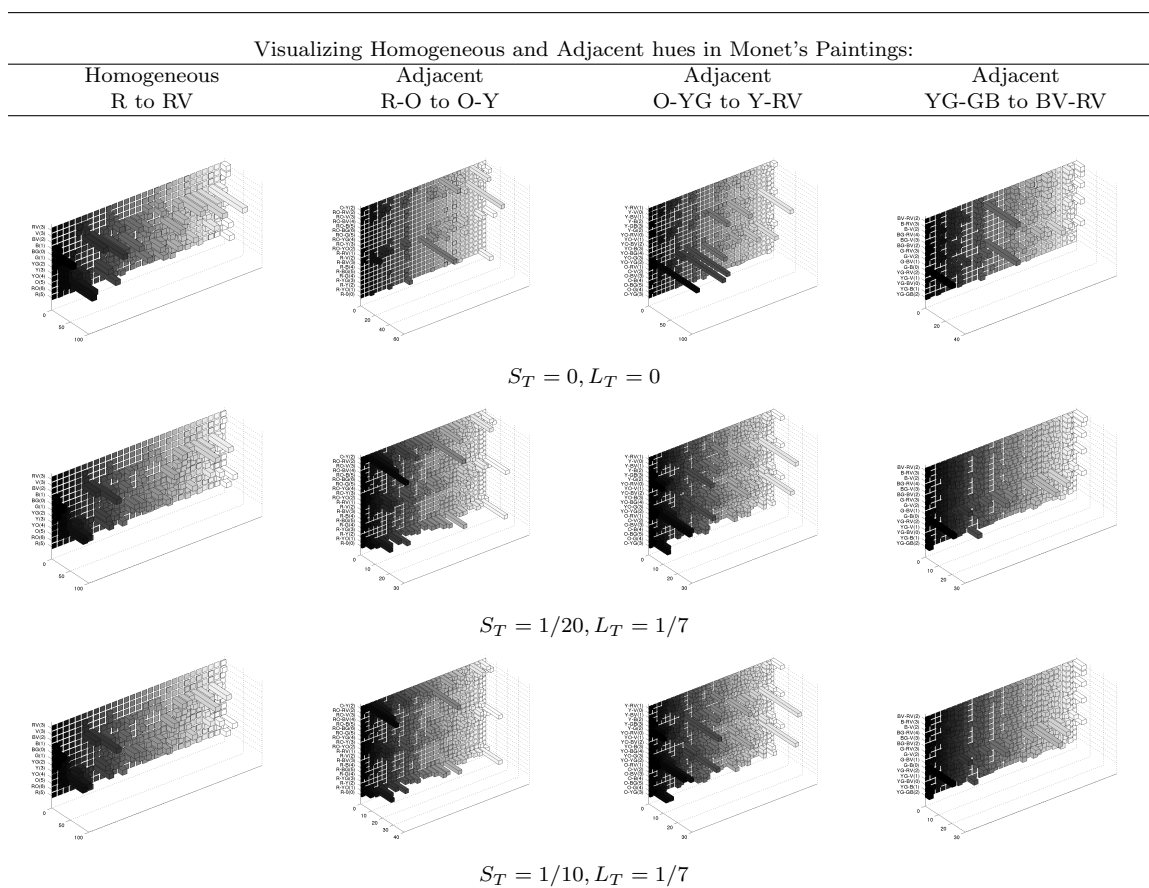


Figure 4.26: Monet Visualization- Histogram of homogeneous regions with warmth indices and warmth contrast strengths for adjacencies listed in parentheses.



(a) Painting

Homogeneous regions

$S_{T_1} = 0, L_{T_1} = 0$		$S_{T_1} = 1/20, L_{T_1} = 1/7$		$S_{T_1} = 1/10, L_{T_1} = 1/7$	
Warmth Index	Warmth Index	Warmth Index	Warmth Index	Warmth Index	Warmth Index
BG(59%)	0	BG(31%)	0	BG(31%)	0
G(15%)	1	O(16%)	5	O(16%)	5
B(15%)	1	G(12%)	1	G(12%)	1
O(3%)	5	B(7%)	1	B(7%)	1
RO(1%)	6	YO(4%)	4	YO(4%)	4
YO(1%)	4	RO(2%)	6	RO(2%)	6
		YG(2%)	2	YG(2%)	2
		Y(1%)	3	Y(1%)	3

Adjacencies

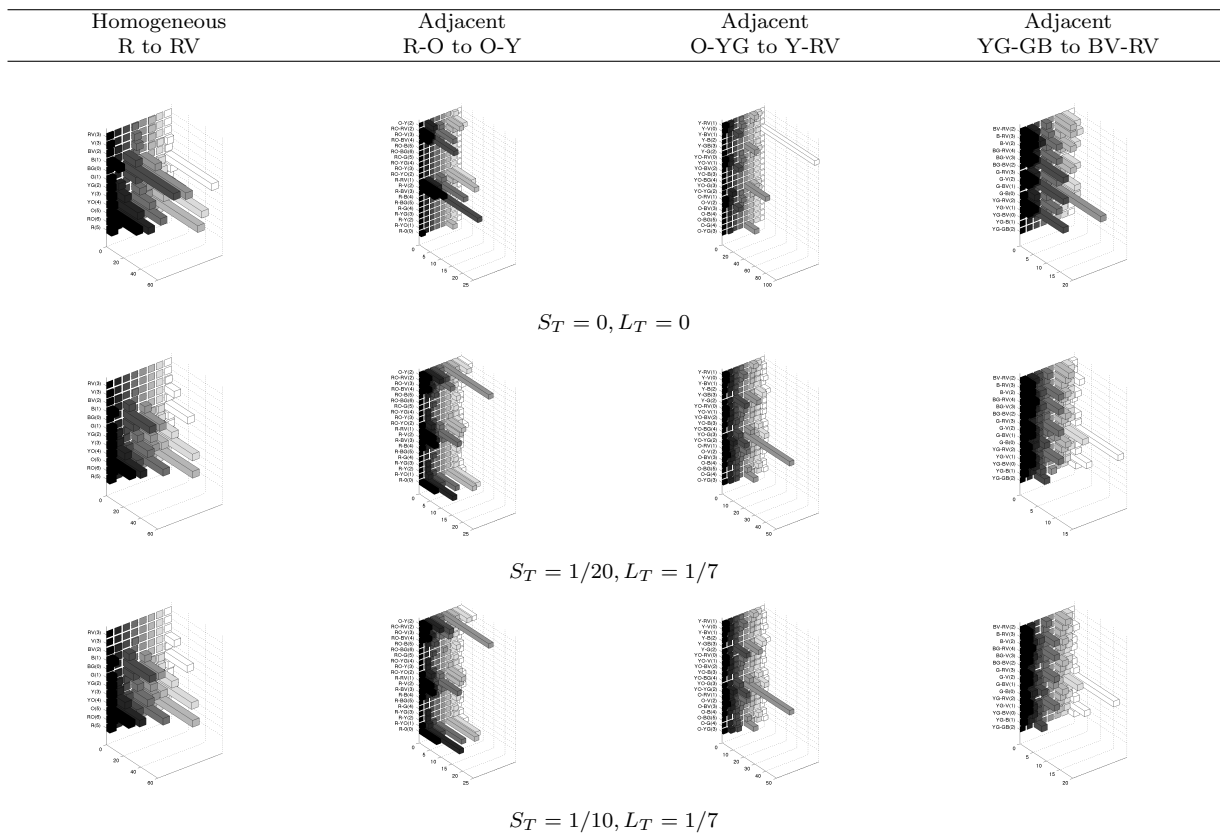
$S_{T_1} = 0, L_{T_1} = 0$		$S_{T_1} = 1/20, L_{T_1} = 1/7$		$S_{T_1} = 1/10, L_{T_1} = 1/7$	
Contrast Strength	Contrast Strength	Contrast Strength	Contrast Strength	Contrast Strength	Contrast Strength
R-BV(22%)	3	Y-G(11%)	2	YO-YG(12%)	2
RO-BV(11%)	4	YO-YG(11%)	2	Y-G(12%)	2
O-BV(11%)	3	O-Y(7%)	2	O-Y(9%)	2
YO-BV(11%)	2	R-O(5%)	0	YO-G(6%)	3
Y-BV(11%)	1	YO-G(5%)	3	R-O(5%)	0
YG-BV(11%)	0	G-B(3%)	0	O-YG(4%)	3
G-BV(11%)	1	YG-BG(3%)	2	G-B(3%)	0
BG-BV(11%)	2	O-G(2%)	4	O-G(3%)	4
		R-V(2%)	2	YG-BG(3%)	2
		O-YG(2%)	3	O-B(2%)	4

(b) Normalized co-occurrences

Figure 4.27: Pissaro - Entree du Village



(a) Pissaro



(b) Visualizing Homogeneous regions and Adjacencies

Figure 4.28: Pissaro Visualization- Histogram of homogeneous regions with warmth indices and warmth contrast strengths for adjacencies listed in parentheses.



(a) Painting

Homogeneous regions

$S_{T_1} = 0, L_{T_1} = 0$		$S_{T_1} = 1/20, L_{T_1} = 1/7$		$S_{T_1} = 1/10, L_{T_1} = 1/7$	
Warmth Index	Warmth Index	Warmth Index	Warmth Index	Warmth Index	Warmth Index
G(16%)	1	G(12%)	1	G(12%)	1
O(10%)	5	O(7%)	5	O(6%)	5
B(10%)	1	B(5%)	1	B(5%)	1
YG(7%)	2	YG(5%)	2	YG(4%)	2
BG(4%)	0	BG(4%)	0	BG(4%)	0
RO(4%)	6	YO(3%)	4	YO(3%)	4
YO(2%)	4	Y(3%)	3	Y(2%)	3
Y(2%)	3	RO(2%)	6	RO(2%)	6
R(2%)	5	R(2%)	5	R(2%)	5
BV(1%)	2				
V(1%)	3				

Adjacencies

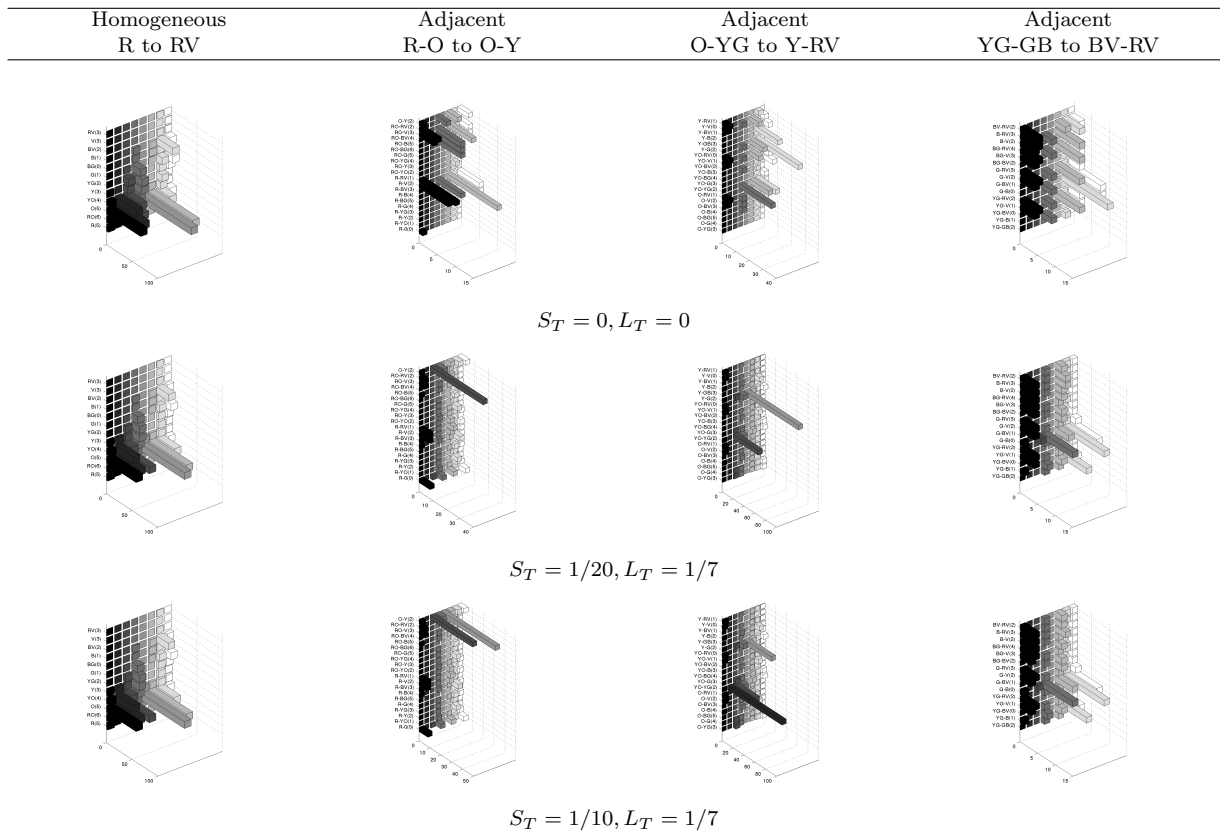
$S_{T_1} = 0, L_{T_1} = 0$		$S_{T_1} = 1/20, L_{T_1} = 1/7$		$S_{T_1} = 1/10, L_{T_1} = 1/7$	
Contrast Strength	Contrast Strength	Contrast Strength	Contrast Strength	Contrast Strength	Contrast Strength
G-B(9%)	0	G-B(8%)	0	G-B(8%)	0
YO-BV(9%)	2	Y-G(6%)	2	R-O(6%)	0
G-BV(9%)	1	R-O(6%)	0	Y-G(6%)	2
R-BV(6%)	3	O-Y(6%)	2	O-Y(6%)	2
Y-BV(6%)	1	YO-YG(5%)	2	YO-YG(5%)	2
R-V(6%)	2	O-G(4%)	4	O-G(5%)	4
YO-V(6%)	1	YO-G(4%)	3	YO-G(4%)	3
O-Y(3%)	2	O-YG(4%)	3	O-YG(4%)	3
YO-YG(3%)	2	R-G(2%)	4	YG-B(3%)	2
YO-G(3%)	3	YG-B(2%)	1	R-G(2%)	4

(b) Normalized co-occurrences

Figure 4.29: Renoir - The two sisters

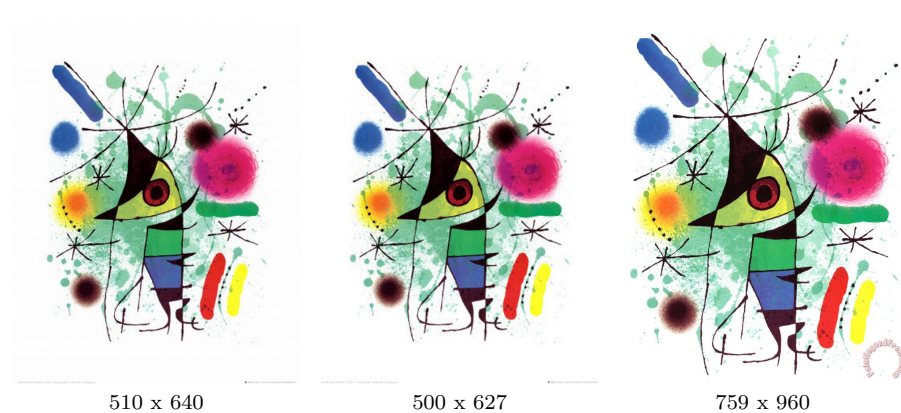


(a) Renoir

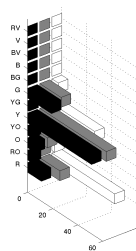


(b) Visualizing Homogeneous regions and Adjacencies

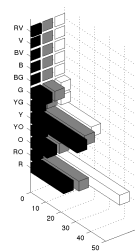
Figure 4.30: Renoir Visualization - 3D histogram of homogeneous regions with warmth indices and warmth contrast strengths for adjacencies listed in parentheses.



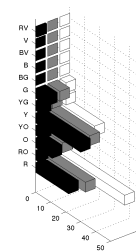
(a) Miró



$$S_T = 0, L_T = 0$$



$$S_T = 1/20, L_T = 1/7$$



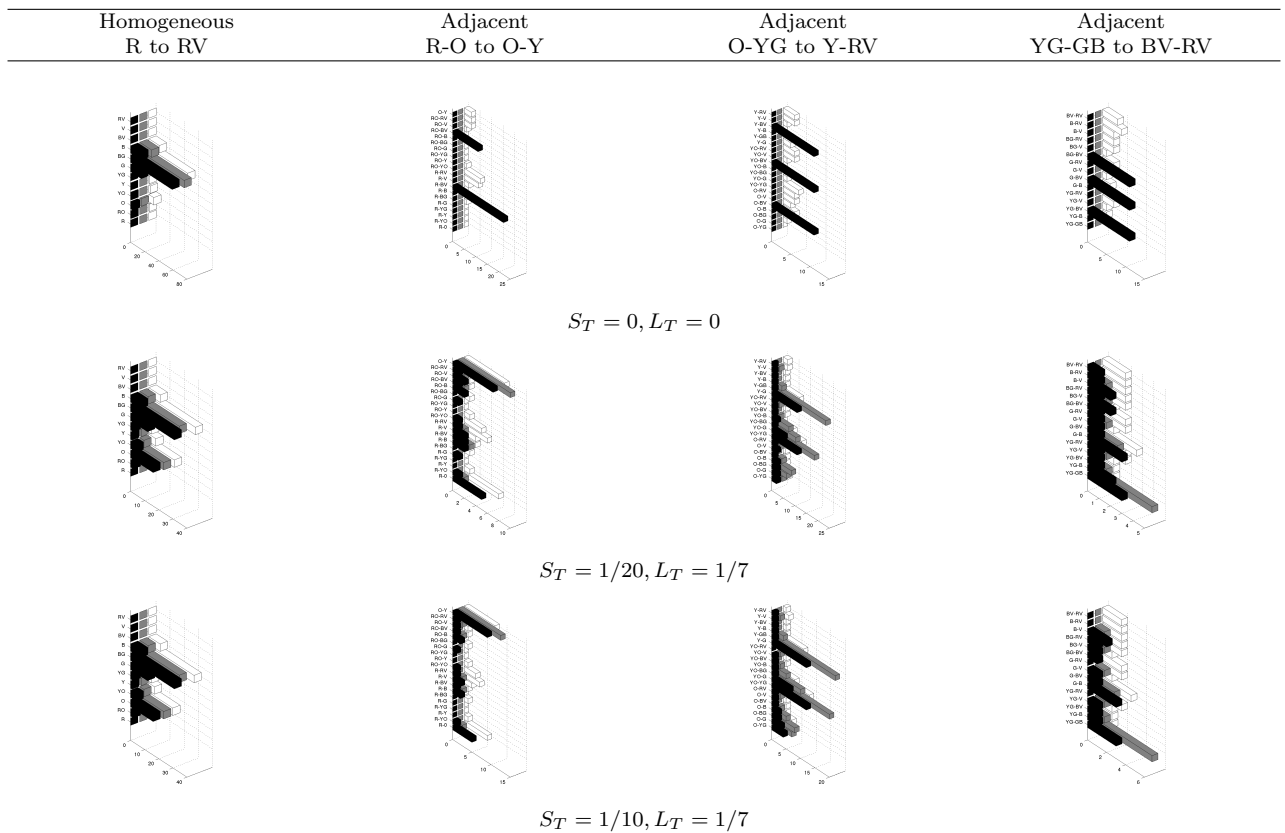
$$S_T = 1/10, L_T = 1/7$$

(b) Visualizing Homogeneous regions

Figure 4.31: Robustness Visualization for *contrast of hue* - 3D histogram of homogeneous regions



(a) Robustness for cold-warm contrast



(b) Visualizing Homogeneous regions and Adjacencies

Figure 4.32: Robustness Visualization for *cold-warm contrast* - 3D histogram of homogeneous regions and adjacencies.

4.3.6 Discussion

Our 3D visualization of chromatic information in a painting is novel. We proposed simple quantitative descriptors for *modulation* and our experimental results show that

the measures are consistent with Itten’s comments and explanations. With a database of paintings described in detail by Itten, and a database of additional images organized by artist, we establish that our computational models for capturing the *contrast of hue* and *cold-warm contrast* are valuable tools in the assessment of these contrasts and they offer important insight in the color composition of images.

In the *contrast of hue*, co-occurrence matrices reflect the order of the size of homogeneous regions, and may contribute to predicting whether *contrast of hue* is at play. Homogeneous regions reflect the number of dominant hues in the image and adjacencies provide spatial information about the color composition. The first range of parameters ($S_{T1} = 0, L_{T1} = 0$) is ideal for capturing the *contrast of hue* in good quality images. In the *cold-warm contrast*, co-occurrence matrices are helpful in analyzing the contrast, but not predictive on their own. The warmth contrast indices, however can be indicative high and low *cold-warm contrast* in images. For *cold-warm contrast*, homogeneous regions reflect the distribution of dominant hues over the cold and warm ranges, adjacencies reflect the subtle inter-hue relationships that create a sense of heat and depth. The second range of parameters ($S_{T1} = 1/20, L_{T1} = 1/7$) is ideal for capturing *cold-warm contrast* in good quality images. Our experimental results show that our computational models for *contrast of hue* and *cold-warm contrast*, as well as exploring artists’ styles are consistent with Itten’s comments and explanations.

Limitations: Our work has two limitations. First, several of the images we analyzed are digital copies of paintings from a few hundred years ago, and as a result the quality has suffered due to aging, discoloration, damage and digitization artifacts. In those cases, we found it helpful to broaden the range of parameters on which we measure the co-occurrences for the poor quality images. Second, the pixel count is an essential piece of information for both *contrast of hue* and *cold-warm contrast*, and is not captured in our computational models. In using the v-8 neighbourhood, we overcount each pixel by up to 8 times. The effect is that a slight increase in a homogeneous regions creates significantly more co-occurrences. To improve our interpretation of co-occurrences, we normalize the diagonal results (for homogeneous regions) separately from the off-diagonals (for adjacencies).

<i>Hue Sector</i>	Ingres 'Reclining Odalisque'			Seurat 'Un Dimanche à la Grande Jatte'			Limbourg 'May- Day excursion'			Monet 'Houses of Parliament in fog'		
	μ_{dist} *10 ³	σ_{dist} *10 ³	<i>N</i>	μ_{dist} *10 ³	σ_{dist} *10 ³	<i>N</i>	μ_{dist} *10 ³	σ_{dist} *10 ³	<i>N</i>	μ_{dist} *10 ³	σ_{dist} *10 ³	<i>N</i>
Red	0.39	2.41	2227	0.14	1.38	5969	1.47	2.48	820	0.12	0.65	8987
Red-Orange	0.72	1.49	1429	0.26	0.84	2803	1.42	2.06	940	0.32	0.83	3576
Orange	0.13	0.36	9235	0.2	0.68	4918	0.27	1.59	4821	0.51	1.02	2176
Yellow-Orange	0.11	0.50	9264	0.34	1.08	2760	0.13	0.40	7089	2.27	7.90	315
Yellow	0.22	0.27	3573	0.07	0.51	7331	0.12	0.70	7279	3.24	16.14	194
Yellow-Green	0.36	1.28	1274	0.1	0.53	4083	0.04	0.44	18974	1.88	5.30	170
Green	0.47	1.40	385	0.05	0.40	20300	0.07	0.85	9706	0.67	2.58	387
Blue-Green	0.34	1.04	265	0.24	1.13	2978	0.59	1.89	1073	0.92	7.1	523
Blue	0.13	0.65	2092	0.10	0.3	6133	0.11	0.25	10463	0.04	0.56	23840
Blue-Violet	0.07	0.45	5006	0.06	0.37	5324	1.13	4.72	456	0.07	0.72	4624
Violet	0.22	1.21	1835	0.16	0.95	3075	1.03	4.44	168	0.19	1.79	2177
Red-Violet	0.64	2.42	459	0.63	4.17	1086	4.86	17.73	53	5.36	3.65	768

(a) Modulation measures for paintings shown in Figure 4.1 on page 61

<i>Hue Sector</i>	Matisse 'Le Piano'			de la Tour 'Newborn Babe'			Cézanne 'Apples and Oranges'			Witz 'The Synagogue'		
	μ_{dist} *10 ³	σ_{dist} *10 ³	<i>N</i>	μ_{dist} *10 ³	σ_{dist} *10 ³	<i>N</i>	μ_{dist} *10 ³	σ_{dist} *10 ³	<i>N</i>	μ_{dist} *10 ³	σ_{dist} *10 ³	<i>N</i>
Red	0.16	1.57	8621	0.10	0.98	10924	0.06	0.16	23158	0.12	0.60	7521
Red-Orange	0.18	0.25	7487	0.14	0.75	8069	0.16	0.40	7320	0.24	1.55	3204
Orange	0.11	0.25	11840	0.57	1.08	2064	0.12	0.52	9876	0.09	0.50	9948
Yellow-Orange	0.28	1.24	2086	1.70	5.70	583	0.30	0.86	1536	0.23	0.78	4045
Yellow	0.52	3.44	743	8.33	50.91	112	0.67	1.74	460	0.61	0.71	1280
Yellow-Green	0.61	4.62	462	0	0	0	1.49	3.49	127	2.59	5.91	267
Green	0.10	0.91	9156	0	0	0	0.38	1.47	57	0.59	2.45	359
Blue-Green	2.00	11.78	171	0	0	0	0	0	0	0.35	0.57	536
Blue	0.18	0.91	3198	1.07	5.83	152	0.44	2.75	322	0.14	0.31	3253
Blue-Violet	0.36	2.26	1204	0.33	1.31	296	0.14	0.95	3542	0.12	0.91	2134
Violet	0.34	2.75	732	0.36	1.11	680	0.13	0.57	7614	0.1	1.02	2482
Red-Violet	0.52	2.70	386	0.58	2.15	538	0.33	0.86	3137	0.19	1.02	1165

(b) Modulation measures for paintings shown in Figure 4.2 on page 62

Table 4.6: Modulation measures for paintings shown in Figure 4.1 and Figure 4.2 on page 61-62

Chapter 5

Application of proposed methods on business documents

5.1 Business documents

Business documents are communication tools for organizations, and are used for both internal and external purposes. These purposes vary: reporting, communicating new directions, providing instructions for new procedures, marketing strategies, and advertising campaigns. Examples of business documents include financial reports, presentations, posters, letters, and magazines.

Organizations place a significant amount of information in documents. Most of them focus on the completeness of the content at the expense of design considerations, leaving the reader to extract the pertinent messages from the document. Document designers work on creating document layouts that allow the reader to better process and understand the content of the document. Document design topics include typesetting, layout, color and messaging.

Karen Schriver[54, p. 10] defines document design as follows: “*Document design is the field concerned with creating texts(broadly defined) that integrate words and pictures in ways that help people to achieve their specific goals for using texts at home, school or work. [...] Document design is the act of bringing together prose, graphics and typography for purposes of instruction, information, or persuasion*”.

The remainder of the chapter is structured as follows: we will discuss the importance of color in business documents (section 5.2), our proposed methods (section 5.3), describe our results (section 5.4) and discuss the use the contrasts in business

documents (section 5.5).

5.2 Color in business documents

The spatial composition and color combination of a document are important aspects of communicating the flow of a document to the reader. When document designers choose color combinations, they intentionally select combinations that suit the purpose of the document. A well constructed document will guide the reader to the important messages and will give clear cues about the hierarchy of important content. Emphasis is a design principle *“concerned with the creation of areas of importance for the viewer to focus upon”*[16]. Color and contrast are properties by which people group figures in their mind[54]. *‘Any sharp contrast will draw the reader’s attention. Moreover, the sharper the contrast the more salient the effect’*[54].

In document design, color can be used to focus the reader’s attention on a particular portion of document. According to Itten, when the color combination of an image is static, the combination is harmonious, and the set of colors in the image is centered at a medium gray [23, pp. 19–20]. Feisner states that harmony is the *“visual agreement of all parts of a work. [...] Two or more colors are harmonious if their mixture yields gray; combinations that do not yield gray have high visual impact”*[16, pp. 74 – 75]. Feisner’s comments are in line with Itten’s color harmony constructs. Harmonious (or static) color combination allow the reader to read the text and view charts without distraction. On the other hand, if the designer’s intention is to ensure the reader starts with a portion of the document, a discordant color can help create the salient effect required, essentially a highlight. Discord is *“the effect obtained when the value of a hue is opposite to its natural order”*[16, p. 40]. See Table 5.1 for the natural order of hue values.

When using figures in business documents, Schriver recommends the use of ‘strong figures’, which she describes as having good gestalt properties such as ‘simplicity’, ‘regularity’ and ‘symmetry’. Strong figures also tend to be ‘closed’, surrounded by a continuous contour. This contour allows strong figures to be more resistant to ‘contextual influences’ than other types of figures. Circles for instance are strongest because they are symmetrical to any angle, and simple figures are more effective than complex figures.[54, p. 316]

In business documents, charts with colored segments are common. Since pie charts are common visualizations that employ color, and fit the description of strong figures,



Figure 5.1: The values of hues. This diagram shows the relative values of hues at full intensity. The horizontal broken line corresponds to middle-value gray[16, p. 39]

we focus our analysis of color in business documents on pie charts. We assess our computational models for the analysis of *contrast of hue* and *cold-warm contrast* in pie charts.

5.3 Analysis of contrasts in pie charts

Our motivation to study the use of contrasts in business documents stems from a research collaboration with SAP, where we set out to improve the readability of business documents through the automation of design principles. SAP is a software company that provides business solutions and applications to a variety of business sectors. Their customer reports contain results of their data analysis, which include graphical representations of data presented in pie charts. Part of the task of improving the readability of the reports was to take some first steps in adjusting the color combinations in the pie charts so that they support readability rather than distract the reader. To assess the existing contrasts in pie charts, we apply our computational models to a database of 111 images of pie charts segmented from business documents SAP provided.

We classified the images into charts with up to 3 hues, and charts with more than 3 hues, and further into subgroups as represented in Table 5.1. Our images are digitally created pie charts. We therefore assume that all pixels in a pie slice







Sample image	Grouping	Number of images	Properties
	1	6	up to 3 hues low saturation colors uniform size segments
	2	14	up to 3 hues bright colors mixed size segments
	3	16	up to 3 hues mixed colors mixed size segments
	4	28	4 or more hues lower saturation uniform size segments
	5	18	4 or more hues bordered images mixed colors small slices
	6	29	4 or more hues mixture colors mixed sized slices

Table 5.1: Classification of pie charts in SAP business documents

are homogeneously composed of the same hue, saturation and light. We test our computational models for the analysis of *contrast of hue* and *cold-warm contrast*, as described in Chapter 3 on each subgroup of images.

We have adjusted the parameters over which we test our computational models of *contrast of hue* and *cold-warm contrast* to better fit pie charts. Our images are digitally created pie charts. We therefore assume that all pixels in a pie slice are homogeneously composed of the same hue, saturation and light.

The criteria for *contrast of hue* is that the colors in a pie chart must be fully saturated colors. Therefore, homogeneous regions are fully saturated ($S \geq 0.8$). The criteria for *cold-warm contrast* is that the pixels of the homogeneous regions must be in the center light range ($0.4 \leq L \leq 0.6$). We also require adjacent hues to be within the center light region ($0.4 \leq L \leq 0.6$). For both contrasts, we set a loose uniformity requirement ($S_{T1} = 1/10, L_{T1} = 1/7$) to account for fading between slices.

5.4 Results

The *contrast of hue* and *cold-warm contrast* results for pie charts in group 1 are displayed in Table 5.2. In the *contrast of hue* results, we observe peaks at green and orange only, meaning that the violet is not sufficiently saturated to be detected. Therefore this group of pie charts do not meet the criteria of *contrast of hue*. In the *cold-warm contrast* results, we observe only one peak per image the homogeneous regions, which means that some of the pie slices do not meet the *cold-warm contrast* criteria. The peaks in the adjacencies show some adjacent hues with mild to medium *contrast strength*.

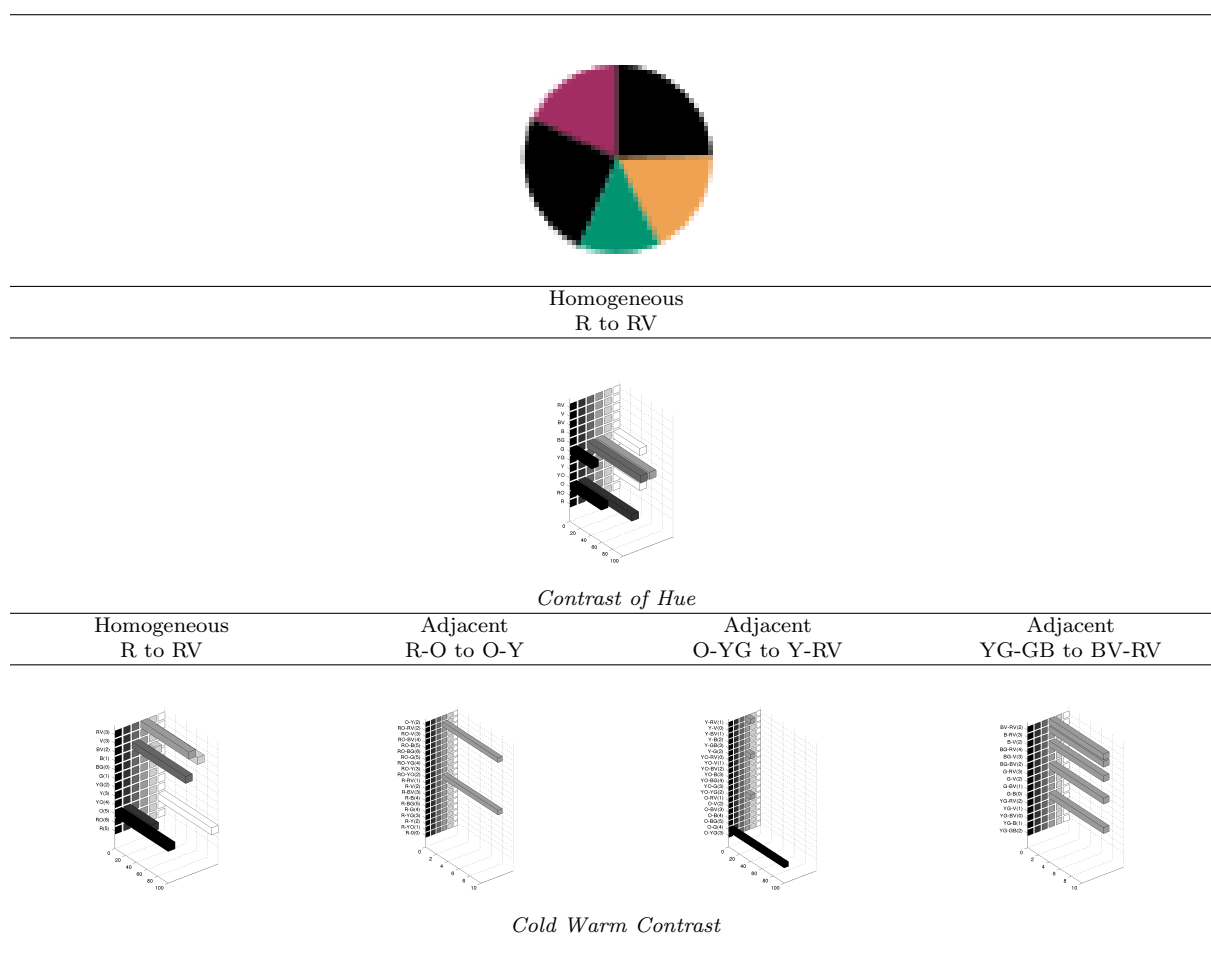


Figure 5.2: 3D Histograms of *contrast of hue* and *cold-warm contrast* in group 1 pie charts

The *contrast of hue* and *cold-warm contrast* results for pie charts in group 2

are displayed in Table 5.3. The homogeneous regions are almost the same for both contrasts, showing that the colors are fully saturated, and the light values are within $0.4 \leq L \leq 0.6$. Many expected hue adjacencies are missing, this is caused by the poor resolution of the pixels near the border surrounding each pie slice, causing the light values of the pixels to be outside the light range ($0.4 \leq L \leq 0.6$). The set of images in this group appear to meet the criteria for both *contrast of hue* and *cold-warm contrast*. Some of the images show a high *contrast strength*(5) between adjacent slices.

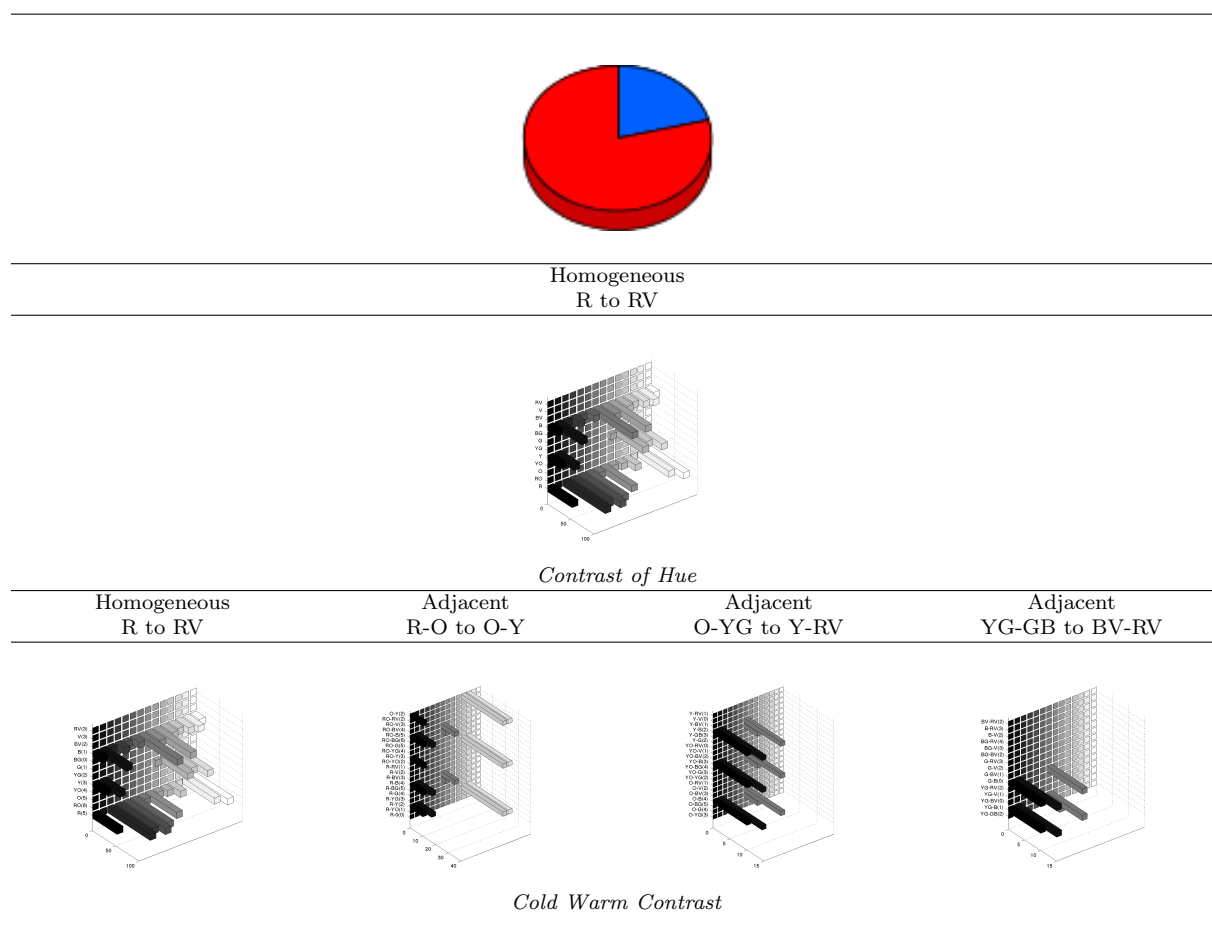


Figure 5.3: 3D Histograms of *contrast of hue* and *cold-warm contrast* in group 2 pie charts

The *contrast of hue* and *cold-warm contrast* results for pie charts in group 3 are displayed in Table 5.4. The overlap between the two 3D histograms of homogeneous regions captured by the *contrast of hue* and *cold-warm contrast* shows that the hues

are both fully saturated and in the light range $0.4 \leq L \leq 0.6$. The presence of adjacencies in the *cold-warm contrast* results shows that adjacent pie slices fit the criteria of *cold-warm contrast*. The *contrast strength* of the adjacencies ranges from mild to high.

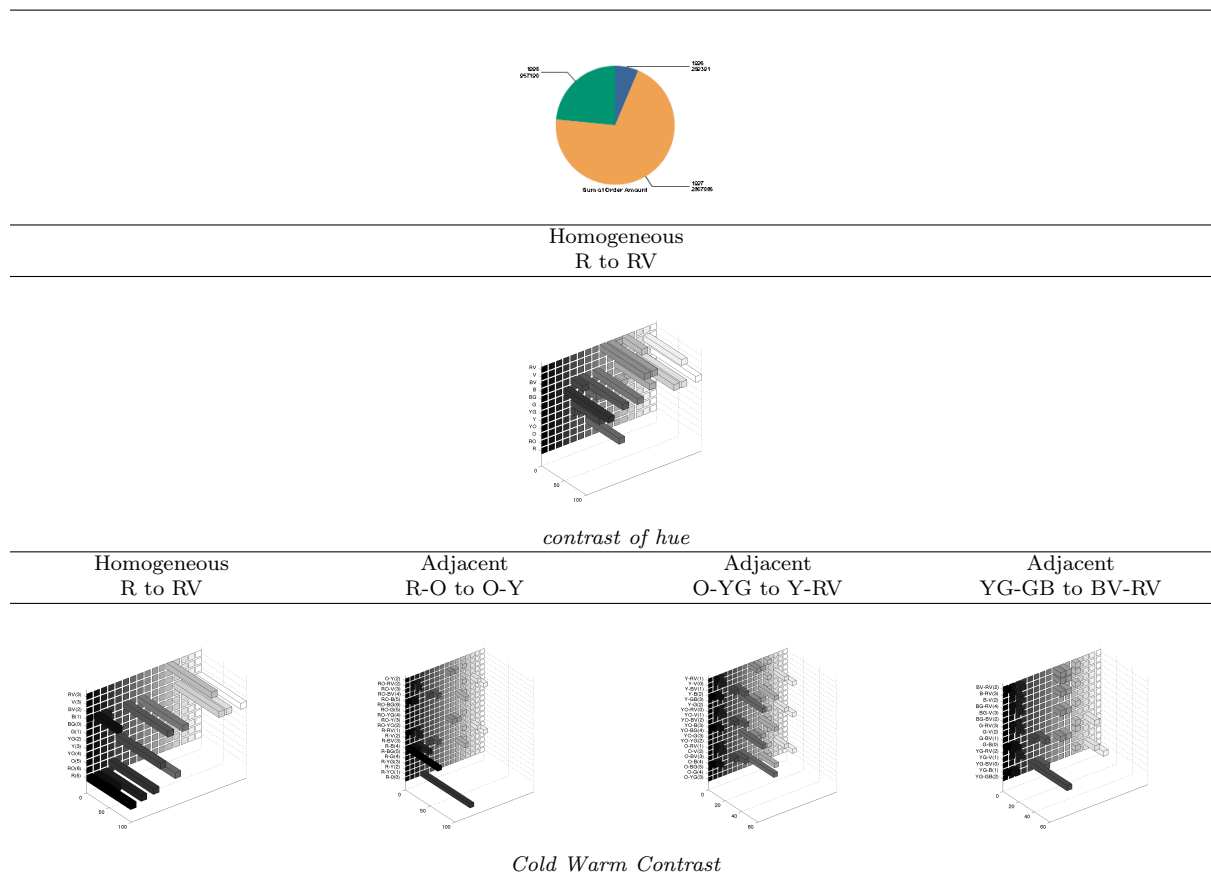


Figure 5.4: 3D Histograms of *contrast of hue* and *cold-warm contrast* in group 3 pie charts

The *contrast of hue* and *cold-warm contrast* results for pie charts in group 4 are displayed in Table 5.5. The images in this set are similar to each other. The overlapping peaks between the 3D histograms of both the *contrast of hue* and *cold-warm contrast* show that some pie slices are fully saturated and in the light range $0.4 \leq L \leq 0.6$. The presence of adjacencies in the *cold-warm contrast* results shows that some adjacent pie slices fit the criteria of *cold-warm contrast*. The *contrast strength* of the adjacencies ranges from mild to high.

The *contrast of hue* and *cold-warm contrast* results for pie charts in group 5 are

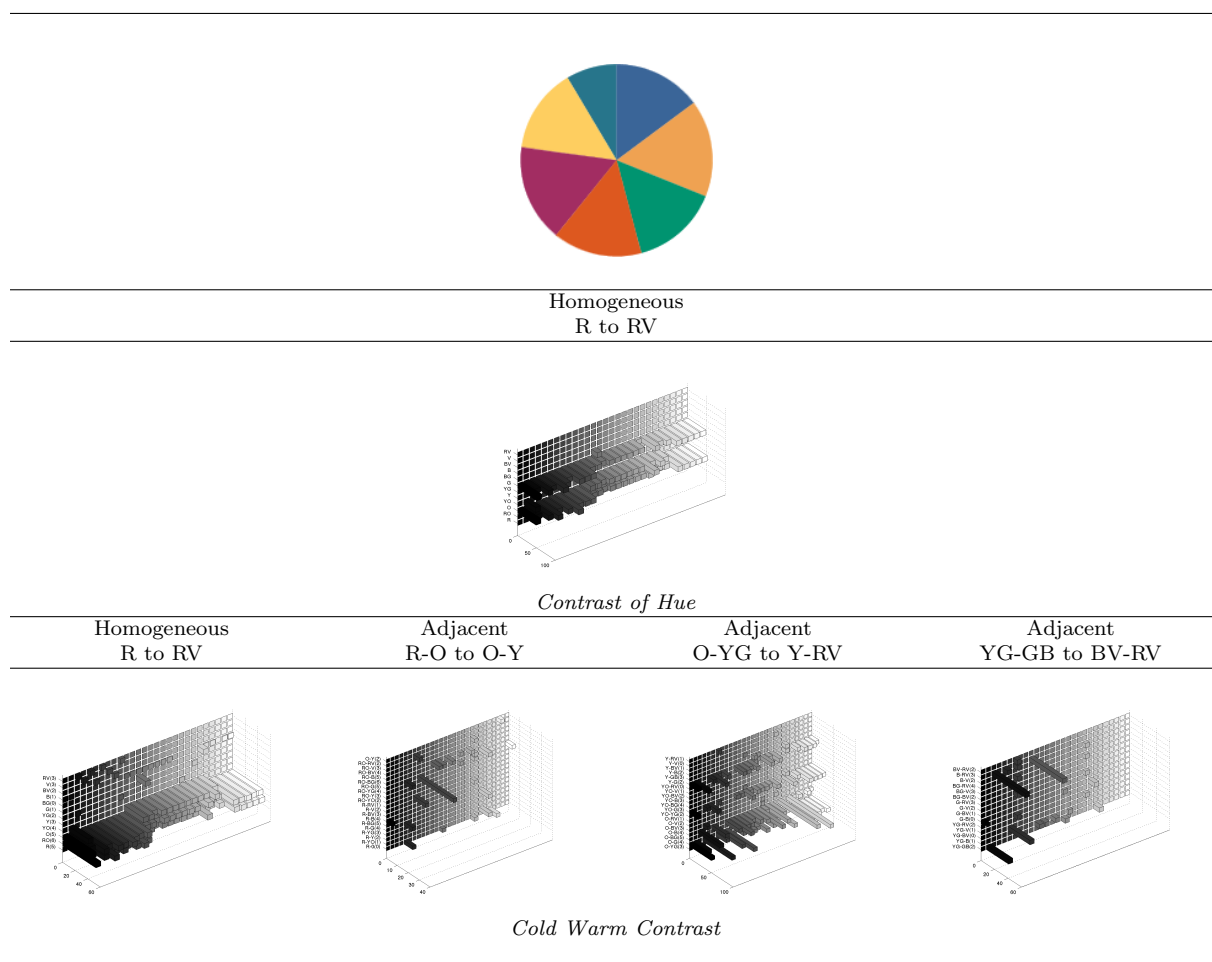


Figure 5.5: 3D Histograms of *contrast of hue* and *cold-warm contrast* in group 4 pie charts

displayed in Table 5.6. The images in this set are similar to each other, with several pie slices containing a mixture of saturations, and light levels. The overlapping peaks between the 3D histograms of both the *contrast of hue* and *cold-warm contrast* show that some pie slices are fully saturated and in the light range $0.4 \leq L \leq 0.6$. The presence of adjacencies in the *cold-warm contrast* results shows that some adjacent pie slices fit the criteria of *cold-warm contrast*. The *contrast strength* of the adjacencies is mostly high.

The *contrast of hue* and *cold-warm contrast* results for pie charts in group 6 are displayed in Table 5.7. The images contain a mixture of hue, saturation and light values and are not similar to each other. The *contrast of hue* results show that some images fit the *contrast of hue* criteria. The results support that the images meet the

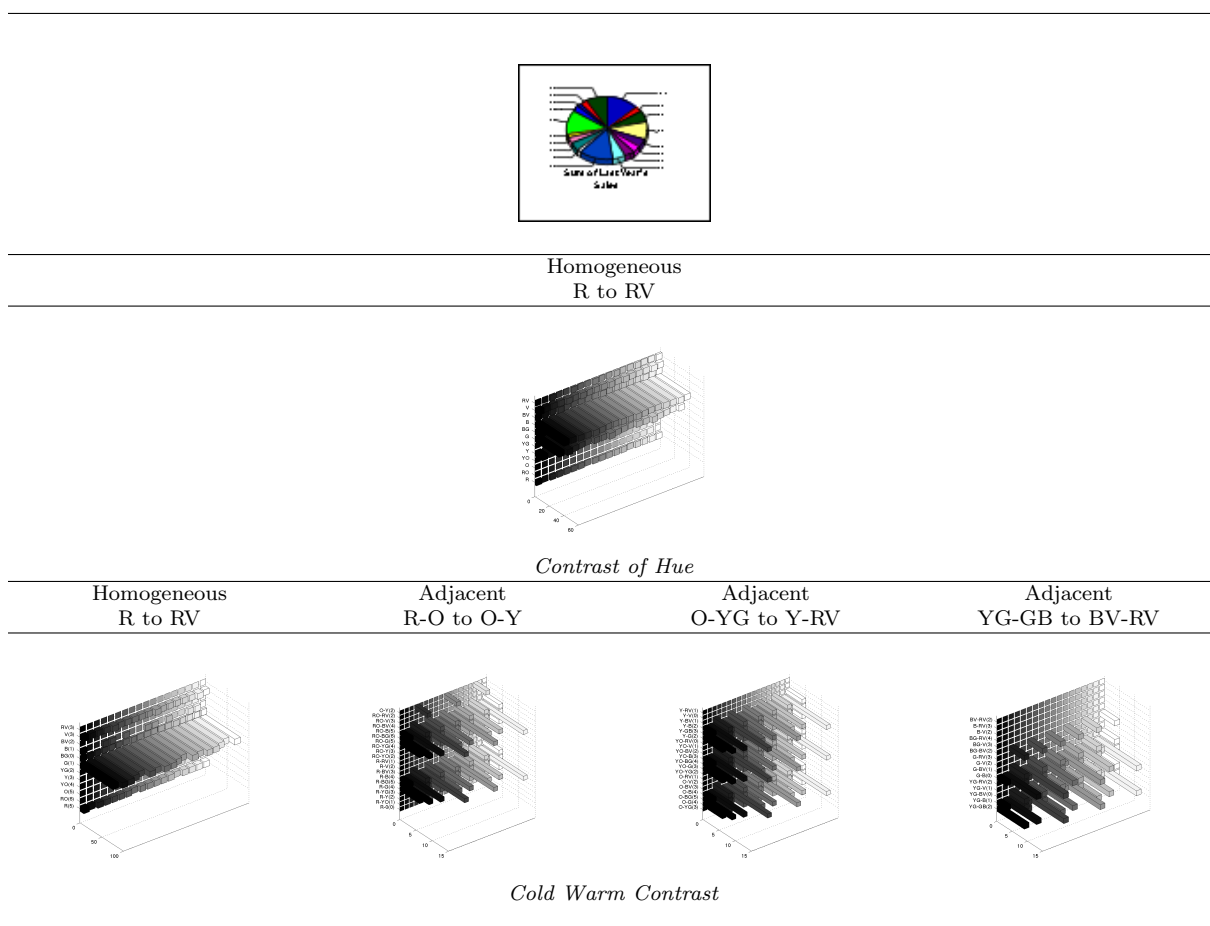


Figure 5.6: 3D Histograms of *contrast of hue* and *cold-warm contrast* in group 5 pie charts

cold-warm contrast criteria well, with varying *cold-warm contrast strengths*.

We observe that group 2, 3 and 6 mostly meet both the criteria for *contrast of hue* and *cold-warm contrast*, while fewer images from groups 1,4 and 5 met the criteria. The main difference between the pie charts that met the criteria and those that did not, was the pie charts that met the requirements had fairly uniform light and saturation ranges.

5.5 Discussion

The requirements of *contrast of hue* are difficult to implement for pie charts as they often need more than three hues. *Cold-warm contrast* however offers a variety of

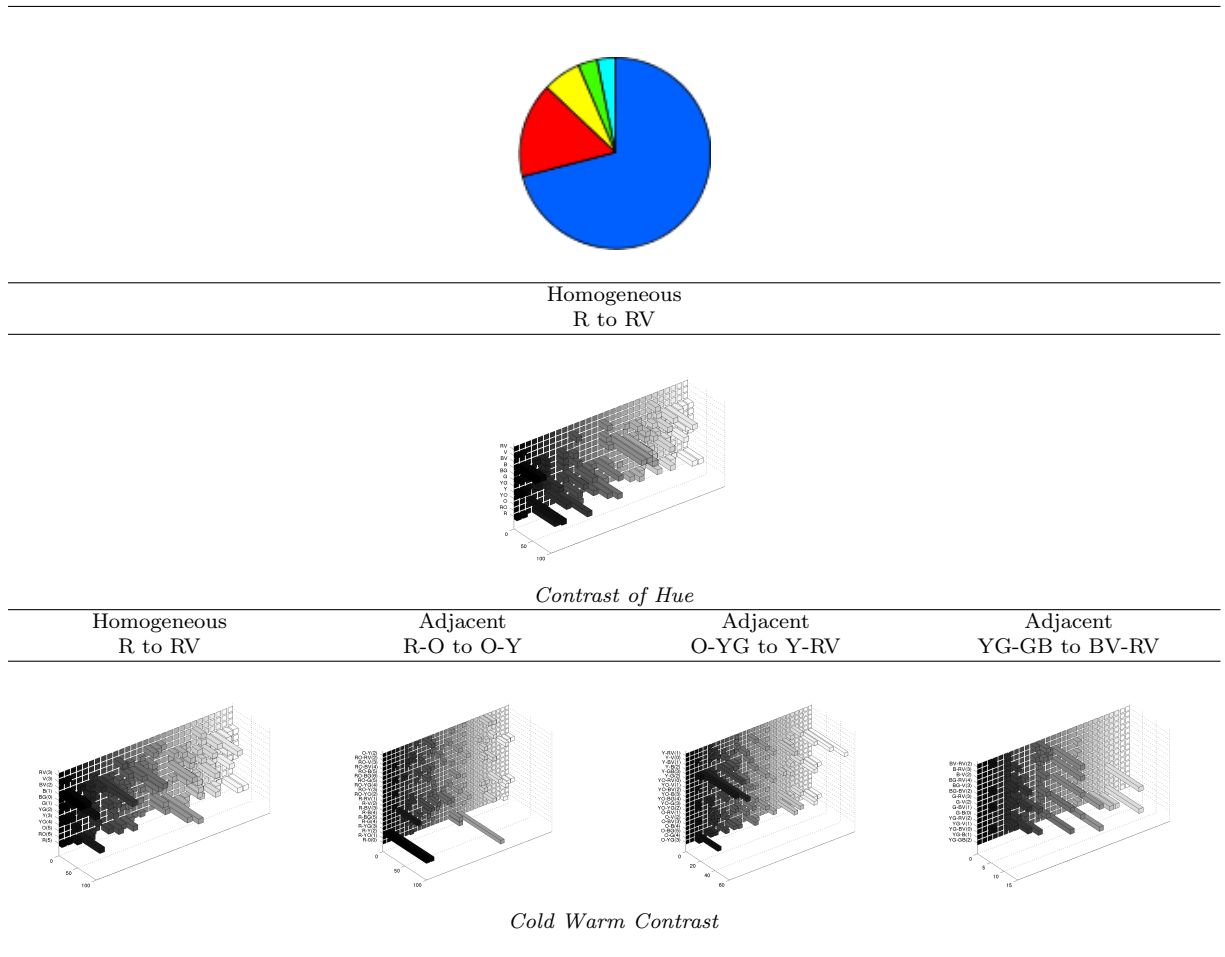


Figure 5.7: 3D Histograms of *contrast of hue* and *cold-warm contrast* in group 6 pie charts

options, with 12 hues, and a larger range of saturation levels to choose from. The *contrast strengths* in the adjacencies would also allow designers to select adjacent hue with intentional choices of mild, medium or high *cold-warm contrast*.

Chapter 6

Conclusion and future work

6.1 Conclusion

Color is an important feature in the aesthetic classification of images, however knowledge of color-based aesthetic theories in the Computer Vision community is limited. Thus the color-related features developed do not necessarily differentiate well between aesthetically high quality and low quality images. Our work aims at improving the state-of-the-art methods of extracting relevant color information by introducing concepts from color-based aesthetic theories and measures grounded in Itten's theories. We have made the following contributions:

1. Visualization: a 3D color palette of a painting in a metric color space consistent with Itten's color space
2. Computational models to measure:
 - (a) *modulation* using second order statistics
 - (b) *contrast of hue* in a painting, as well as assess patterns of *contrast of hue* in a collection of paintings from an artist
 - (c) *cold-warm contrast*. In this model, we developed a uniform quantization of *warmth indices* for hues, as well as a *warmth contrast strength* measure of contrast between homogeneous regions of different hues, and adjacent hues. We further developed a model to assess patterns of *cold-warm contrast* in a collection of paintings from an artist

3. An assessment of color use in business documents, namely assessing pie charts for the presence of *contrast of hue* and *cold-warm contrast*

6.2 Future work

Computer Vision researchers working the aesthetic classification of images would benefit from closer collaborations with the visual arts community. Such a collaboration would improve the outcome of the Computer Vision aesthetic classification systems, as design paradigms are learned from the visual art community. As such, our focus on Itten's color theories opens up many opportunities for research to further enrich Computer Vision with color-based aesthetic theory knowledge. We envision the following research projects:

Our work on *modulation* provides insight into the color palette of a painting. We also touched upon *modulation* in paintings that employed *cold-warm contrast*. Further research needs to be done to establish relationships between our *modulation* measures and the various contrasts at play in a painting. Our work on the color contrasts was focussed on two out of seven contrasts. Five contrasts remain to be explored: *contrast of light*, *contrast of saturation*, *complementary contrast*, *simultaneous contrast*, and *contrast of extension*. The study of contrast is directly related to color harmony. The following excerpt from Itten provides a description of his color harmony model: '*Suppose we have a double pointed needle universally pivoted at the center of the color sphere. Let one point of the needle be directed at any spot on the sphere; then the other point will indicate the symmetrical spot or complementary color value.... Thus not only the opposite hues but also all their degrees of brilliance are in complementary relation to each other*' [23, p.70]. This description inspires the exploration of geometric relationships among contrasting and harmonious color combinations, based on the spatial juxtaposition of the colors in the color sphere.

An extension of our work is in content-based-image-retrieval, an area of research in Computer Vision where given a probe image, a ranked list of similar images is retrieved from a larger collection. Typical techniques include computing the similarity of the probe image with the images in the collection, based on features such as color, texture and spatial composition. We anticipate that our color contrast features would improve the precision and recall measures of the images.

Other extensions of our work on contrasts include generating a heat map to visualize the cold and warm contrasts in images based on the hue warmth indices we

developed. Further, the co-occurrences for homogeneous regions can be re-interpreted by evaluating their square roots, as our current methods overcount the co-occurrences due to the V-8 relationship between a pixel and its neighbours. Re-interpretation of the results in this new light may provide more concise comparisons of the homogeneous regions for both the *contrast of hue* and *cold-warm contrast*.

Finally, we discuss future work on business documents. Pie charts can be recolored with a modified version of Cohen-Or's[8] harmonization algorithm. Since *contrast of hue* requires about three hues, and pie charts often contain more than 3 slices, recoloring pie charts to meet the criteria of *contrast of hue* may not be helpful. *Cold-warm contrast* however can create interesting color combinations for pie charts. Using the *cold-warm contrast* strengths from Chapter 3, it would be interesting to explore recoloring pie charts such that the strength of the *cold-warm contrast* in adjacent pie slices is controlled to be mild, medium or high.

Bibliography

- [1] Dpchallenge - a digital photography challenge. <http://www.dpchallenge.com/>. Accessed: 27/06/2014.
- [2] Flickr. <https://www.flickr.com/>. Accessed: 27/06/2014.
- [3] Photo.net - a site for photographers by photographers. <http://www.photo.net/>. Accessed: 27/06/2014.
- [4] Rule of thirds. <http://digital-photography-school.com/rule-of-thirds/>. Accessed: 04/07/2014.
- [5] A. Borji and L. Itti. State-of-the-art in visual attention modeling. *Pattern Analysis and Machine Intelligence, IEEE Transactions on*, PP(99):1, 2012.
- [6] Kenneth E Burchett. Color harmony. *Color Research & Application*, 27(1):28–31, 2002.
- [7] Marisa Carrasco. Visual attention: The past 25 years. *Vision research*, 51(13):1484–1525, 2011.
- [8] Daniel Cohen-Or, Olga Sorkine, Ran Gal, Tommer Leyvand, and Ying-Qing Xu. Color harmonization. *ACM Trans. Graph.*, 25(3):624–630, jul 2006.
- [9] Martin Constable and Xiaoyan Zhang. Depth-based analyses of landscape paintings and photographs according to itten’s contrasts. In *Image and Video Technology (PSIVT), 2010 Fourth Pacific-Rim Symposium on*, pages 481–486. IEEE, 2010.
- [10] Ritendra Datta, Dhiraj Joshi, Jia Li, and James Z Wang. Studying aesthetics in photographic images using a computational approach. In *Computer Vision–ECCV 2006*, pages 288–301. Springer, 2006.

- [11] Ritendra Datta, Jia Li, and James Ze Wang. Algorithmic inferencing of aesthetics and emotion in natural images: An exposition. In *Image Processing, 2008. ICIP 2008. 15th IEEE International Conference on*, pages 105–108. IEEE, 2008.
- [12] ER Davey. 'Soft framing': a comparative aesthetics of painting and photography. *Journal of European Studies*, 30(118):133–155, 2000.
- [13] Larry S. Davis, Steven A. Johns, and J.K. Aggarwal. Texture analysis using generalized co-occurrence matrices. *Pattern Analysis and Machine Intelligence, IEEE Transactions on*, PAMI-1(3):251–259, 1979.
- [14] Brigitte Borja De Mozota. *Design management: using design to build brand value and corporate innovation*. Skyhorse Publishing Inc., 2003.
- [15] S. Dhar, V. Ordonez, and T.L. Berg. High level describable attributes for predicting aesthetics and interestingness. In *Computer Vision and Pattern Recognition (CVPR), 2011 IEEE Conference on*, pages 1657 –1664, jun 2011.
- [16] Edith Feisner. *Color Studies*. Fairchild Publications, 2nd edition, 2006.
- [17] V. Gopalakrishnan, Y. Hu, and D. Rajan. Salient region detection by modeling distributions of color and orientation. *IEEE Transactions on Multimedia*, 11(5):892–905, 2009.
- [18] Soumyajit Gupta, Rahul Agrawal, Ritwik Layek, and Jayanta Mukhopadhyay. Psychovisual saliency in color images. In *Computer Vision, Pattern Recognition, Image Processing and Graphics (NCVPRIPG), 2013 Fourth National Conference on*, pages 1–4. IEEE, 2013.
- [19] Nick Harkness. The colour wheels of art, perception, science and physiology. *Optics & Laser Technology*, 38(4):219–229, 2006.
- [20] Florian Hoenig. Defining computational aesthetics. In *Proceedings of the First Eurographics conference on Computational Aesthetics in Graphics, Visualization and Imaging*, pages 13–18. Eurographics Association, 2005.
- [21] P. Isola, Jianxiong Xiao, A. Torralba, and A. Oliva. What makes an image memorable? In *Computer Vision and Pattern Recognition (CVPR), 2011 IEEE Conference on*, pages 145 –152, jun 2011.

- [22] Johannes Itten. *The Art of Color*. Van Nostrand Reinhold Company, 1961.
- [23] Johannes Itten. *The elements of color*. Van Nostrand Reinhold Company, 1970.
- [24] L. Itti. Visual salience. 2(9):3327, 2007.
- [25] L. Itti and C. Koch. Computational modelling of visual attention. *Nat. Rev. Neurosci.*, 2(3):194–203, Mar 2001.
- [26] L. Itti, C. Koch, and E. Niebur. A model of saliency-based visual attention for rapid scene analysis. *Pattern Analysis and Machine Intelligence, IEEE Transactions on*, 20(11):1254–1259, nov 1998.
- [27] C Richard Johnson, Ella Hendriks, Igor J Bereznoy, Eugene Brevdo, Shannon M Hughes, Ingrid Daubechies, Jia Li, Eric Postma, and James Z Wang. Image processing for artist identification. *Signal Processing Magazine, IEEE*, 25(4):37–48, 2008.
- [28] Dhiraj Joshi, Ritendra Datta, Elena Fedorovskaya, Quang-Tuan Luong, James Z Wang, Jia Li, and Jiebo Luo. Aesthetics and emotions in images. *Signal Processing Magazine, IEEE*, 28(5):94–115, 2011.
- [29] Timothée Jost, Nabil Ouerhani, Roman von Wartburg, René Müri, and Heinz Hügli. Assessing the contribution of color in visual attention. *Computer Vision and Image Understanding*, 100(1):107–123, 2005.
- [30] Yan Ke, Xiaou Tang, and Feng Jing. The design of High-Level features for photo quality assessment. In *Computer Vision and Pattern Recognition, 2006 IEEE Computer Society Conference on*, volume 1, pages 419 – 426, jun 2006.
- [31] Shehroz S Khan and Daniel Vogel. Evaluating visual aesthetics in photographic portraiture. In *Proceedings of the Eighth Annual Symposium on Computational Aesthetics in Graphics, Visualization, and Imaging*, pages 55–62. Eurographics Association, 2012.
- [32] Helmut Leder, Benno Belke, Andries Oeberst, and Dorothee Augustin. A model of aesthetic appreciation and aesthetic judgments. *British Journal of Psychology*, 95(4):489–508, 2004.

- [33] Congcong Li and Tsuhan Chen. Aesthetic visual quality assessment of paintings. *Selected Topics in Signal Processing, IEEE Journal of*, 3(2):236–252, 2009.
- [34] Jia Li, Lei Yao, Ella Hendriks, and James Z Wang. Rhythmic brushstrokes distinguish van gogh from his contemporaries: findings via automated brushstroke extraction. *Pattern Analysis and Machine Intelligence, IEEE Transactions on*, 34(6):1159–1176, 2012.
- [35] Zhi Liu, Wenbin Zou, and O. Le Meur. Saliency tree: A novel saliency detection framework. *Image Processing, IEEE Transactions on*, 23(5):1937–1952, May 2014.
- [36] Florent Perronnin (Xerox (XRCE) Grenoble) Luca Marchesotti (Xerox). Learning beautiful (and ugly) attributes. In *Proceedings of the British Machine Vision Conference*. BMVA Press, 2013.
- [37] Wei Luo, Xiaogang Wang, and Xiaoou Tang. Content-based photo quality assessment. In *Computer Vision (ICCV), 2011 IEEE International Conference on*, pages 2206–2213. IEEE, 2011.
- [38] Matija Males, Adam Hedi, and Mislav Grgic. Aesthetic quality assessment of headshots. In *ELMAR, 2013 55th International Symposium*, pages 89–92. IEEE, 2013.
- [39] Luca Marchesotti, Florent Perronnin, Diane Larlus, and Gabriela Csurka. Assessing the aesthetic quality of photographs using generic image descriptors. In *Computer Vision (ICCV), 2011 IEEE International Conference on*, pages 1784–1791. IEEE, 2011.
- [40] Daniele Marini and Alessandro Rizzi. A computational approach to color adaptation effects. *Image and Vision Computing*, 18(13):1005–1014, 2000.
- [41] P. Moon and D. Spencer. Geometric formulation of classical color harmony. *J. Opt. Soc. Am.*, 34(1):46–50, Jan 1944.
- [42] N. Murray and L. Marchesotti. Ava: A large-scale database for aesthetic visual analysis. In *Computer Vision and Pattern Recognition (CVPR), 2012 IEEE Conference on*, jun 2012.

- [43] M. Nishiyama, T. Okabe, I. Sato, and Y. Sato. Aesthetic quality classification of photographs based on color harmony. In *Computer Vision and Pattern Recognition (CVPR), 2011 IEEE Conference on*, pages 33–40, June 2011.
- [44] P. Obrador, L. Schmidt-Hackenberg, and N. Oliver. The role of image composition in image aesthetics. In *Image Processing (ICIP), 2010 17th IEEE International Conference on*, pages 3185–3188, Sept 2010.
- [45] Pere Obrador, Michele Saad, Poonam Suryanarayan, and Nuria Oliver. Towards category-based aesthetic models of photographs. In Klaus Schoeffmann, Bernard Merialdo, Alexander Hauptmann, Chong-Wah Ngo, Yiannis Andreopoulos, and Christian Breiteneder, editors, *Advances in Multimedia Modeling*, volume 7131 of *Lecture Notes in Computer Science*, pages 63–76. Springer Berlin / Heidelberg, 2012.
- [46] Li-Chen Ou, Patrick Chong, M Ronnier Luo, and Carl Minchew. Additivity of colour harmony. *Color Research & Application*, 36(5):355–372, 2011.
- [47] Li-Chen Ou and M Ronnier Luo. A colour harmony model for two-colour combinations. *Color Research & Application*, 31(3):191–204, 2006.
- [48] Li-Chen Ou, M Ronnier Luo, Andrée Woodcock, and Angela Wright. A study of colour emotion and colour preference. part i: Colour emotions for single colours. *Color Research & Application*, 29(3):232–240, 2004.
- [49] Rajarshi Pal, Jayanta Mukherjee, and Pabitra Mitra. How do warm colors affect visual attention? In *Proceedings of the Eighth Indian Conference on Computer Vision, Graphics and Image Processing*, page 24. ACM, 2012.
- [50] Stephen E. Palmer, Karen B. Schloss, and Jonathan Sammartino. Visual aesthetics and human preference. *Annual Review of Psychology*, 64(1):77–107, 2013. PMID: 23020642.
- [51] Gabriele Peters. Aesthetic primitives of images for visualization. In *Information Visualization, 2007. IV'07. 11th International Conference*, pages 316–325. IEEE, 2007.
- [52] C. Platzer and A. Broder. Most people do not ignore salient invalid cues in memory-based decisions. *Psychon Bull Rev*, 19(4):654–661, Aug 2012.

- [53] Jorge Sánchez, Florent Perronnin, Thomas Mensink, and Jakob Verbeek. Image classification with the fisher vector: Theory and practice. *International journal of computer vision*, 105(3):222–245, 2013.
- [54] Karen Schriver. *Dynamics in document design*. Wiley Computer Publishing, 2nd edition, 1997.
- [55] Hae Jong Seo and P. Milanfar. Nonparametric bottom-up saliency detection by self-resemblance. In *Computer Vision and Pattern Recognition Workshops, 2009. CVPR Workshops 2009. IEEE Computer Society Conference on*, pages 45 –52, june 2009.
- [56] Martin Solli and Reiner Lenz. Color based bags-of-emotions. In *Computer Analysis of Images and Patterns*, pages 573–580. Springer, 2009.
- [57] Huixuan Tang, N. Joshi, and A. Kapoor. Learning a blind measure of perceptual image quality. In *Computer Vision and Pattern Recognition (CVPR), 2011 IEEE Conference on*, pages 305 –312, jun 2011.
- [58] Masataka Tokumaru, Noriaki Muranaka, and Shigeru Imanishi. Color design support system considering color harmony. In *Fuzzy Systems, 2002. FUZZ-IEEE'02. Proceedings of the 2002 IEEE International Conference on*, volume 1, pages 378–383. IEEE, 2002.
- [59] S Treue and S Katzner. Visual attention. *Encyclopedia of Neuroscience*, 10:243–250, 2009.
- [60] Norman Turner. Cézanne, Wagner, Modulation. *The Journal of Aesthetics and Art Criticism*, 56(4):pp. 353–364, 1998.
- [61] S. Westland, K. Laycock, V. Cheung, and F. Henry, P.and Mahyar. Color harmony. *Colour: Design & Creativity*, 1(1):1–15, 2007.
- [62] Victoria Yanulevskaya, Jasper Uijlings, Elia Bruni, Andreza Sartori, Elisa Zamboni, Francesca Bacci, David Melcher, and Nicu Sebe. In the eye of the beholder: employing statistical analysis and eye tracking for analyzing abstract paintings. In *Proceedings of the 20th ACM international conference on Multimedia*, pages 349–358. ACM, 2012.

- [63] Qi Zhao and Christof Koch. Learning a saliency map using fixated locations in natural scenes. *Journal of vision*, 11(3):9, 2011.